

REPUBLIC OF CAMEROON

Peace - Work - Fatherland
Ministry of Higher Education



DEPARTEMENT DE GENIE CIVIL
DEPARTMENT OF CIVIL ENGINEERING

REPUBLIQUE DU CAMEROUN

Paix - Travail - Patrie
Ministère de l'Enseignement Supérieure



**UNIVERSITÀ
DEGLI STUDI
DI PADOVA**

DEPARTMENT OF CIVIL, ARCHITECTURAL
AND ENVIRONMENTAL ENGINEERING

**THE BEHAVIOUR OF CONCRETE BUILDINGS DESIGNED IN THE
ELASTIC AND PLASTIC FIELDS.
CASE STUDY: LINEAR AND NON-LINEAR ANALYSIS ON THE
ADMINISTRATIVE BUILDING IN THE NATIONAL ADVANCED
SCHOOL OF PUBLIC WORKS YAOUNDE**

A thesis submitted in partial fulfilment of the requirements for the degree of Master of
Engineering (MEng) in Civil Engineering.

Curriculum: **Structural Engineering**

Proposed by:

CHEFOR MBAFOR WAZIBI

Student number: **15TP20979**

Supervisor:

Prof Eng. Carmelo MAJORANA

Co-Supervisors:

Dr Eng. Guillaume Hervé POH'SIE

Eng. Giuseppe CARDILLO

Academic year: **2019-2020**

DEDICATION

This work is dedicated to the memory of my beloved daughter

AMAZING-GRACE

*Baby, you left this world too soon, but as I look at this project every day, I'll
have your wonderful smile and laughter forever in my heart.*

ACKNOWLEDGEMENTS

Special thanks go to God Almighty father of our Lord Jesus Christ for His grace, wisdom and motivation given to me during my training and especially for this thesis.

The **President of this jury** for the honour given to me in accepting to preside this jury.

The **Examiner** for the time he spent to check this work and the remarks he made.

I would also like to thank my supervisors **Prof Carmelo MAJORANA** and **Eng. Giuseppe CARDILLO** who were involved in the validation survey for this research. Without their participation and input, the validation survey could not have been successfully conducted.

I would extend my gratitude to **Dr Eng. Guillaume Hervé POH'SIE** for his continual survey and supervision for the accomplishment of this thesis and as reporter of my work.

I thank the Director and Assistant director in charge of studies in the respective persons of **Prof NKENG George ELAMBO** and **Dr BWEMBA Charles** for all their administrative and academic support throughout these years spent at NASPW in this MEng program as they worked in partnership with the University of Padua;

I would also thanks **Prof MBESSA Michel**, head of the Department of Civil Engineering for his availability encouragement and relentless efforts to assist me during the entire preparation of this dissertation.

I would like to express my gratitude to all the teaching staff of the National Advanced School of Public Works and University of Padova for their collaborations and support in bringing out the best results of this wonderful partnership.

I am thankful to the administrative staff of the National Advanced School of Public Works for their kind assistance during the whole preparation of this thesis.

I would like to express my deepest gratitude to my beloved parents **Mr & Mrs CHEFOR**, my uncle and professional mentor **Mr MA-APOH Augustine**, my brothers and lovely sisters, for their endless encouragement, support and patience throughout the project period,

I thank my classmates of '**6e PROMO MEng**' for their moral support throughout my training in ENSTP and the organisation of special tutorials we called "*Messes*".

I thank the group **MATRICE** for accompanying me throughout my training in ENSTP especially during the tough times of the first and second years of my training.

I also want to thank **Eng. NGOUO Idriss** for the close follow-up of my master thesis work despite his busy schedule.

Finally, I thank the **Etoug-ebe Baptist Church** family, my spiritual mentor **Mr FAJONG David**, my friends and all those who directly or indirectly have supported me all these while.

GLOSSARY

ADRS: Acceleration-Displacement Response Spectrum

CCSZ: Cameroon Shear Zone

CEM: Cement class

EC: Eurocode

EN: European Norm

FEMA: Federal Emergency Management Agency

FIM : Fondation Input Motion

LSA: linear static analysis

MDOF: Multiple degrees of freedom

NDP: Nationally Determined Parameters

NLTHA: Nonlinear time history analysis

PA: Pushover Analysis

PEER: Pacific Earthquake

RCC: Reinforced Cement Concrete

RC: Reinforced Concrete

SAP: Structural Analysis Program

SDOF: Single degree of freedom

SSI: Soil structure interaction

SSR: Seismic Source Region

SSZ: Sanaga Shear Zone

SLS: Serviceability limit state

Ti: Periods

ULS: Ultimate Limit State

W/C: Water to Cement ratio

NOTATIONS AND SYMBOLS

ϕ	<i>Strength reduction factor</i>
v_n	<i>Nominal joint shear stress</i>
τ_c	<i>Shear stress in concrete</i>
A	<i>Area of the cross-section</i>
A_c	<i>Area of the concrete cross-section</i>
A_{min}	<i>Minimum section area</i>

A_{net}	<i>Net area of the cross-section</i>
A_s	<i>Area of the steel reinforcement section</i>
A_{sw}	<i>The Cross-sectional area of the shear reinforcement</i>
A_{jv}	<i>Area of vertical shear reinforcement</i>
A_g	<i>Gross area of concrete</i>
A_{st}	<i>Total are of stirrups</i>
A_{jh}	<i>Area of horizontal shear reinforcements</i>
A_{sh}	<i>Area of horizontal steel reinforcement</i>
A_{s1}	<i>Area of steel at the top of beam section</i>
A_{s2}	<i>Area of steel section at the bottom of beam section</i>
b	<i>Width of the bottom flange of the beam</i>
b_c	<i>Width of column</i>
b_w	<i>Width of the beam</i>
$C_{min, b}$	<i>Minimum cover due to bond requirement</i>
$C_{min, dur}$	<i>Minimum cover due to environmental conditions</i>
C_{min}	<i>Minimum concrete cover</i>
d	<i>Effective depth section</i>
d_t	<i>Concrete tensile damage parameter</i>
d_c	<i>Concrete compressive damage parameter</i>
f_{ywd}	<i>Design yield strength of stirrups</i>
f_c'	<i>Unconfined compressive strength of concrete</i>
f_{sy}	<i>Yield strength of stirrup</i>
f_{cd}	<i>The design value of concrete compressive strength</i>
f_{ctm}	<i>mean value of tensile strength of concrete</i>
f_{yd}	<i>The design value of yield strength of steel</i>
G	<i>Shear Modulus</i>
$G1k$	<i>Structural load of the building</i>
$G2k$	<i>Non-structural load apply to the building</i>
H	<i>Total height of the building</i>
I	<i>Moment of inertia</i>
h	<i>Storey height</i>
h_c	<i>Cross-sectional depth of the column</i>

M_{Ed}	<i>Bending moment at support</i>
M_{Rd}	<i>Resisting moment</i>
M_{Sd}	<i>Soliciting bending moment</i>
M_{Ed}	<i>Bending moment at support</i>
V_{juh}	<i>Maximum induced horizontal shear force in the joint</i>
N_{Ed}	<i>Design axial compression force</i>
N_{Ed}	<i>The tensile axial force inside the element</i>
$N_{Pl,Rd}$	<i>Design tension resistance of a steel section</i>
N_{Rd}	<i>Minimum area section of the column</i>
N_{Sd}	<i>Axial load compute using the recovery area of the column</i>
$N_{u,Rd}$	<i>Designed ultimate resistance</i>
$S_{cl,max}$	<i>Minimum spacing of the transverse reinforcement</i>
V_{Ed}	<i>Acting shear</i>
$V_{Rd,C}$	<i>Design shear resistance of the member without shear reinforcement</i>
c	<i>Concrete cover</i>
$s_{l,max}$	<i>Maximum longitudinal spacing</i>
$s_{t,max}$	<i>Maximum transversal spacing</i>
x	<i>Neutral Axis Position</i>
α	<i>The angle between shear reinforcement and the beam axis perpendicular to the shear force</i>
α_{cw}	<i>Coefficient taking account the state of stress in the compression cord</i>
$\Delta C_{dur,ad}$	<i>Add reduction of minimum cover for use of additional protection</i>
d	
$\Delta C_{dur,st}$	<i>Reduction of minimum cover for use of stainless steel</i>
$\Delta C_{dur,\gamma}$	<i>Additive safety element</i>
$\phi_{l,min}$	<i>Minimum diameter of the longitudinal bars</i>
ϕ_{ef}	<i>Effective creep ratio</i>
γ	<i>Specific weight</i>
γ_s	<i>Partial safety factor for steel</i>
Ψ_E	<i>Combination coefficient for variable action</i>
λ	<i>Slenderness</i>
λ_{lim}	<i>The limit value of slenderness</i>
ν	<i>Poisson's ratio</i>

ABSTRACT

The aim of this work was to show the behaviour of a reinforced concrete building following elastic and plastic designs. A six floor existing storey building in the National Advanced School of Public Works located in Yaounde-Cameroon was studied. In recent times, most attention has been drawn to the ductility of steel used for reinforcement in reinforced concrete, which can deform in-elastically to required deformations imposed by a ground vibration without loss of strength. This implies damage, but not collapse since design level of ground vibrations or earthquakes are rare events. The elastic design was done by performing a linear static analysis for the study of horizontal and vertical structural elements following standards given in Eurocode 2 by using SAP 2000v.22 for the beam modelling and load combinations, and Microsoft Excel for the treatment of the results obtained. The structure is then modelled on SAP 2000v.22 using the sections obtained from the previous elastic design, then a modal analysis is performed in the same software to get the periods of oscillation of the structure. From the first three modes of our building, it was observed a rotational dominant effect due to the ratio between the length and width of the studied part of the building which should normally require a structural joint. The plastic design is then carried out by performing a non-linear static analysis (pushover analysis) still in SAP 2000v.22 by applying plastic hinges in the areas where failure is most likely to occur and see how they behave under the action of a given ground force. The results of this pushover analysis showed that the structure behaves differently in the x and y directions from the displacements obtained in the respective directions. The displacements were more in the y direction than in the x direction because the pillars obtained from the elastic analysis were rectangular (giving rise to a variation of moments of inertia in each direction). It is more favourable for beams to collapse before columns in structure so that the entire building goes down progressively, but this was not the case for our structure (where fixed footings are considered). It was noticed that the columns went in to collapse before the beams. The structure was modelled a second time, taking in to consideration the soil structure interaction and the modal and pushover analysis performed again where it was noticed a different behaviour of the structure with an observed increase in the floor displacements and a modification in the collapse mechanism as beams now went in to collapse before columns. It was also noticed that the inter-storey drift ratio was within the limit values, which is a plus in the stability of our structure in terms of life safety.

Keywords: Reinforced concrete buildings, linear static analysis, modal analysis, non-linear static analysis, soil structure interaction.

RESUME

Le but de ce travail était de montrer le comportement d'un bâtiment en béton armé suivant des conceptions élastiques et plastiques. Un immeuble de 6 étages à l'Ecole Nationale Supérieure des Travaux Publics a été étudié. Ces derniers temps, la plus grande attention a été attirée sur la ductilité de l'acier utilisé pour le renforcement du béton armé, qui peut se déformer de manière inélastique aux déformations requises imposées par une vibration du sol sans perte de résistance. Cela implique des dommages, mais pas un effondrement puisque le niveau de conception des vibrations du sol ou des tremblements de terre sont des événements rares. Le dimensionnement élastique a été fait en réalisant une analyse statique linéaire pour l'étude des éléments de structure horizontaux et verticaux suivant les normes données dans l'EC2 en utilisant SAP 2000 pour la modélisation des poutres et les combinaisons de charges, et Microsoft Excel pour le traitement des résultats obtenus. L'ensemble de la structure est ensuite modélisé sur SAP en utilisant les sections obtenues, puis une analyse modale est effectuée dans le même logiciel pour obtenir les périodes d'oscillation de la structure. Dès les trois premiers modes de notre bâtiment, il a été observé un effet dominant de rotation dû au rapport entre la longueur et la largeur de la partie étudiée du bâtiment qui devrait normalement nécessiter un joint structurel. La conception plastique est ensuite réalisée en effectuant une analyse statique non linéaire toujours dans SAP en appliquant des charnières en plastique dans les zones où la défaillance est la plus susceptible de se produire et de voir comment elles se comportent sous l'action d'une force terrestre donnée. Les résultats de cette analyse pushover ont montré que la structure se comporte différemment dans les directions x et y suivant les déplacements obtenus dans les 2 directions. Les déplacements étaient plus dans la direction y que dans la direction x car les poteaux obtenus à partir de l'analyse élastique étaient rectangulaires (donnant lieu à une variation des moments d'inertie). Il est plus favorable que les poutres s'effondrent avant les poteaux en structure pour que l'ensemble du bâtiment s'effondre progressivement, mais ce n'était pas le cas pour notre structure. Il est apparu que les poteaux s'effondraient avant les poutres. La structure a été modélisée une deuxième fois en tenant compte de l'interaction sol-structure, et l'analyse modale et pushover ont été effectuée à nouveau où il a été remarqué un comportement différent de la structure avec une augmentation observée des déplacements des planchers et une amélioration dans le schéma de ruine. Il a été aussi constaté que le rapport de déplacement inter-étage sur la hauteur était dans les valeurs limites, ce qui est un plus dans la stabilité de notre structure en terme de sécurité des personnes.

Mots clés : Bâtiments en béton armé, analyse statique linéaire, analyse modale, analyse statique non linéaire, interaction sol-structure.

LIST OF FIGURES

Figure 1.1.	Particle size distribution curves of sand and gravel	3
Figure 1.2.	Water/cement ratio for different compressive strength (http://www.google.cm).....	5
Figure 1.3.	Cylinder and cubic specimens in compressive strength evaluation (EN 1992-1-1:2004).....	7
Figure 1.4.	Strength class and deformation for concrete (EN 1992-1-1:2004)	8
Figure 1.5.	Stress Strain Curve for concrete under compression.....	10
Figure 1.6.	Stress-strain diagrams for reinforcing steel (EN 1992-1-1:2004)	11
Figure 1.7.	Equivalence of ductility and behaviour factor (Ahmed Y. 2016)	12
Figure 1.8.	Flexural cracks in RC beams (Haseeb Jamal, 2018)	14
Figure 1.9.	Honey combing in concrete (Haseeb Jamal, 2018)	15
Figure 1.10.	Factors affecting concrete durability (L. H. Son et al., 1993)	16
Figure 1.11.	Capacity curves for: SDOF system (a), (Roberta, 2010), MDOF system (b) (Chopra et al., 2004).....	22
Figure 1.12.	Typical pushover curve (Mouzzoun et al., 2013).....	23
Figure 1.13.	Kobe Earthquake 1995	24
Figure 1.14.	Stress strain curve.....	25
Figure 1.15.	Methods of seismic analysis	25
Figure 1.16.	Schematic illustration of a direct analysis of SSI (NIST, 2012).	26
Figure 1.17.	Substructure method for modelling the soil–pile–structure interaction (Van Nguyen et al, 2017).....	28
Figure 1.18.	Schematic illustration of deflections caused by lateral force applied to: (a) structure with fixed base, (b) structure with flexible base (NIST, 2012).	30
Figure 1.19.	Illustration of the SSI effect on base shear due to the period lengthening and change in damping (NIST, 2012).....	31
Figure 1.20.	Maximum inter-storey drifts of the structure for different type of foundation under the influence of El Centro earthquake (Hokmabadi, 2015).	33
Figure 2.1.	Concrete cover	37
Figure 2.2.	Moment reduction at supports (Djeukoua Nathou, G. L. 2019).....	38
Figure 2.3.	Shifting of the moment curve (Djeukoua Nathou, G. L. 2019).....	39
Figure 2.4.	Example of transversal beam section with longitudinal reinforcements....	40
Figure 2.5.	Neutral axis position in the beam section.....	40

Figure 2.6.	Maximum longitudinal spacing and transversal spacing of the legs	42
Figure 2.7.	Geometric characteristics of a transversal beam section	43
	The moment of inertia of the uncracked section is given by equation 2.20:	43
Figure 2.8.	M-N diagram computation of a rectangular column section in both loading directions.....	44
Figure 2.9.	Example of M-N diagram (D'Antino et al., 2016).....	46
Figure 2.10.	Force- Deformation for hinge formation	50
Figure 2.11.	Colour codification for performance identification in SAP 2000	50
Figure 2.12.	Pushover curve and bilinear idealisation scheme (P. Fajfar et al. 2004)....	51
Figure 2.13.	Subgrade modulus for different soil types (Forni, sd).....	51
Figure 3.1.	Administrative building in the NASPW Yaounde	55
Figure 3.2.	Formwork plan of the building.....	56
Figure 3.3.	Formwork plan of block B	57
Figure 3.4.	Section A-A of block B	57
Figure 3.5.	Section B-B of block B.....	58
Figure 3.6.	Selected beam for design.....	61
Figure 3.7.	Dimensions of the beam section.....	62
Figure 3.8.	Load combinations at ULS	63
Figure 3.9.	Beam model with simple supports	64
Figure 3.10.	Beam model with fixed supports.....	64
Figure 3.11.	Bending moment solicitation curves of the beam	64
Figure 3.12.	Shear solicitation curves on the beam	65
Figure 3.13.	Envelope curve for bending moment	65
Figure 3.14.	Envelope curve for shear solicitation	66
Figure 3.15.	Recapitulative curve for bending moment verification of the beam	66
Figure 3.16.	Recapitulative curve for shear verification of the beam.....	67
Figure 3.17.	Bending moment solicitation curves for the beam at SLS	67
Figure 3.18.	Envelope curve for bending moment at SLS.....	68
Figure 3.19.	Recapitulative curve of the stress verification of the beam.....	69
Figure 3.20.	Recapitulation of beam detailing.....	70
Figure 3.21.	Choice of the studied column	71
Figure 3.22.	Dimensions of the beam section.....	71
Figure 3.23.	Bending moment solicitation curves on the columns.....	73
Figure 3.24.	Axial load solicitation curve on the column.....	73

Figure 3.25.	Envelope curve of bending moment on the column.....	74
Figure 3.26.	Envelope curve of axial load on column.....	75
Figure 3.27.	Interaction diagram of the column F2 in the x-direction.....	75
Figure 3.28.	Interaction diagram of the column F2 in the y-direction.....	76
Figure 3.29.	Shear force solicitation curve on the column.....	77
Figure 3.30.	Shear force envelope on the column.....	78
Figure 3.31.	Recapitulative of the column detailing.....	79
Figure 3.32.	Reinforcement detail for studied frame.....	80
Figure 3.33.	Load on footing.....	80
Figure 3.34.	Structural model with fixed footings.....	81
Figure 3.35.	First vibrational mode, translational in the x-direction.....	82
Figure 3.36.	Second vibrational mode, translational-rotation in the y-direction.....	82
Figure 3.37.	Third vibrational mode, rotational.....	82
Figure 3.38.	formation of plastic hinge non the entire structure.....	83
Figure 3.39.	Push on frame in direction OXZ.....	84
Figure 3.40.	Hinge formation for push on frame in direction OXZ.....	84
Figure 3.41.	Push X on frame frame in direction OYZ.....	85
Figure 3.42.	Hinge formation due to push X on frame in direction OYZ.....	85
Figure 3.43.	Floor displacement in the X- direction.....	86
Figure 3.44.	Floor displacement in the Y direction.....	86
Figure 3.45.	Storey drift.....	87
Figure 3.46.	Failure mode of structure.....	87
Figure 3.47.	Building model considering SSI.....	88
Figure 3.48.	First mode of vibration considering SSI.....	89
Figure 3.49.	Second mode of vibration considering SSI.....	89
Figure 3.50.	Third mode of vibration considering SSI.....	90
Figure 3.51.	Formation of plastic hinges after considering SSI.....	90
Figure 3.52.	Hinge formation in Y-direction considering SSI.....	91
Figure 3.53.	Pushover curve for push Y considering SSI.....	91
Figure 3.54.	Comparison for push Y.....	92
Figure 3.55.	Hinge formation in x-direction considering SSI.....	92
Figure 3.56.	Pushover curve for push X considering SSI.....	93
Figure 3.57.	Comparison for push X.....	93
Figure 3.58.	Floor displacement in x-direction considering SSI.....	94

Figure 3.59.	Floor displacement in y-direction considering SSI	94
Figure 3.60.	Floor displacement comparison in the x-direction	95
Figure 3.61.	Floor displacement comparison in the y-direction	95
Figure 3.62.	Storey drift considering SSI	96
Figure 3.63.	Failure mode after considering SSI	96

LIST OF TABLES

Table 1.1.	Classification of common cement types by strength (EN 197-1:2000)	4
Table 1.2.	Properties of reinforcement (EN 1992-1-1:2004)	6
Table 1.3.	Exposure classes related to environmental conditions (EN 206-1:2006).....	9
Table 3.1.	Concrete characteristics.....	58
Table 3.2.	Longitudinal reinforcement characteristics	59
Table 3.3.	Structural loads of building	60
Table 3.4.	Non-structural loads of the building.....	60
Table 3.5.	Parameter for the computation of λ_{lim}	78
Table 3.6.	Characterisation of foundation geometry	80

TABLE OF CONTENT

DEDICATION	i
ACKNOWLEDGEMENTS	ii
GLOSSARY.....	iii
ABSTRACT.....	vi
RESUME.....	vii
LIST OF FIGURES.....	viii
LIST OF TABLES.....	xi
SOMMAIRE... ..	xii
GENERAL INTRODUCTION	1
Chapter 1. LITERATURE REVIEW	2
INTRODUCTION.....	2
1.1 GENERALITIES ON REINFORCED CONCRETE	2
1.1.1 <i>Definition of reinforced concrete</i>	2
1.1.2 <i>Components of reinforced concrete</i>	3
1.1.3 <i>Properties of reinforced concrete</i>	6
1.1.4 <i>Uses of reinforced concrete</i>	13
1.1.5 <i>Defects of reinforced concrete</i>	14
1.2 ELASTICITY AND PLASTICITY.....	17
1.2.1 <i>Elasticity</i>	17
1.2.2 <i>Plasticity</i>	17
1.2.3 <i>Differences between elastics and plastics</i>	18
1.3 METHODS OF ANALYSIS OF STRUCTURES.....	19
1.3.1 <i>Linear analysis</i>	19
1.3.2 <i>Nonlinear analysis:</i>	20
1.4 SOIL STRUCTURE INTERACTION	26
1.4.1 <i>Numerical methods in the soil structure interaction analysis</i>	26
1.4.2 <i>Effects of SSI on building performance</i>	29
CONCLUSION	33
Chapter 2. METHODOLOGY OF ANALYSIS AND DESIGN	34
INTRODUCTION.....	34
2.1 GENERAL RECOGNITION OF THE SITE.....	34

2.2	SITE VISIT.....	34
2.3	DATA COLLECTION	34
2.4	GENERAL PROCEDURE AND STANDARDS	34
2.4.1	<i>Evaluation procedure of actions on the building.....</i>	<i>35</i>
2.4.2	<i>Loads acting on the structure.....</i>	<i>35</i>
2.4.3	<i>Combination of actions.....</i>	<i>36</i>
2.5	LINEAR STATIC DESIGN METHODOLOGY	37
2.5.1	<i>Concrete cover and durability.....</i>	<i>37</i>
2.5.2	<i>Horizontal structural element design.....</i>	<i>38</i>
2.5.3	<i>Vertical structural element design.....</i>	<i>44</i>
2.5.4	<i>Footing design</i>	<i>48</i>
2.6	MODAL ANALYSIS METHODOLOGY	49
2.6.1	<i>Fundamental period of vibration.....</i>	<i>49</i>
2.6.2	<i>Vibration modes</i>	<i>49</i>
2.7	PUSHOVER ANALYSIS METHODOLOGY	49
2.8	SOIL STRUCTURE INTERACTION ANALYSIS.....	51
	CONCLUSION	52
Chapter 3.	RESULTS.....	53
	INTRODUCTION.....	53
3.1	GENERAL PRESENTATION OF THE SITE	53
3.1.1	<i>Geographic location</i>	<i>53</i>
3.1.2	<i>Geology.....</i>	<i>53</i>
3.1.3	<i>Relief.....</i>	<i>53</i>
3.1.4	<i>Climate.....</i>	<i>54</i>
3.1.5	<i>Hydrology</i>	<i>54</i>
3.1.6	<i>Population and</i>	<i>54</i>
3.1.7	<i>Socio-economic activities.....</i>	<i>54</i>
3.2	PRESENTATION OF THE PROJECT	54
3.3	PRESENTATION OF DATA COLLECTED.....	58
3.3.1	<i>Geotechnical data.....</i>	<i>58</i>
3.3.2	<i>Material properties.....</i>	<i>58</i>
3.4	ACTIONS ON THE BUILDING AND LOAD COMBINATIONS.....	59
3.4.1	<i>Permanent action</i>	<i>60</i>

3.4.2	<i>Variable actions and load combinations</i>	60
3.4.3	<i>Load combinations</i>	60
3.5	LINEAR STATIC DESIGN	61
3.5.1	<i>Durability and concrete cover to reinforcement</i>	61
3.5.2	<i>Horizontal structural component</i>	61
3.5.3	<i>Vertical structural elements</i>	71
3.5.4	<i>Footing design</i>	80
3.6	MODAL ANALYSIS	81
3.7	PUSHOVER ANALYSIS	83
3.8	ANALYSIS INCLUDING SOIL STRUCTURE INTERACTION.....	88
3.8.1	<i>Modelling including soil structure interaction</i>	88
3.8.2	<i>Time period for soil structure interaction</i>	89
3.8.3	<i>Pushover curves for soil structure interaction</i>	90
3.8.4	<i>Storey displacement for soil structure interaction</i>	94
3.8.5	<i>Storey drift considering soil structure interaction</i>	96
3.8.6	<i>Failure mode of the structure</i>	96
	CONCLUSION	97
	GENERAL CONCLUSION	98
	REFERENCES	99

GENERAL INTRODUCTION

One of the emerging fields in design of structures is the performance-based design. The subject is still in the realm of research and is only slowly emerging out into the practitioner's arena. As seen today, concrete is the most used material for construction due to its high compressive strength. Several types of concrete are seen which have different adaptations, methods of applications and strength. Structural design is slowly transforming from a stage where a linear elastic analysis for a structure was sufficient for both its elastic and ductile design, to a stage where a special dedicated non-linear procedure is to be done, which finally influences the structural behaviour as a whole. As a consequence, new structural design provisions require structural engineers to perform both static and dynamic analysis for the design of structures. The advanced calculation rules as prescribed in EN 1998 and the FEMA (Federal Emergency Management Agency) regulations provide a course of action for the achievement of a level of safety.

The primary purpose of this study is to present the elastic and plastic behaviour of a reinforced concrete building after its design through linear and non-linear methods of analysis. Using the pushover curves which gives the interaction between a particular base shear or ground force with respect to the displacement of the highest point of the buildings height.

The present study is divided into three main chapters. Chapter 1 presents the generalities on reinforced concrete from its composition to having a good mix, the structural characteristics of a building from its centres of mass and rigidity to the regularity criteria. Some examples of reinforced concrete structures accomplished in Cameroon are seen alongside these criteria. Chapter 2 discusses the methodology of analysis starting from general recognition of the site of study to running right down to the pushover analysis. Chapter 3 presents our case study which is a 6-storey irregular building, the software used, the material properties and the action on the building. The results of the analysis are presented, where the behaviour of the structure is seen and discussed.

Chapter 1. LITERATURE REVIEW

Introduction

Today, second only to water, concrete is the most consumed material, with three tons per year used for every person in the world. In this chapter we shall talk about reinforced concrete where we'll go from its definition, components, and the properties of reinforced and equally its uses in the construction domain. We'll also have an overview of the concept of elasticity and plasticity from where we'll move to the different analysis methods used in the design of concrete buildings. Pushover analysis we'll be elaborated in its fullness before closing up with soil structure interaction as we'll have the numerical methods of the the SSI and finally the effects of SSI in the performance of buildings.

1.1 Generalities on reinforced concrete

1.1.1 Definition of reinforced concrete

Reinforced concrete (RC) also called reinforced cement concrete (RCC) is a composite material in which concrete's relatively low tensile strength and ductility are counteracted by the inclusion of reinforcement having higher tensile strength or ductility. The reinforcement is usually, though not necessarily, steel reinforcing bars (rebar) and is embedded passively in the concrete before the concrete sets. Reinforcing schemes are generally designed to resist tensile stresses in some regions of the concrete that might cause unacceptable cracking and/or structural failure. The economy, the efficiency, the strength and the stiffness of reinforced concrete make it an attractive material for a wide range of structural applications. For its efficient use as structural material, concrete must satisfy the following conditions:

- (1) The structure must be strong and safe. The idea of structural collapse in buildings is due to poor dimensioning of the structure and this must be avoided.
- (2) The structure must be rigid and “appear unblemished”. Care must be taken to control deflections under service loads and to limit the crack width to an acceptable level.
- (3) The structure must be economical. Materials must be used efficiently, since the difference in unit cost between concrete and steel is relatively large.

1.1.2 Components of reinforced concrete

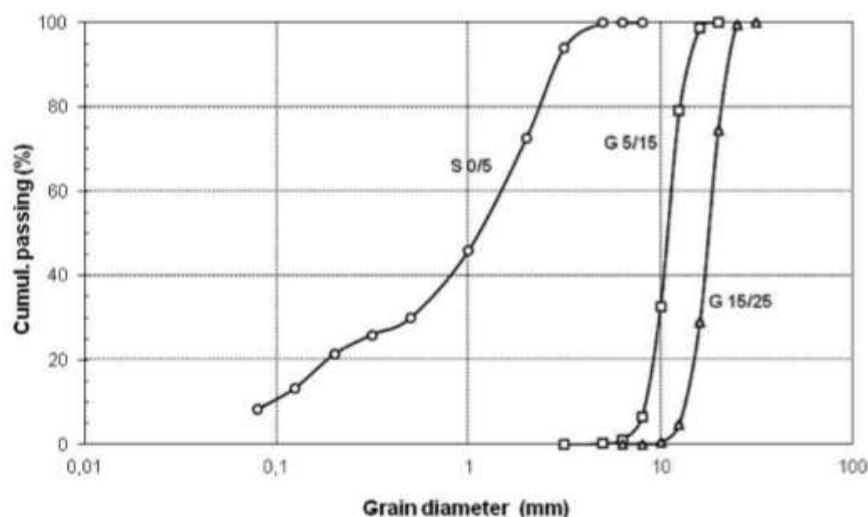
The main components of reinforced concrete are concrete and steel. As contrast to normal concrete, steel is embedded in reinforced concrete to add more strength and ductility making it capable of resisting any design loads applied to it.

1.1.2.1 Concrete components

Concrete, usually **Portland cement concrete** is a composite material composed of fine and coarse aggregate bonded together with a fluid cement paste that hardens over time. The factors which have the greatest effect upon the strength of concrete are the cement-to-aggregate ratio, the compaction, the water-to-cement ratio or the mix, and the method of curing. The component of concrete are aggregates, cement, water and admixtures.

a. Aggregates

Aggregates are a broad category of fine to coarse grained particle materials used in construction, including sand, gravel, crushed stone, slag, recycled concrete and geosynthetic aggregates. This mixture of grains ranges from 0 to 125mm. Aggregates occupy more than 70% of concrete volume and intervene directly on its properties of dried concrete as well as wet (Mbessa, 2000). Their availability in nature and consequently its relatively low cost gives it an advantage both economically and mechanically (Dreux & Festa, 1998). The range of particle sizes in aggregate is illustrated in Figure 1.1.



Particle size distribution curves of sand and gravel (Makhloufi et al. 2014)

b. Cement

Cement is a binder, a substance used for construction that sets, hardens, and adheres to other materials to bind them together. Cement mixed with fine aggregate produces mortar for masonry, or with sand and gravel, produces concrete. The 27 products in the family of common cements, covered by EN 197-1, they are grouped into five main cement types as follows:

- CEM I Portland cement
- CEM II Portland-composite cement
- CEM III Blast-furnace cement
- CEM IV Pozzolanic cement
- CEM V Composite cement

The standard strength of a cement is the compressive strength determined in accordance with EN 196-1 at 28 days of maturation and is shown in table 1.1.

Table 1.1. Classification of common cement types by strength (EN 197-1:2000)

Strength class	Characteristic compressive strength (N/mm ²)	Absolute minima (N/mm ²)		Characteristic 28-day compressive strength (N/mm ²)		Absolute minima (N/mm ²) 28 days
		7 days	2/7 days	Minimum	Maximum	
32.5N	-	≥16	≥14	32.5	52.5	≥30.0
32.5R	≥10	-	≥8			
42.5N	≥10	-	≥8	42.5	62.5	≥40.0
42.5R	≥20	-	≥8			
52.5N	≥20	-	≥18	52.5	-	≥50.0
52.5R	≥30	-	≥28		-	

Where,

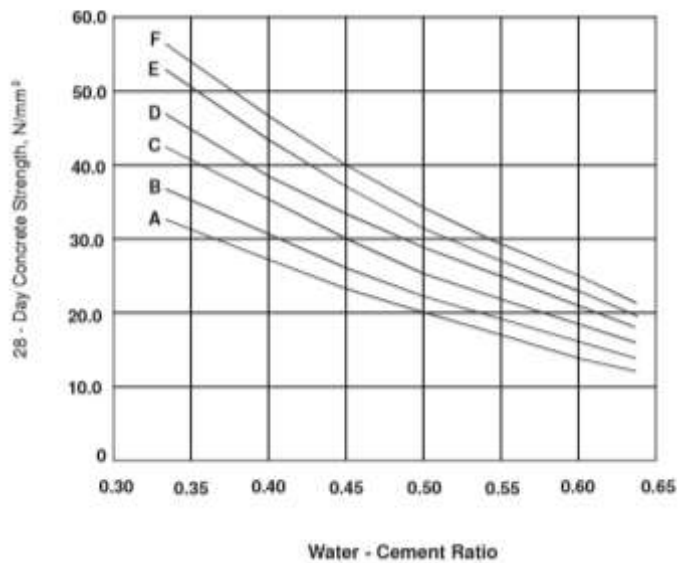
N: Normal (subclass; indicates the rate of early strength development)

R: Rapid

c. Water

It takes about 35% water for the cement to be hydrated. The excess contributes more or less to the manoeuvrability (workability) than to the decrease in resistance; Resistance and manoeuvrability evolve concomitantly (the more manoeuvrability increases, the more resistance

decreases). Water to cement ratio is the single most important factor governing the strength and durability of concrete (Durocrete 2013). Figure 1.2 shows the strength of a concrete with different water to cement ratio.



Water/cement ratio for different compressive strength (<http://www.google.cm>)

d. Admixtures

Admixtures are those ingredients in concrete other than cement, water, and aggregates that are added to the mixture immediately before or during mixing (Kosmatka et al. 2003). The amount of admixture recommended by the manufacturer or the optimum amount determined by laboratory tests should be used. Admixtures can be classified into many functions such as:

1. Air-entraining and water-reducing admixtures
2. Plasticizers
3. Accelerating and Retarding admixtures and many others.

1.1.2.2 Reinforcing Steel

Steel reinforcement bar, also known as rebar (reinforcing bar, and reinforcing steel) is a steel bar or mesh of steel wires used as tension device in reinforced concrete and reinforced masonry structures to strengthen and aid the concrete under tension. Steel is also considered an ideal material for carrying out seismic resistant construction due to its ductility and high energy absorption capacity. Concrete (Rafi et al., 2013) is a weak material in tension and cracks when local tensile stresses exceed its tensile strength. Consequently, concrete is reinforced to enable it to resist these stresses. According to Annex C, the design rules in EN 1992 are applicable to steel reinforcement

with characteristic yield strength in the range 400–600 N mm⁻². The properties of reinforcement steel is shown in Table 1.2 as given in Eurocode.

Table 1.2. Properties of reinforcement (EN 1992-1-1:2004)

Product form	Bars and De-coiled rods			Wire fabrics		
Class	A	B	C	A	B	C
Characteristic yield strength f_{yk} or $f_{0.2k}$ (N/mm ²)	400-600					
$k = (f_t/f_y)_k$	≥1.05	≥1.08	≥1.15 <1.35	≥1.05	≥1.08	≥1.15 <1.35
Characteristic strain at maximum force ϵ_{uk} (%)	≥2.5	≥5.0	≥7.5	≥2.5	≥5.0	≥7.5
Bendability	Bend/Re-bend test					
Maximum bar size deviation from normal mass (%)				± 6.0		
				±4.5		

1.1.3 Properties of reinforced concrete

The two main constituents of reinforced concrete are, the concrete itself and then the reinforcing steel members. Their properties are allowed separately as follows

1.1.3.1 Properties of concrete

The concrete which is greater in volume in the heterogeneous mixture of reinforced concrete will be outlined here in its strength, durability and then its stress-strain relationship

a. Strength

Among all the characteristics of the material, the most common factor used to measure concrete quality is its compressive strength. It is the fundamental parameter, which allows identifying the concrete class of resistance.

It is defined, in accordance with EN 206-1, by the characteristic value f_{ck} (5% fractile of distribution) obtained through the elaboration of compression tests executed at 28 days on cylindrical specimens of diameter 150mm and height 150mm as shown in figure 1.3. It can also be defined by another characteristic value $f_{ck,cube}$. They are both recognized and they are related by the following expression, described in Eurocode 2:

$$f_{ck} = 0.83 f_{ck,cube} \quad \text{Eq. 1.1}$$

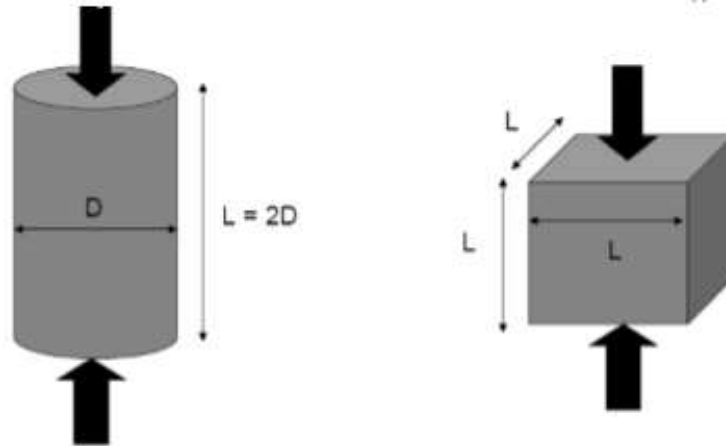
The design compressive strength of concrete, f_{cd} , used in design to Eurocode 2 is taken as:

$$f_{cd} = \alpha_{cc} f_{ck} / \gamma_c \quad \text{Eq. 1.2}$$

Where f_{ck} = characteristic cylinder compressive strength of concrete at 28 days,

γ_c = partial (safety) factor for concrete (1.5)

α_{cc} = a coefficient to allow for long term and loading effects (0.85).



Cylinder and cubic specimens in compressive strength evaluation (EN 1992-1-1:2004)

The different strength of concrete class is depicted in figure 1.4.

Strength classes for concrete															Analytical relation / Explanation
f_{ck} (MPa)	12	18	20	25	30	35	40	45	50	55	60	70	80	90	
$f_{ck,cube}$ (MPa)	15	20	25	30	37	45	50	55	60	67	75	85	95	105	
f_{cm} (MPa)	20	24	28	33	38	43	48	53	58	63	68	78	88	98	$f_{cm} = f_{ck} + 8$ (MPa)
f_{ctm} (MPa)	1,6	1,9	2,2	2,6	2,9	3,2	3,5	3,8	4,1	4,2	4,4	4,6	4,8	5,0	$f_{ctm} = 0,30 + f_{cm}^{(0,7)} \leq C50/60$ $f_{ctm} = 2,12 \cdot \ln(1 + (f_{cm}/10)) \leq C50/60$
$f_{ctk,0,05}$ (MPa)	1,1	1,3	1,5	1,8	2,0	2,2	2,5	2,7	2,9	3,0	3,1	3,2	3,4	3,5	$f_{ctk,0,05} = 0,7 \cdot f_{ctm}$ 5% fractile
$f_{ctk,0,95}$ (MPa)	2,0	2,5	2,9	3,3	3,8	4,2	4,6	4,9	5,3	5,5	5,7	6,0	6,3	6,6	$f_{ctk,0,95} = 1,3 \cdot f_{ctm}$ 95% fractile
E_{cm} (GPa)	27	29	30	31	33	34	35	36	37	38	39	41	42	44	$E_{cm} = 22 \cdot (f_{cm}/10)^{1,3}$ (f_{cm} in MPa)
ϵ_{cu1} (‰)	1,8	1,9	2,0	2,1	2,2	2,25	2,3	2,4	2,45	2,5	2,6	2,7	2,8	2,8	see Figure 3.2 $\epsilon_{cu1}(f_{ck}) = 0,7 \cdot f_{cm}^{-0,31} \approx 2,8$
ϵ_{cu1} (‰)	3,5								3,2	3,0	2,8	2,8	2,8	see Figure 3.2 for $f_{ck} \geq 50$ Mpa $\epsilon_{cu1}(f_{ck}) = 2,8 + 27 / (98 - f_{ck}) \cdot \sqrt{100}^4$	
ϵ_{cu2} (‰)	2,0								2,2	2,3	2,4	2,5	2,6	see Figure 3.3 for $f_{ck} \geq 50$ Mpa $\epsilon_{cu2}(f_{ck}) = 2,0 + 0,085 \cdot (f_{ck} - 50)^{0,85}$	
ϵ_{cu2} (‰)	3,5								3,1	2,9	2,7	2,8	2,8	see Figure 3.3 for $f_{ck} \geq 50$ Mpa $\epsilon_{cu2}(f_{ck}) = 2,6 + 35 \cdot ((90 - f_{ck}) / 100)^4$	
n	2,0								1,75	1,6	1,45	1,4	1,4	for $f_{ck} \geq 50$ Mpa $n = 1,4 + 23,4 \cdot ((90 - f_{ck}) / 100)^4$	
ϵ_{cu3} (‰)	1,75								1,8	1,9	2,0	2,2	2,3	see Figure 3.4 for $f_{ck} \geq 50$ Mpa $\epsilon_{cu3}(f_{ck}) = 1,75 + 0,55 \cdot (f_{ck} - 50) / 40$	
ϵ_{cu3} (‰)	3,5								3,1	2,9	2,7	2,8	2,8	see Figure 3.4 for $f_{ck} \geq 50$ Mpa $\epsilon_{cu3}(f_{ck}) = 2,6 + 35 \cdot ((90 - f_{ck}) / 100)^4$	

Strength class and deformation for concrete (EN 1992-1-1:2004)

The tensile strength is determined by the tensile splitting test, EN 1992-1-1 permits the axial tensile strength to be calculated, from the tensile splitting strength, and it is taken as

$$f_{ct} = 0,90 f_{ct,sp} \tag{Eq. 1.3}$$

For normal structural uses, the mean axial tensile strength, f_{ctm} , is related to the characteristic cylinder strength by the equations. For compressive strength classes $\leq C50/60$

$$f_{ctm} = 0,3 \cdot f_{ck}^{2/3} \tag{Eq. 1.4}$$

The value of the design tensile strength, f_{ctd} , is defined as

$$f_{ctd} = \alpha_{ct} f_{ctk} \frac{0,05}{\gamma_c} \tag{Eq. 1.5}$$

Where f_{ck} = characteristic tensile strength of concrete at 28 days,

γ_c = partial (safety) factor for concrete

α_{ct} = a coefficient to allow for long term and loading effects (0.85).

b. Durability

(J. Gonzalez 2018) defined durability as the conservation of the physical and mechanical characteristics of the structure and the materials with which the structures are constructed. One of the main properties of concrete is its ability to be durable. By (Mosley et al. 2007), the durability of concrete is affected by factors such as:

- The exposure conditions;
- The cement type;
- The concrete cover reinforcement

Exposure conditions are chemical and physical conditions to which the structure is exposed in addition to the mechanical actions and are illustrated in table 1.3.

Table 1.3. Exposure classes related to environmental conditions (EN 206-1:2006)

Exposure classes	Description of the environment	Informative examples where exposure classes may occur
XF1	Moderate water saturation, without de-icing agent	Vertical concrete surfaces exposed to rain and freezing
XD2	Wet, rarely dry	Concrete components exposed to industrial waters containing chlorides
XC3	Moderate humidity	Concrete inside buildings with moderate or high air humidity External concrete sheltered from rain
XC4	Cyclic wet and dry	Concrete surfaces subject to water contact, not within exposure class XC2

The nominal cover to reinforcement, c_{nom} , is obtained from the minimum cover, c_{min} , by adding an allowance for likely deviations during construction, Δc_{dev}

$$c_{nom} = c_{min} + \Delta c_{dev} \quad \text{Eq. 1.6}$$

The recommended value of Δc_{dev} for reinforced concrete is normally taken as 10 mm

The minimum cover to reinforcement c_{min} is given by the following expression

$$c_{min} = \max\{c_{min,dur}; c_{min,b}; 10 \text{ mm}\} \quad \text{Eq. 1.7}$$

Where

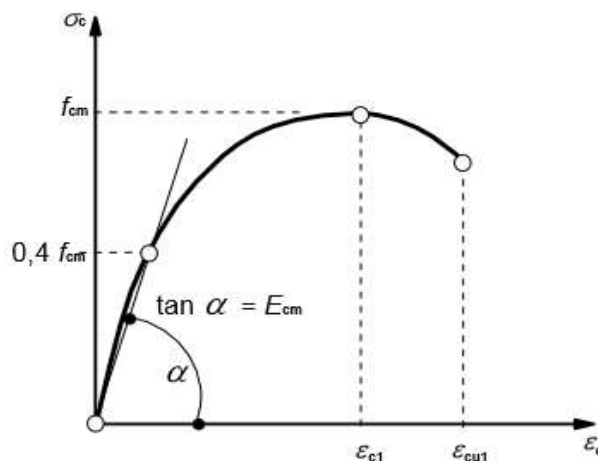
$C_{min,dur}$ is the minimum cover for durability

$C_{min,b}$ is the minimum cover for bond

Values of minimum cover, $C_{min,dur}$, requirements with regard to durability for reinforcement steel and prestressing steel is chosen in accordance with EN 1992-1-1:2004

c. Stress- strain relation for nonlinear structural analysis

Like many other structural materials, concrete is, to a certain degree, elastic. A material is said to be perfectly elastic if strain appears and disappears immediately on application and removal of stress. Stress strain curve of concrete is a graphical representation of concrete behaviour under load, as shown in figure 1.5 below. It is produced by plotting concrete compress strain at various interval of concrete compressive loading (stress).



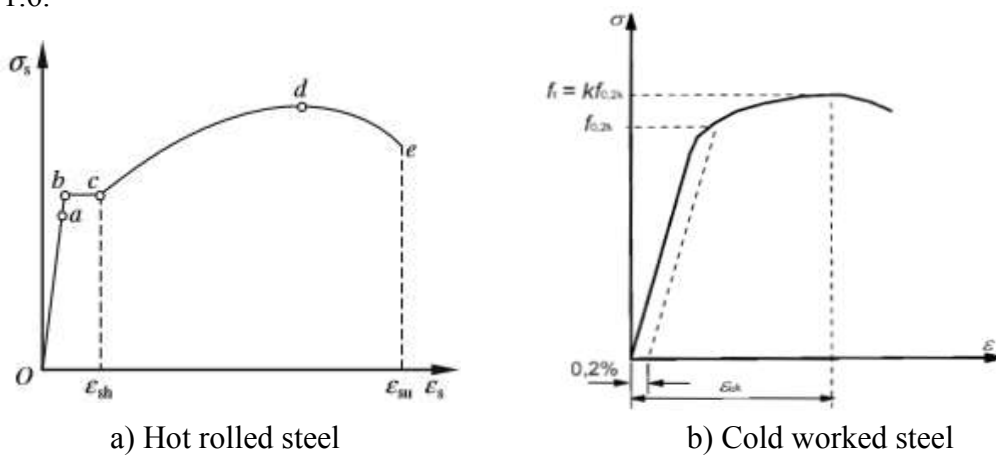
Stress Strain Curve for concrete under compression (EN 1992-1-1:2004)

Concrete has a non-linear behaviour both in tension and compression. This behaviour results from progressive micro cracking, which begins on the interface between coarse aggregate and cement paste and spreads to the whole concrete with time.

1.1.3.2 Properties of the reinforcing steel

a. Strength

Concrete is a weak material in tension and cracks when local tensile stresses exceed its tensile strength. Consequently, concrete is reinforced to enable it to resist these stresses. Reinforcing steel must be strong in tension and, at the same time, be ductile enough to be shaped or bent cold. The application rules for design and detailing in Eurocode are valid for a specified yield strength range, $f_{yk} = 400$ to 600 N/mm². The grade of reinforcement steel denotes the specified characteristic yield stress (f_{yk}). The stress-strain diagram for both hot rolled steel and cold worked steel is shown in figure 1.6.



Stress-strain diagrams for reinforcing steel (EN 1992-1-1:2004)

The curves exhibit an initial linear elastic portion. The stress at point **bc** is called the yield strength. The stress corresponding to the highest point is the ultimate strength of steel bars. Segment **cd** is the strain-hardening range. After point **d**, the strain increases rapidly accompanied by the area reduction of the weakest section, i.e. necking, and finally fracture occurs at point **e**.

b. Ductility

Designing structures to remain elastic in large earthquakes is likely to be uneconomic as the force demands will be very large. A more economical design can be achieved by accepting some level of damage short of complete collapse and making use of the ductility of the structure to reduce the force demands to acceptable levels. Ductility is defined as the ability of a structure or member to withstand large deformations beyond its yield point without fracture and can be expressed in terms of the maximum imposed deformation. The displacement ductility factor is

$$\mu = \Delta_{max} / \Delta_y \quad \text{Eq. 1.8}$$

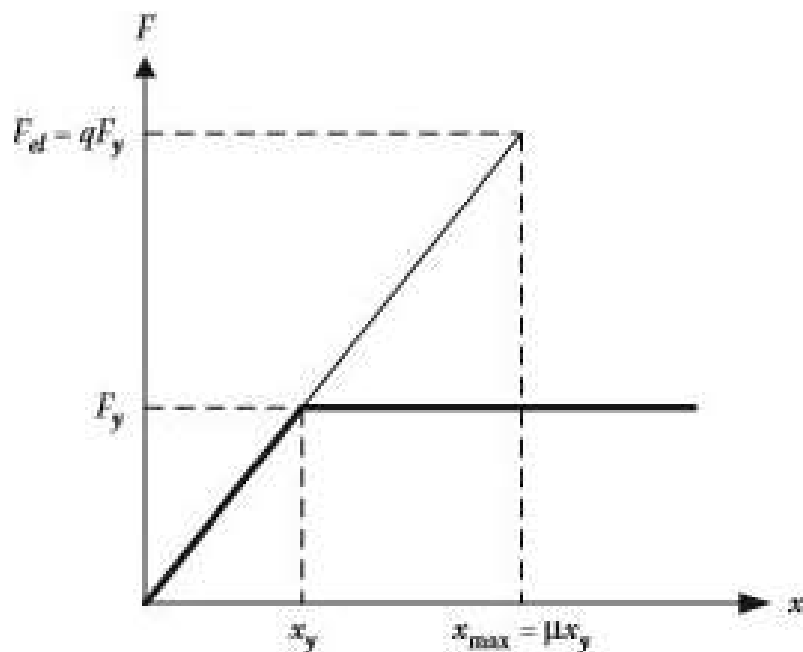
Where, Δ_{max} is the maximum displacement and

Δ_y is the displacement at yield

Ductility characterizes the deformation capacity of members after yielding, or their ability to dissipate energy. Yielding of a structure also has the effect of limiting the peak force that it must sustain. In EC8, this force reduction is quantified by the behaviour factor, q

$$q = \frac{F_{el}}{F_y} \quad \text{Eq. 1.9}$$

Where F_{el} is the peak force, and F_y is the yield load of the system. Figure 1.7 shows the ductility and behaviour factor of a system.



Equivalence of ductility and behaviour factor (Ahmed Y. 2016)

The reinforcement shall have adequate ductility as defined by the ratio of tensile strength to yield stress (f_t/f_{yk}) and elongation (ϵ_{uk}) at maximum force. With reference to the ultimate strain of the material, three ductility classes are distinguished:

- Class A (Low ductility) with $\epsilon_{uk} \geq 2.5\%$ $f_t/f_{yk} \geq 1.05$
- Class B (Normal ductility) with $\epsilon_{uk} \geq 5.0\%$ $f_t/f_{yk} \geq 1.08$
- Class C (High ductility) with $\epsilon_{uk} \geq 7.5\%$ $f_t/f_{yk} \geq 1.15 = 7,5$

1.1.4 Uses of reinforced concrete

CIM BÉTON experts in one of their technical sheets entitled " Les bétons: formulation, fabrication et mise en œuvre " divided the use of concrete into two major areas of construction which are buildings and public works.

1.1.4.1 Buildings

Concrete plays an essential role in modern urban planning. This seems normal when considering its use in the construction of dwellings (for the construction of walls, structural elements and for floors, concrete is practically the ideal material). Concrete has also been heavily established in the construction of other buildings such as offices, hospitals, premises, as well as large public buildings and industrial buildings.

1.1.4.2 Bridges

Technological advances and, in particular, the evolution of concrete characteristics, allow ranges of up to several hundred meters to be achieved.

1.1.4.3 Tunnels

For large tunnels whose examples are multiplying in the world, concrete is either poured on site or used in prefabricated voussoirs. These are laid to the advancement of the tunnelling machine.

1.1.4.4 Dams

Large dams are most often made of concrete, allowing settlements in the most difficult sites.

1.1.4.5 Roads

Concrete pavement is becoming increasingly important in major road and motorway roads, thanks to the development of modern techniques such as continuous reinforced concrete, thick slabs, surface treatment, low-traffic roads and urban development, show a renewed interest in concrete solutions, which ensure them durability and low maintenance costs.

1.1.4.6 Other works

It is also important to mention unusual structures: offshore structures or nuclear power plants, whose requirements require concretes with high mechanical characteristics and durability.

1.1.5 Defects of reinforced concrete

Like any other material, concrete is subjected to chemical attack by an aggressive environment or suffers some physical damage. Serious carbonation, alkali aggregate reaction, chemical attack on the concrete, cracking, spalling and honeycombing due to poor-quality materials or workmanship, and/or corrosion of the reinforcement are all signs of distress that indicate a concrete of low durability.

1.1.5.1 Cracking

Cracks in concrete occur as a result of tensile stresses introduced in the concrete. The crack widths and distribution is controlled by the reinforcement in reinforced and prestressed concrete, whereas in plain concrete there is no such control.

1.1.5.2 Spalling

In spalling large chunks of concrete separate from the parent member. This indicates a severe weakness in some parts or the entire project. It is more likely to happen during freeze thaw conditions. Spalling is a continuation of the delamination process which is caused by the actions of external loads, pressure exerted by the corrosion of reinforcement or by the formation of ice in the delaminated area results in the breaking off of the delaminated concrete. The spalled area left behind is characterized by sharp edges as shown in figure 1.9.



Flexural cracks in RC beams (Haseeb Jamal, 2018)

1.1.5.3 Honeycombing

Honeycombing occurs due to the improper or incomplete vibration of the concrete which results in voids being left in the concrete where the mortar failed to completely fill the spaces between the coarse aggregate particles (figure 1.10).



Honey combing in concrete (Haseeb Jamal, 2018)

1.1.5.4 Scaling

Scaling is a defect in concrete in which local flaking, or loss of the surface portion of concrete or mortar as a result of the freeze-thaw deterioration of concrete occurs. Scaling is common in non-air-entrained concrete, but can also occur in air-entrained concrete in the fully saturated condition. Scaling is prone to occur in poorly finished or overworked concrete where too many fines and not enough entrained air is found near the surface.

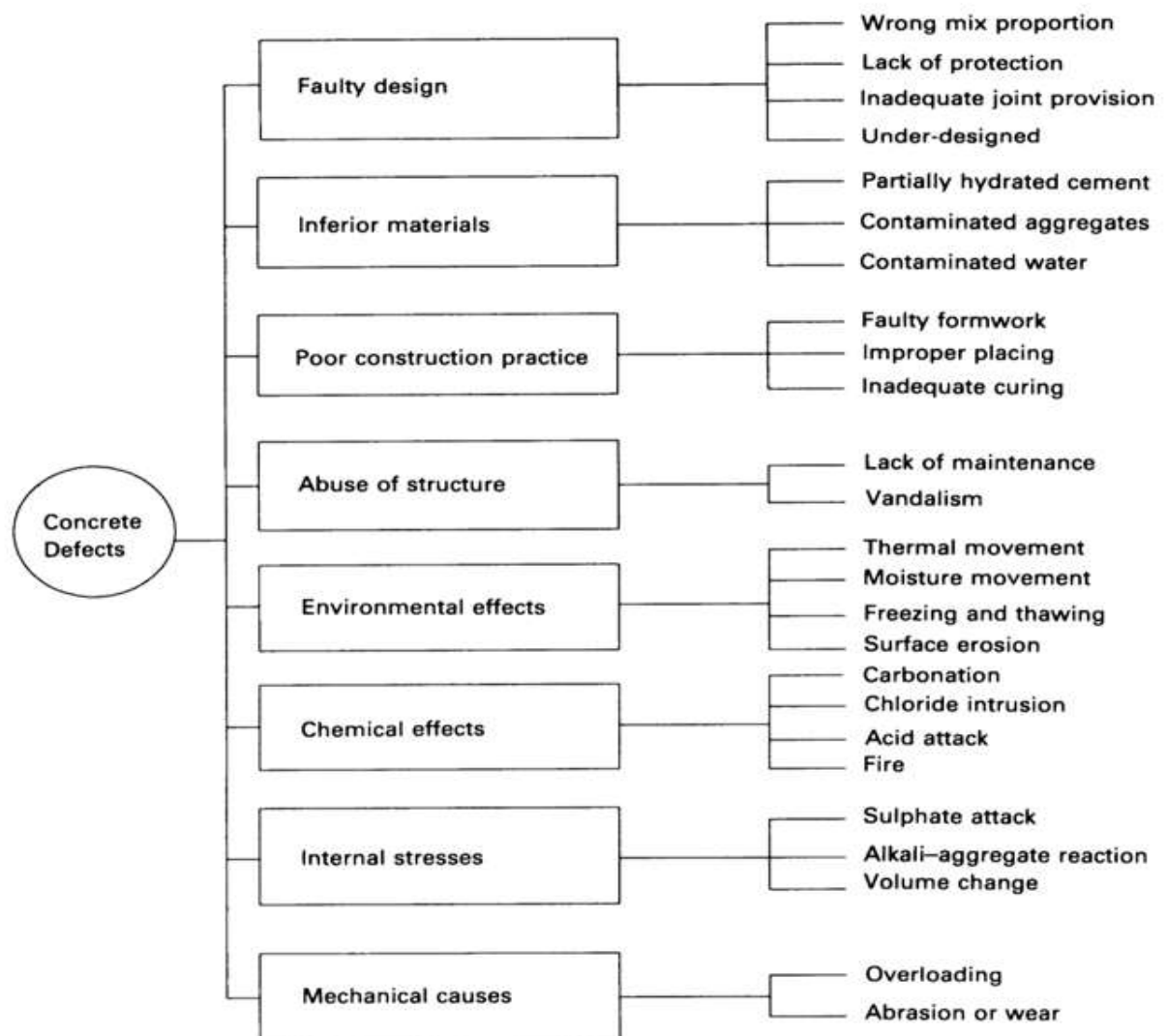
1.1.5.5 Delamination

Delamination is a defect in hardened concrete which is defined as a discontinuity of the surface concrete which is substantially separated but not completely detached from concrete below or above it. Visibly, it may appear as a solid surface but can be identified as a hollow sound by tapping or chain dragging. Delamination begins with the corrosion of reinforcement and subsequent cracking of the concrete. However, in the case of closely spaced bars, the cracking extends in the plane of the reinforcement parallel to the exterior surface of the concrete. Delamination or debonding may also occur in concrete that has been patched or overlaid due to the continued deterioration of the older concrete. This may happen even in the absence of any rusting of reinforcing steel.

1.1.5.6 Alkali aggregate reaction

Chemical attack can occur because concrete is alkaline and chemically reactive. It can be attacked by acids; some alkalis; numerous salt solutions; and organics such as fermenting liquids, sugars, and animal oils, especially if they contain free acids. Seawater will attack concrete. Corrosive solutions penetrating to the steel reinforcing rods may be particularly destructive because the large displacement of the corrosion products of the steel can cause cracking and spalling of the concrete.

A summary of concrete defects is shown on figure 1.10 (L. H. Son et al, Building Maintenance Technology 1993).



Factors affecting concrete durability (L. H. Son et al., 1993)

1.2 Elasticity and plasticity

When a force is exerted on a body, that body undergoes a deformation which is directly proportional to the applied force. This deformation can either be elastic or plastic.

1.2.1 Elasticity

Elasticity is a property of a material to be flexible or buoyant in nature. When an external force is applied to a body, the body falls apart. This happens because the distance between the lattice atoms increases and each atom tries to pull its neighbour closer to itself. The pull creates a force in the material which tries to resist the deformation. This force is termed as strain, and the deforming force is termed as stress. Although, it is a reversible property, there is a limit to the magnitude of the force which is applied to the body. This limit is called the elastic limit of a body.

The ‘elastic limit’ of a body is defined as the maximum extent to which a solid may be stretched without permanent deformation. This property can be easily explained on the basis of Hooke’s law. The law states that, the elasticity of that material depends on the ratio of the stress and strain acting on the body.

Which means, if the applied stress is linear or equal to the strain on the body, then body is under elastic limit, and is elastic in nature. But, when the force or stress on the body increases and the elastic limit is broken, the body becomes deformed and turns plastic in nature. This limit is known as the yield strength of the material, wherein an elastic body turns plastic in nature.

1.2.2 Plasticity

Plasticity is defined as the ability of a body to change its shape and size permanently, when an external force is applied. In a plastic body, when a force is applied, from the many layers of atoms, two of these layers slide from their crystal planes, and lose their elastic limit, which causes the deformation in the body.

Based on the above explanation, one can say that a change in these properties only happen, when a body undergoes elastic deformation to enter plastic deformation. Thus, it can be said that both these properties are inter-related. Further differences between the two can be read in the table below.

1.2.3 Differences between elastics and plastics

	Plastic	Elastic
Definition	The property on account of which a body does not regain its original size and shape on removal of applied force is called as plastic body.	The property on account of which a body regains its original size and shape on removal of external deforming force is called as elastic body.
Process	It is irreversible.	It is reversible.
Ductility	They are highly ductile in nature.	It is less ductile in nature.
Resilience	They have low yield strength.	They have high yield strength.
Modulus of elasticity (ratio)	The ratio of stress to strain is high.	The ratio of stress to strain is low or equal.
Toughness	They do not have the ability to absorb energy up to a fracture.	They have the ability to absorb energy up to a fracture.
Bonds	The molecular bonds are fractured.	The molecular bonds do not get fractured.
Shape and size	The shape and size changes permanently.	The shape and size does change permanently,
Example	Plasticine.	Rubber.

1.3 Methods of analysis of structures

There are two (2) main methods of analysis which are the linear and non-linear analysis which come from the variation of strain with respect to stress. These methods are further broken into either static or dynamic.

1.3.1 Linear analysis

Linear simply means that there is a linear relationship between the deformations (strain) of the body under a particular applied force (stress)

1.3.1.1 Linear static analysis (equivalent static analysis):

A linear static analysis is an analysis where a linear relation holds between applied forces and displacements. In practice, this is applicable to structural problems where stresses remain in the linear elastic range of the used material. In a linear static analysis the model's stiffness matrix is constant, and the solving process is relatively short compared to a nonlinear analysis on the same model. Therefore, for a first estimate, the linear static analysis is often used prior to performing a full nonlinear analysis.

In this analysis, an array of forces is used to represent the consequence of earthquake ground motion. It follows the assumption that the building is responsive in its fundamental mode. This is applicable for low rise building and the building which do not rotate significantly about its axis. Further researches have been made to increase its application to high rise buildings and low level of rotation about its axis.

1.3.1.2 Linear dynamic analysis (response spectrum of analysis):

In circumstances where structures are either too irregular or too tall, the response spectrum analysis is no longer applicable and more complex analysis is often required, such as non-linear static analysis or dynamic analysis. This analysis can be performed either by mode superposition method or response spectrum method and elastic history time method. This analysis generates higher vibration modes and actual distribution of forces in the elastic range in a good way. The difference between Linear Static Analysis and Dynamic Static analysis is the force distribution along the height of the structure and the level of force. Apart from this, the response of the structure to ground motion is calculated in the domain of time, and hence all phase information is maintained.

The response spectrum analysis is carried out when modes other than the fundamental one significantly affect the response of the structure. Here, the response of Multiple-Degree-of-

Freedom System (MDOF) is represented as the superposition of modal response where each modal response is determined from the spectral analysis of Single-Degree-of-Freedom-System (SDOF). All these are then amalgamated to calculate the total response.

1.3.2 Nonlinear analysis:

A nonlinear analysis is an analysis where a nonlinear relation holds between applied forces and displacements. Nonlinear effects can originate from geometrical nonlinearity's (i.e. large deformations), material nonlinearity's (i.e. elasto-plastic material), and contact. These effects result in a stiffness matrix which is not constant during the load application. This is opposed to the linear static analysis, where the stiffness matrix remained constant. As a result, a different solving strategy is required for the nonlinear analysis and therefore a different solver.

Modern analysis software makes it possible to obtain solutions to nonlinear problems. However, experienced skill is required to determine their validity and these analyses can easily be inappropriate. Care should be taken to specify appropriate model and solution parameters. Understanding the problem, the role played by these parameters and a planned and logical approach will do much to ensure a successful solution.

The source of this nonlinearity can be attributed to multiple system properties, for example, materials, geometry, nonlinear loading and constraints.

1.3.2.1 Non-linear static analysis (pushover analysis):

It is an improvement of linear static or dynamic analysis as it allows the inelastic behaviour of the structure. But one thing is unchanged as it assumes a set of static incremental lateral load over the height of the structure. This analysis is also known as “pushover analysis”. A pattern of forces is applied to a structural model including non-linear properties and the total force is plotted with reference to displacement to depict a capacity curve. This can then be combined with a demand curve (typically in the form of an Acceleration-Displacement Response Spectrum (ADRS)) hence reducing the problem to an SDOF System. Moreover, this analysis is simpler, gives information on strength, deformation, ductility and the distribution of demands. Along with advantages it has some limitation like it neglects the variation in loading patterns and also the effect of resonance and higher modes influence on buildings.

a) Objectives and definition of pushover analysis

One of the emerging fields in seismic design of structures is the Performance Based Design. The subject is still in the realm of research and academics, and is only slowly emerging out into

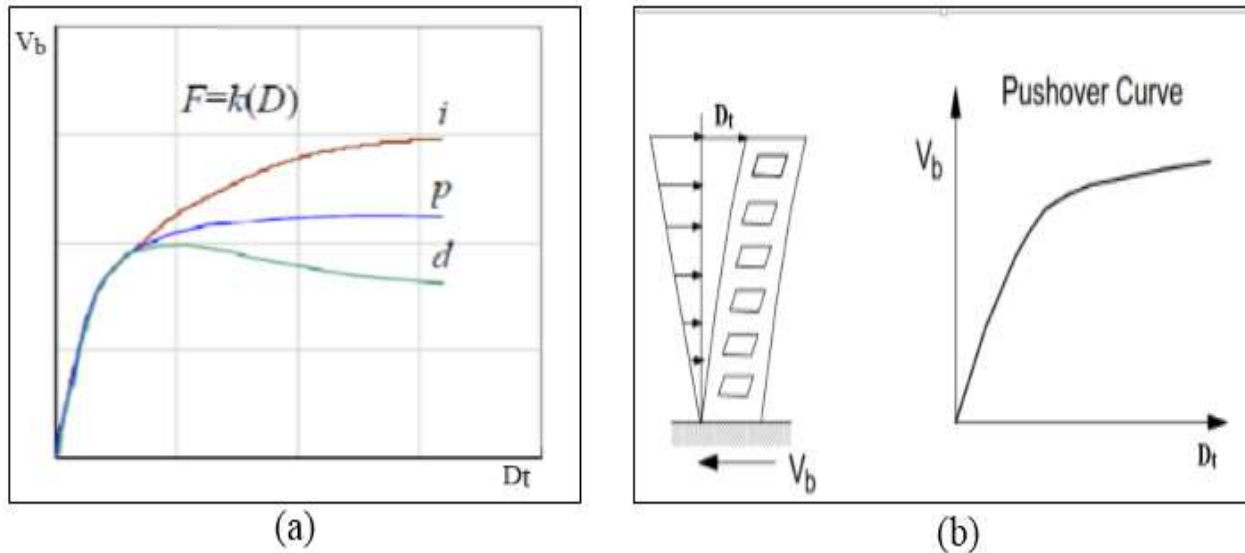
the practitioner's arena. Seismic design is slowly transforming from a stage where a linear elastic analysis for a structure was sufficient for both its elastic and ductile design, to a stage where a special dedicated non-linear procedure is to be done, which finally influences the seismic design as a whole. The basis for the linear approach lies in the concept of the Response Reduction factor R . When a structure is designed for a Response Reduction factor of, say, $R = 5$, it means that only 1/5th of the seismic force is taken by the Limit State capacity of the structure. Further deflection is in its ductile behaviour and is taken by the ductile capacity of the structure. In Reinforced Concrete (RC) structures, the members (i.e. beams and columns) are detailed such as to make sure that the structure can take the full impact without collapse beyond its Limit State capacity up to its ductile capacity. In fact we never analyse for the ductile part, but only follow the reinforcement detailing guidelines for the same. The drawback is that the response beyond the limit state is neither a simple extrapolation, nor a perfectly ductile behaviour with predeterminable deformation capacity. This is due to various reasons: the change in stiffness of members due to cracking and yielding, P-delta effects, change in the final seismic force estimated, etc. Although elastic analysis gives a good indication of elastic capacity of structures and shows where yielding might first occur, it cannot account for redistribution of forces during the progressive yielding that follows and predict its failure mechanisms, or detect possibility and location of any premature failure. A non-linear static analysis can predict these more accurately since it considers the inelastic behaviour of the structure. It can help identify critical members likely to reach critical states during an earthquake for which attention should be given during design and detailing.

The need for a simple method to predict the non-linear behaviour of a structure under seismic loads saw light in what is now popularly known as the Pushover Analysis (PA). It can help demonstrate how progressive failure in buildings really occurs, and identify the mode of final failure. Putting simply, PA is a non-linear analysis procedure to estimate the strength capacity of a structure beyond its elastic limit (meaning Limit State) up to its ultimate strength in the post-elastic range. In the process, the method also predicts potential weak areas in the structure, by keeping track of the sequence of damages of each and every member in the structure (by use of what are called 'hinges' they hold).

According to Mouzzoun et al. (2013), pushover analysis is an analysis method in which the structure is subjected to monotonically increasing lateral forces with an invariant height-wise distribution until a target displacement is reached. Pushover analysis consists of a series of sequential elastic analyses, superimposed to approximate a force-displacement curve of the overall structure.

b) Outcome of the pushover analysis:

The aim result of a pushover analysis is the definition of the so called “capacity curve “ or pushover curve , that is the relationship between force and displacement of the studied structure, generally expressed in terms of base shear (V_b) and top displacement (D_t).



Capacity curves for: SDOF system (a), (Roberta, 2010), MDOF system (b) (Chopra et al., 2004)

In the figure 1.11(a), it is plotted for a SDOF, the force-displacement relationships of three behaviours characterized by an initial linear elastic performance to the threshold yield (Linear portion of curve) followed by a post-critical non-linear behaviour which can be: hardening (i), perfect (p) and degrading (d). Each point of the capacity curve defines a specific state of structural damage.

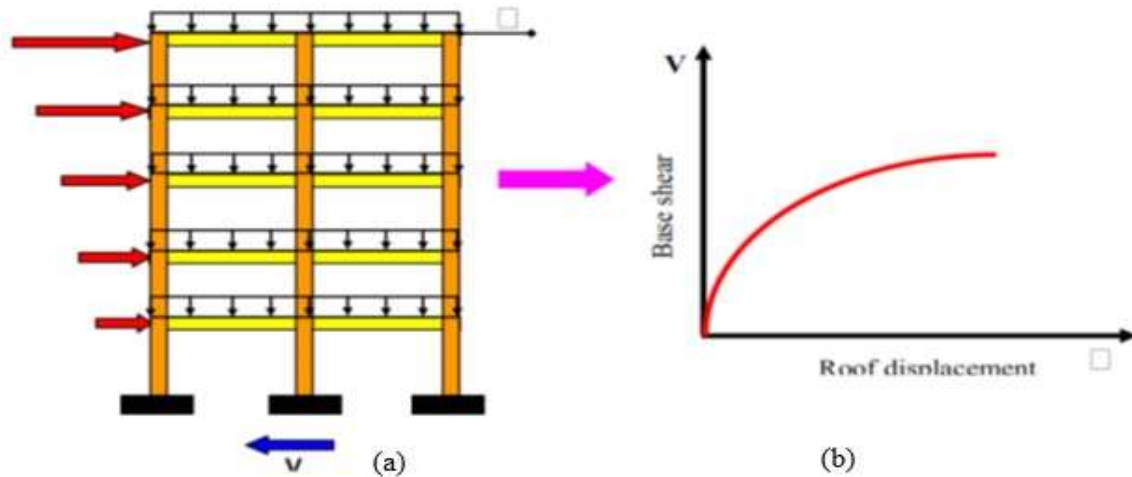
c) Application field of pushover analysis.

The pushover analysis is very useful in estimating several characteristic of the structure such as:

- The capacity of the structure (represented by the base shear versus roof- displacement graph, see Figure 1.12b);
- The maximum rotation and ductility of critical members load;
- The distribution of plastic hinges at the ultimate load;
- The distribution of damage in the structure, as expressed in the form of load damage indices, at the ultimate load;
- The yield lateral resistance of the structure;
- Estimates of understory drifts and its distribution along the building height;

- Determination of force demands on members, such as axial force demands on columns, moment demands on beam-column connections;
- To assess the structural performance of existing or retrofitted buildings.

Pushover analysis can also serve as a compromise between the design based on time history analysis (accurate, complex and time consuming) and linear analysis (less occurred, less complex) (Mouzzoun et al., 2013).



Typical pushover curve (Mouzzoun et al., 2013)

1.3.2.2 Non-linear dynamic analysis:

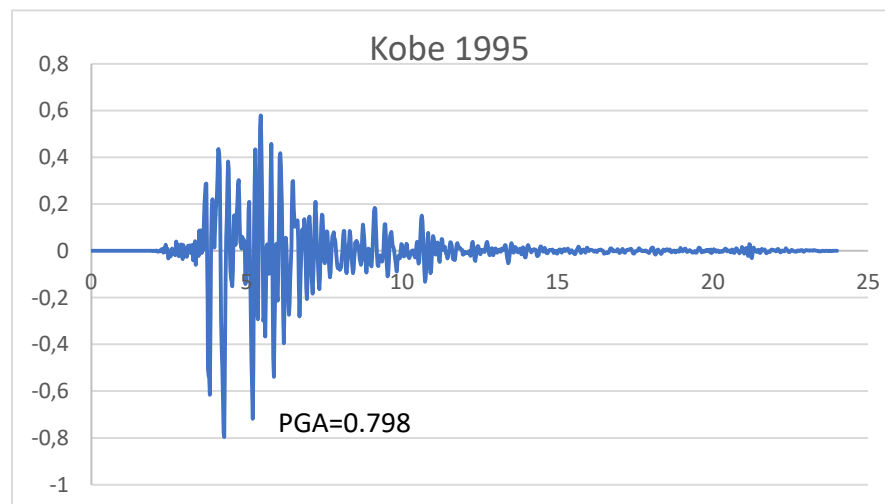
The non-linear time history analysis (NLTHA) provides a more realistic model of structural response to ground shaking. In fact, it provides a more reliable assessment of earthquake performance than non-linear static analysis. Non-linear dynamic analysis is recognized as the more accurate tool for seismic evaluation of structures in the case of both probabilistic assessment and design (Meena, & Viswanath. 2008). Its main practical application is for the retrofit of existing structures. Furthermore, the analysis is also adopted when the effects of higher modes and structural behaviour after the first mechanism are of interest. Additionally, NLTHA provides estimates not only of the peak deformations but of residual ones. The peak deformation is important for the overall safety and integrity of the structure. The residual deformations are the meaningful measure of damage and important for performance-based design. In NLTHA, the non-linear properties of the structure are considered as part of a time domain analysis.

a. Selection and scaling of ground motion

The issue of selecting the seismic input is seen to be one of the most critical in the seismic assessment of structures via non-linear dynamic analysis. According to Iervolino & Manfredi, (2008), it is sometimes considered more important even than structural modelling. Therefore, this

problem has been the subject of large research recently. For a NLTHA, time histories of the ground motions are needed. Those records will be adopted to simulate the earthquakes in the numerical model. To achieve a reliable data of the structural response, several ground motions must be applied. EN 1998-1 requires the application of at least seven ground motions and the average response must be applied in the design. It also states, if only three ground motions are implemented, the result from the most unfavourable one must be used. Depending on the nature of the application and on the information available, the description of the seismic motion may be made using either

- Artificial accelerograms or
- Recorded or simulated accelerograms. Figure 1.13 shows the Kobe earthquake that took place in 1995 with a peak acceleration of 0.798g.

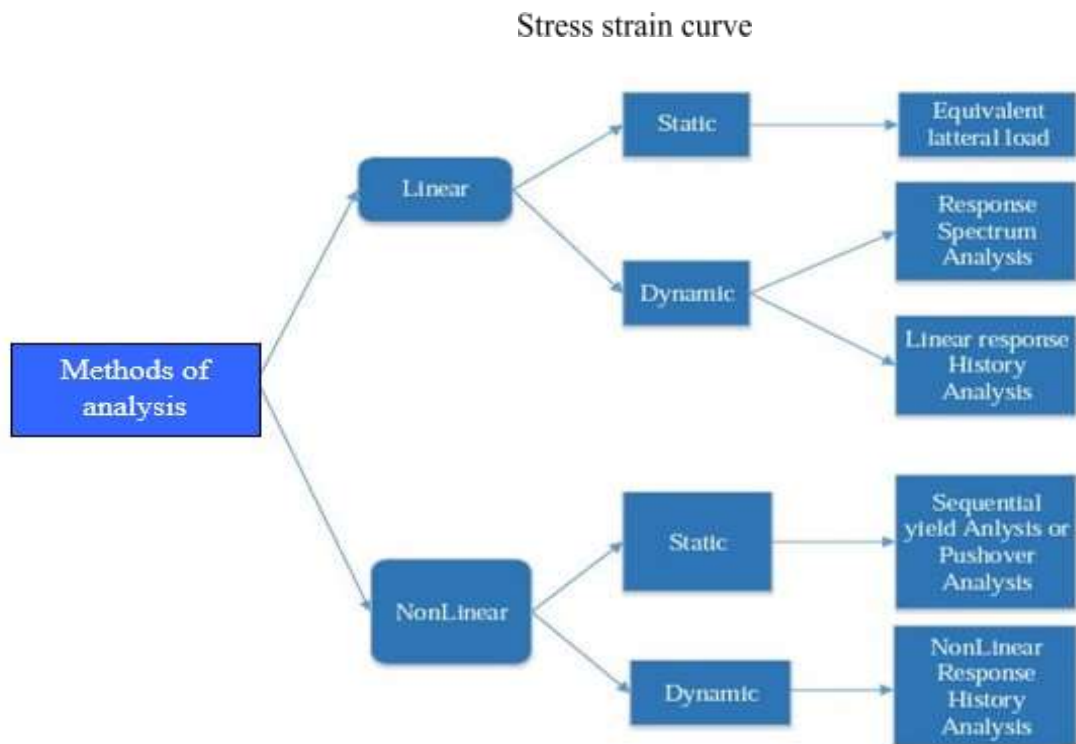
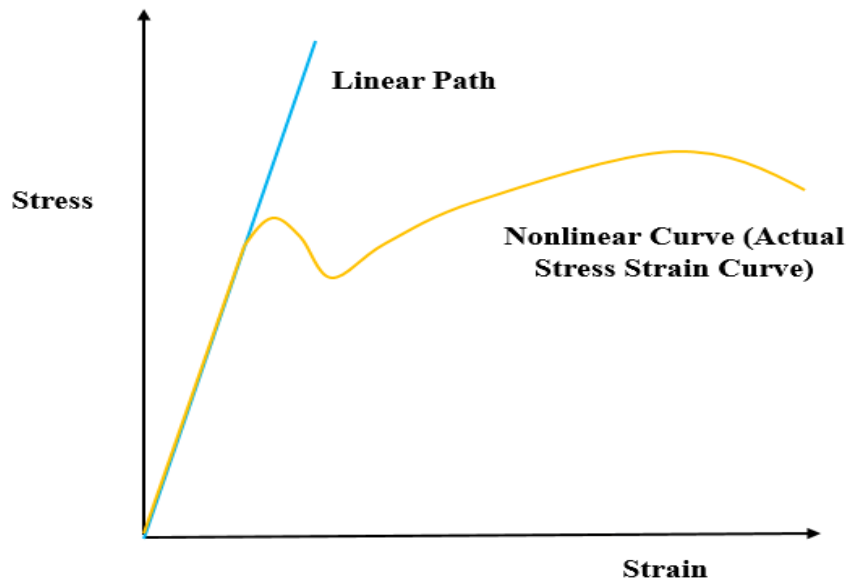


Kobe Earthquake 1995

b. Limitations

One of the main disadvantages of NLTHA is the sensitivity of results to the choice of input ground motions. Furthermore, it is a complicated and requires a lot of time, skill and cost. In addition, NLTHA does not explicitly give the overview of the stiffness, strength and ductility of the structure, thereby, it should be supplemented with Pushover analysis.

In summary we have two big groups of analyses type which could either be linear or non-linear according to the relationship between stress and strain as seen on figure 1.14. These two groups are further broken down in to static or dynamic as shown on figure 1.15.



Methods of seismic analysis

1.4 Soil structure interaction

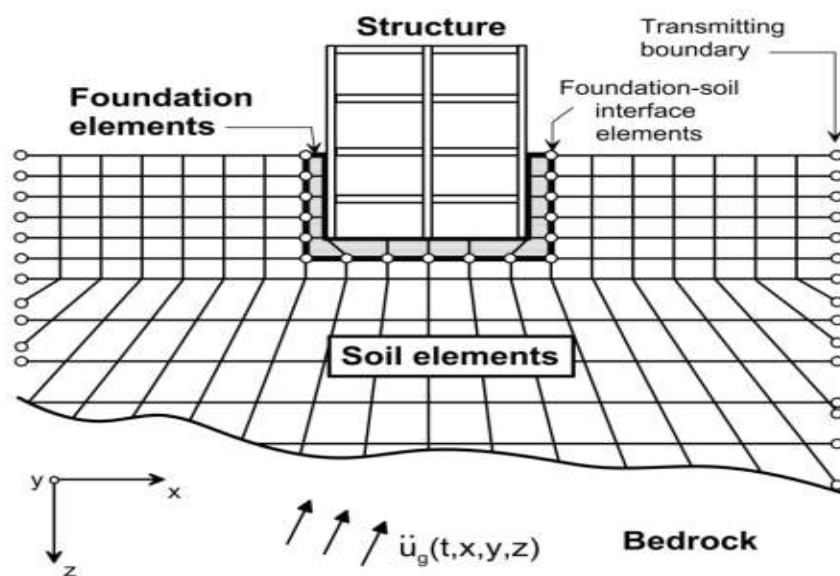
Most civil structures are attached to the ground in one way or another. When an earthquake acts on these structures neither the structural displacement nor the ground displacement are independent of each other. The process in which the response of the soil influences the motion of the structure and vice versa is termed as soil structure interaction (SSI). Conventional structural design methods neglect SSI effects. Unfortunately, the application of SSI for building is hindered by a literature that is often difficult to understand, and codes that contain limited guidance.

1.4.1 Numerical methods in the soil structure interaction analysis

SSI problems have been solved using numerous approaches in literature. Experimental analyses such as shaking table and centrifugal tests have been attempted but they revealed to be expensive. From an analytical point of view, it is challenging or even impossible to obtain solutions (Jia,2018). Therefore, computational models are normally used for solving the problem. Practically, the techniques used are the direct approach and the sub-structural approach

1.4.1.1 Direct approach

In the direct analysis, structure, foundations and surrounding soil are included within the same model and analysed as a complete system. It is performed through finite element methods. In this approach the soil is modelled as a continuum media along with foundation and structural elements, transmitting boundaries at the limits of the soil mesh, and interface elements at the edges of the foundation as shown in figure 1.16. The bedrock motion obtained after the de-convolution of the free field motion is applied at the bottom of the model and the waves travel upwards through the model.



Schematic illustration of a direct analysis of SSI (NIST, 2012).

The transmitting boundary, defined as a special consideration of the external fictitious boundary of the soil model to eliminate wave reflections and to apply seismic excitations, is a requirement of this approach. Lysmer and Kuhlemeyer (1969) proposed a simple viscous local boundary modelling, which comprises two series of dashpots oriented normal and tangential to the boundary of FE mesh.

This approach has the advantage that it can consider nonlinear behaviour of soil and superstructure. If the system is treated as being fully linear, the solution can be carried out in the frequency domain. But if the structure foundation subsystem is modelled as a nonlinear system the solution should be carried out in the time domain. In the latter case, the coupled nonlinear equations of motion are solved using standard step-by-step numerical integration procedures (Arefi,2008).

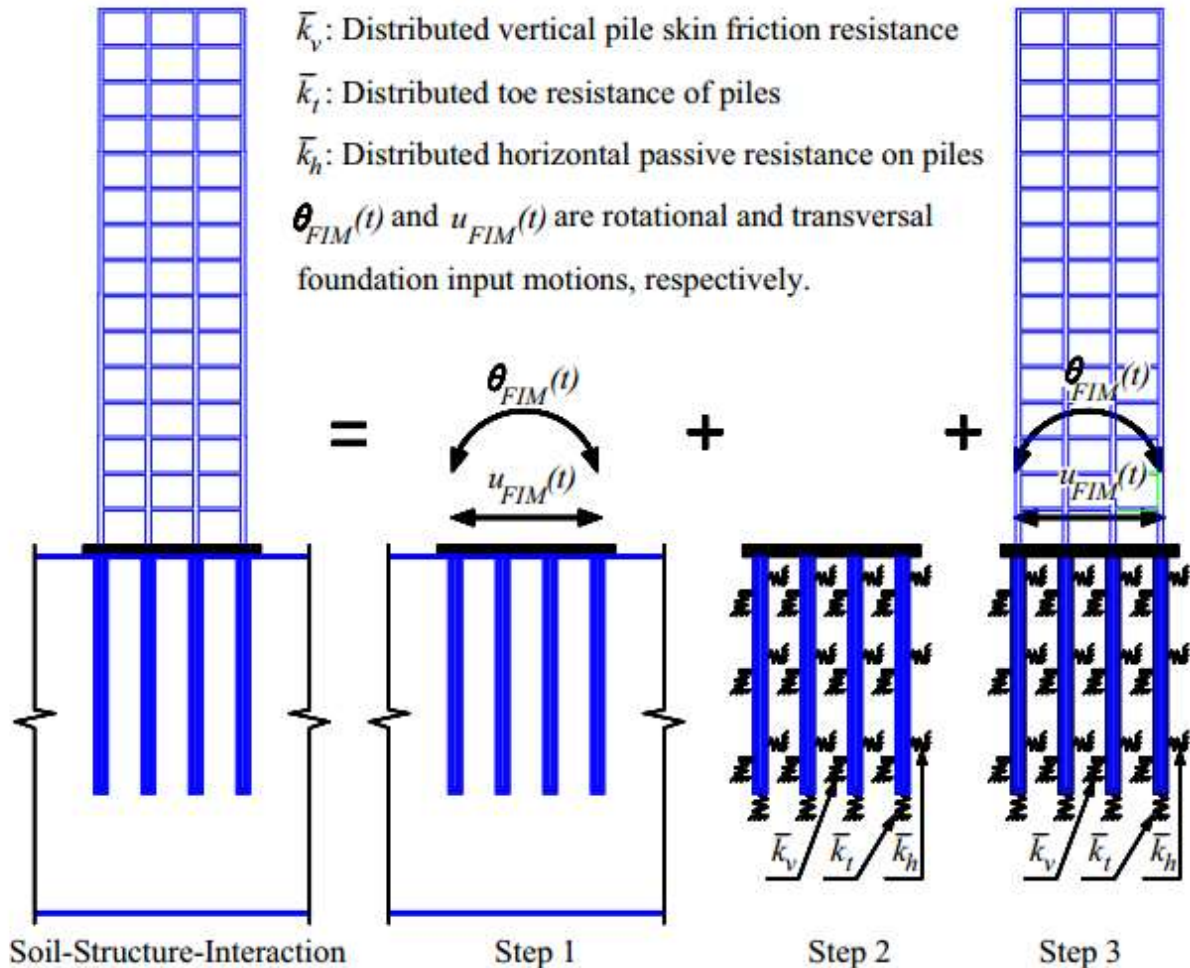
Several researchers (Carbonari et al. 2011; Hayashi and Takahashi 2004; Chu and Truman 2004, Hokmabadi et al. 2014; Tabatabaiefar and Fatahi 2014; Hokmabadi et al. 2015) have studied the seismic responses of soil–pile–structure systems by adopting the direct method for modelling the soil–structure interaction to achieve accurate and realistic outcomes. Because an assumption of superposition is not required, true and accurate nonlinear analyses are possible in this case. The direct analysis approach is better at modelling complex nature of soil structure interaction in dynamic analysis but requires a high computational cost, especially when the system is geometrically complex or contains significant non-linearity in soils or structures. Therefore, it is rarely used in practice.

1.4.1.2 Sub-structural approach

For improving the computational efficiency, the substructure approach can be adopted to assess the effect of soil flexibility even though this cannot explicitly account for the nonlinear effects of SSI. In the substructure approach, the SSI problem is decomposed into three distinct parts that are the soil, the foundation and the superstructure. In this approach, the interaction effects are typically accounted for by modelling a number of frequency-dependent springs and dashpots representing the flexibility of the soil and the radiation of energy away from the foundation, and they are attached to the fixed-base structural model.

By partitioning the soil system into a simpler sets figure 1.17 illustrates the three main steps in the substructure method (Van Nguyen et al ,2017): (1) evaluate the foundation input motion (FIM), which is the motion that would occur on the base slab if the structure and foundation had no mass; (2) determine the impedance function that describes the stiffness and damping

characteristics of the foundation-soil system; and (3) a dynamic analysis of the structure supported on a compliant base that is represented by impedance. It includes both geotechnical analysis (foundation input motion and subgrade impedances) and structural analysis (inertia interaction).



Substructure method for modelling the soil–pile–structure interaction (Van Nguyen et al, 2017).

Numerous studies (Kutunis and Elmas 2001; Carbonari et al. 2011; Allotey and El Naggari 2008; Liu et al. 2015) have been performed using the substructure method to assess the seismic response of structural systems while considering soil–structure interaction. The method has a lot of conveniences for both modelling and computation. However, according to Wolf (1998), since this method is based on the principle of superposition, any predictions would only be accurate for linear soil and structural behaviours, while approximations of soil non-linearity by means of iterative wave propagation analyses, would allow the superposition to be applied to moderately non-linear systems.

1.4.2 Effects of SSI on building performance

Many researches showed that SSI has non-negligible effects on the behaviour of buildings. In fact, SSI changes the building vibration characteristics and behaviours including the base shear, lateral deformation, story drifts, moment at beam ends and force of inner columns.

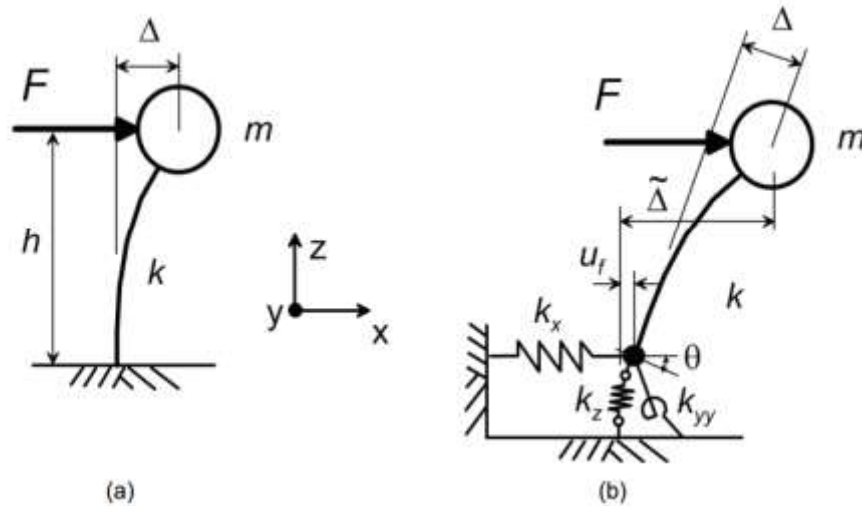
1.4.2.1 Period lengthening

Soil flexibility can be a source of energy dissipation that affects the dynamic properties of the structure-foundation-soil system. A rigid base is the most common support assumption used in practice for modelling structures. This support condition assumes that the soil-foundation interface is infinitely rigid. On the other hand, a flexible base considers the deformability of the foundation system and the soil and it leads to an increase of the system period.

A schematic illustration of the fixed and flexible base conditions for a single-degree-of-freedom structure with a force concentrated at the top can be seen in the figure.1.18 The lateral deflection Δ of the structure with a fixed base presented in the figure 1.18(a) is caused by its translational displacement; however, the lateral deflection, $\tilde{\Delta}$, of this structure with a flexible base illustrated in figure 1.18 b is not just function of its translational displacement, but also the rotation of the foundation system. The undamped period of vibration, T , for the structure with a fixed base can be calculated as function of the circular frequency, ω mass, m , and stiffness, k , using the following commonly used equation (Clough & Penzien, 1993):

$$T=2\pi/\omega=2\pi/\sqrt{(k/m)} \quad \text{Eq. 1.10}$$

For the case of the flexible base, vertical kz , horizontal kx , and rotational springs kyy represent the flexibility of the soil-foundation system (see figure 1.18.b). The undamped period of vibration, T , for a structure with a flexible base can be estimated as a function of the structure height, h , spring constants at the foundation (kz , kx , and kyy), k , and T using the equation suggested by Veletsos & Meek (1974) expressed in equation 1.13. This period ratio is greater than unity based on the degree of flexibility of the structure-soil-foundation system.



Schematic illustration of deflections caused by lateral force applied to: (a) structure with fixed base, (b) structure with flexible base (NIST, 2012).

To see how the type of foundation affects the change in the structure's period, Shiming &Gang (1998) conducted a three-dimensional (3D) linear analysis of SSI on two types of 12-story structures supported by two different types of foundations with and without a pile. The results of their research revealed the enhanced natural period of the structures induced by an interaction between the soil and foundations. Furthermore, pile foundations could lead to a lower increase in the natural period of the structure as compared to a structure lying on a shallow foundation.

1.4.2.2 System damping

The change in damping is one of the effects of the inertial interaction. There are two main sources of foundation damping that are the hysteric and radiation damping. Hysteretic damping is caused by the hysteric behaviour of soil under seismic excitation while radiation damping is originated by the radiation of the reflected wave-field away from the foundation. The damping of a flexible base system is greater compared to the structural damping due to the contribution of the foundation damping.

NIST (2012) presents works done by many researchers to develop analytical models for the evaluation of the foundation damping. Most of these models are frequency-dependent. One exception is the expression suggested by Wolf (1985) using a circular foundation resting on a half-space, which ignores the frequency dependence of the foundation stiffness terms and assumes a linear foundation radiation damping. Similar to a previous study presented by Roësset (1980) considering frequency dependence, the expression initially suggested by Wolf's can be expressed as:

$$\beta_f = \left[\frac{(\tilde{T}/T)^{n_s} - 1}{(\tilde{T}/T)^{n_s}} \right] \beta_s + \frac{1}{(\tilde{T}/T_x)^{n_x}} \beta_x + \frac{1}{(\tilde{T}/T_{yy})^{n_{yy}}} \beta_{yy} \quad \text{Eq. 1.11}$$

Where:

β_s : is the hysteric damping evaluated from information in the literature

β_x : is the translational damping

β_{yy} : is the rotational damping

$n_{s,}$ are exponents that are equal to 2 for linear viscous damping and 3 otherwise

T_x and T_{yy} are the fictitious period defined as:

$$T_x = 2\pi \sqrt{\frac{m}{k_x}} \quad T_{yy} = 2\pi \sqrt{\frac{mh^2}{k_{yy}}} \quad \text{Eq. 1.12}$$

From the increase in the damping it is obvious that when using a general acceleration response spectrum, consideration of SSI effects will reduce the response of the flexible base system.

1.4.2.3 Shear force distribution

As discussed above, SSI tends to increase the period and the damping of the system which leads to a change of the base shear given from the response spectrum as shown in the figure 1.19. The effect of SSI on base shear is related to the slope of the spectrum. Base shear tends to increase when the slope is positive and decrease when the slope is negative. For the common case of buildings with relatively long periods on the descending portion of the spectrum, the use of flexible base shear in lieu of fixed base shear typically results in the reduction of the base shear demand. Conversely, inertial SSI can increase the base shear in relatively short-period structures.

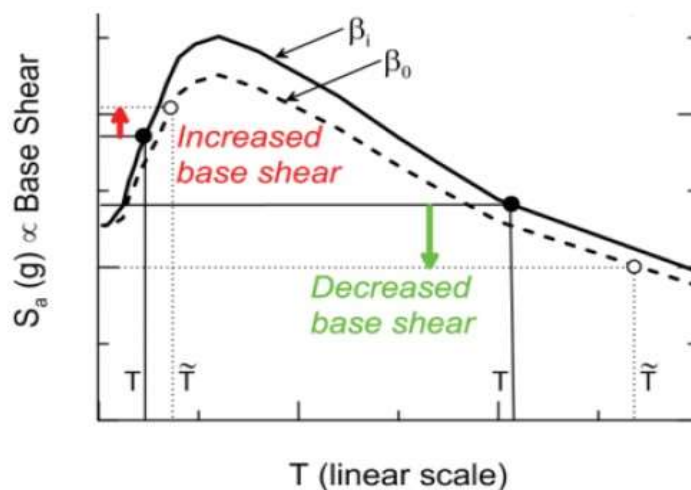


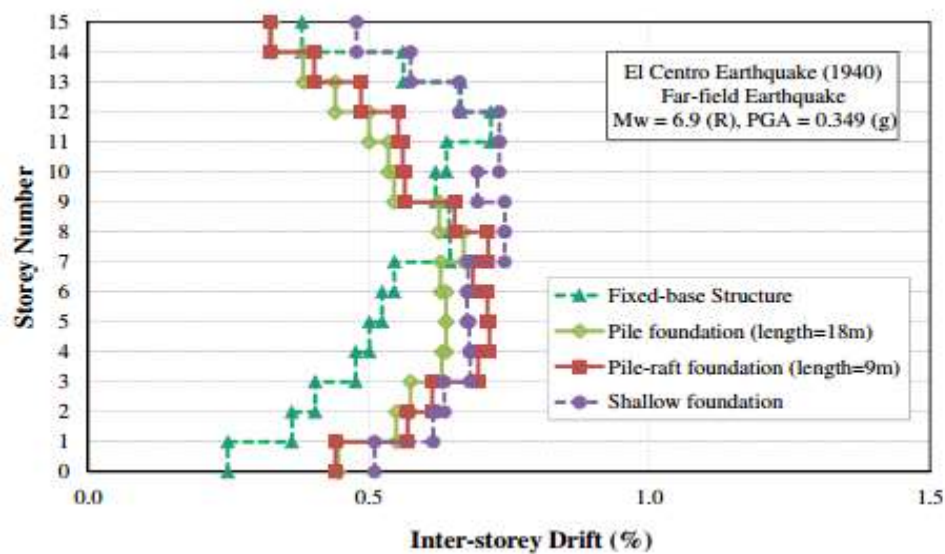
Illustration of the SSI effect on base shear due to the period lengthening and change in damping (NIST, 2012).

SSI also influences how the base shear is distributed in the superstructure. Several researchers (eg Hokmabadi and Fatahi 2015, Abdelraheem 2014, Bargheri et al 2018) studied the effect of SSI on the distribution of shear force in the structural elements of a building and concluded that although SSI reduced the shear forces but the amount and trend of this reduction was not the same at every level. In fact, in the structure analysed by Hokmabadi & Fatahi (2015) the maximum shear force experienced in the first level of the 15 storey superstructure supported by the pile-raft foundation reduced by 38% compared to the fixed-based structure under the impact of the 1994 Northridge earthquake, whereas the seventh level experienced virtually no reduction in the generated shear force (less than 10%). As a consequence, practicing engineers should realise that the reduction ratio for the maximum base shear due to SSI cannot be generalized to all levels of the superstructure because it could result in an unsafe design.

1.4.2.4 Lateral deformation and inter-story drift.

Overall lateral deformation and inter-story drift are the most used damage parameters in the performance-based approach. The increase in the lateral deformation of the building can change the performance level of the structure and is particularly important in tall, slender, and closely spaced structures that can be subjected to pounding when relative displacements are large (Kramer 1996). Moreover, increase in the total deformation of the structure, and in turn secondary P- Δ effect, influences the total stability of the structure as well as the performance of the non-structural elements. Storey drift ratio is the maximum relative displacement of each floor divided by the height of the same floor and is strictly connected to the damage suffered by both structural and non-structural elements.

In general, SSI leads to an increase of the lateral deflection in the superstructure. Hokmabadi et al (2015) reported that the amplification relative to the fixed based approach varied with the type of foundation. It has been shown that a building with shallow foundation deflects more than structure with pile foundation. Layout of the building considered by Hokmabadi et al (2015) for examining SSI effects. SSI may affect the performance level of the structure and shift the performance level of the structure from the life safe zone (less than 1.5% drift) to the near collapse or even the collapse zones, particularly in soft soils. Figure 1.20 shows the corresponding maximum inter-storey drifts of the superstructure for different types of foundations of a 15-story building subjected to El Centro earthquake. It is shown that SSI tended to increase the inter-storey drifts of the superstructure, although the maximum inter-storey drift of the structure supported by the floating pile foundation is less than the corresponding value for the structure supported by shallow foundations and the fixed base condition.



Maximum inter-storey drifts of the structure for different type of foundation under the influence of El Centro earthquake (Hokmabadi, 2015).

Conclusion

The objectives of this chapter were to make touch with reinforced concrete as a construction, material, the design parameters and methods of reinforced concrete buildings and the understanding of linear and non-linear analysis. The response of structure depends on both the type of structure, the behaviour of the materials that constitute the structural elements (its ability to dissipate energy received i.e. ductility) and the severity of the loads. Thus, the type of analysis to be adopted depends on the structure's characteristics. Pushover analysis as seen at the end is a simplified nonlinear analysis method in which the structure is subjected to monotonically increasing lateral forces with an invariant height-wise distribution, with the aim to simulate the behaviour of the structure under a given seismic action. Soil structure interaction was also discussed and we saw her effects in the building design.

Chapter 2. METHODOLOGY

Introduction

Structural analysis involves evaluating the response of a structure due to specified loads or other external effects, such as temperature changes and support movements. For structural design, the response characteristics generally of interest are support reactions, stresses or stress resultants (i.e., axial forces, shears and bending moments) and deflections. This chapter will be focused firstly on the ground condition and seismic action, which part will take into account the assumptions about ground parameters for the seismic analysis. Next, the methods for linear analysis and nonlinear analysis of structures in static equilibrium as well as dynamic function of the structure as a result of time varying loads.

2.1 General recognition of the site

The site recognition will be carried out from a documentary research whose essential goal is to know the location of the site, the climate, the hydrology and socio-economic parameters in the region.

2.2 Site visit

The purpose of this activity is the building description results from the observation and the presentation of the use category, the floor plans and elevation configuration.

2.3 Data collection

Two types of information will be collected. Those related to the geometry and those related to the structure. These data will be taken from different plans available where we can identify the sections and positions of structural elements (beams and columns) and the characteristics of materials used.

2.4 General procedure and standards

The evaluation procedure goes by a series of steps. These steps are concerned with the realization of a construction project. As it is common with most, if not all, construction projects, there is the superstructure (above ground level) and the substructure (below ground level). The steps are as follows:

- The choice of the type of structure, load patterns and analyses;
- Gravity load design and detailing of the building;
- 3D modelling on SAP 2000 version 22 and performance of modal analysis;

- Non-linear static analysis (pushover analyses) of the structure;
- Check failure modes in terms of creation of plastic hinges.

2.4.1 Evaluation procedure of actions on the building

Various design codes are being used all around the world. The design code used in this work is the European Norms (Eurocodes), recommended by the European Committee for standardization. In the Eurocode, with respect to the construction material, the use of the structure and the location of the structure, different codes exist, partitioned according to the field of construction. The various parts made use of in this thesis go thus:

- Eurocode 0: Basis of structural design;
- Eurocode 1: Actions on structures
- Eurocode 2: Design of concrete structures
- Eurocode 8: Design of structures for earthquake resistance

A structure can be subjected to a variety of load types and at the same time. The concern of this thesis is beam- column joints in RC structures, so the type loads applied to the chosen structure will be; permanent loads, and variable loads (imposed loads).

2.4.2 Loads acting on the structure

2.4.2.1 Permanent actions

These are actions acting during the whole nominal life of the structure with negligible time variation of their intensity (that can be considered as constant in time):

- Self-weight of structural elements (G1); self-weight of the soil, if present; forces due to the soil (excluding the effects of the service loads applied to the soil); forces due to water pressure (when they are constant in time);
- Self-weight of non-structural elements (G2); imposed displacements and deformations determined by the designer and realized in-situ;
- Prestressing
- shrinkage and creep (fluage);
- differential displacements

Permanent action or load consist essentially of the weight of the element, whether structural or not. Provisions for the evaluation of the self-weight of these elements are given in Eurocode1.

2.4.2.2 Variable actions

Variable actions are those which, as the name goes, vary with respect to time. They consist of actions on the structure (or on the structural element) with instantaneous values which can be significantly different in time: That is, their magnitude is time dependent.

- with long duration: acting with a significant intensity, also if non-continuously, for a not negligible time compared to the nominal life of the structure;
- with brief duration: acting with brief duration compared to the nominal life of the structure;

This variation is nonnegligible and monotonic. Variable loads fall under two main kinds; Imposed loads and seismic- induced loads.

2.4.3 Combination of actions

A combination of actions, as the name indicates, consist of a set of load values applied to the structure simultaneously to verify its structural reliability for a given limit state (design limit states). They are defined as follows, when designing a building.

2.4.3.1 Fundamental combination

$$\sum_{i \geq 1} \gamma_{G,i} G_{k,i} + \gamma_{Q,1} Q_{k,1} + \sum_{i > 1} \gamma_{Q,i} \Psi_{0,i} Q_{k,i} \quad (\text{Eq. 2.1})$$

Eq. 2.1 above is the fundamental load combination at Ultimate Limit State (ULS) design situation, where the coefficients $\gamma_{G,j}$ and $\gamma_{Q,i}$ are partial factors or again safety coefficients, which minimize the action which tends to reduce the solicitations and maximize the one which tends to increase it. The values of these partial factors recommended by the Eurocode 0 for the structural and Geotechnical (STR and GEO) verifications are:

$$\gamma_{G,} = 1.35$$

$$\gamma_{G,} = 1$$

$$\gamma_{Q,1} = 1.50 \text{ Where unfavourable (0 where favourable)}$$

$$\gamma_{Q,} = 1.50 \text{ Where unfavourable (0 where favourable)}$$

2.4.3.2 The rare combination

This is the load combination for non-reversible Serviceability Limit State (SLS) for the verifications with allowable stress method.

$$\sum_{j \geq 1} G_{k,j} + Q_{k,1} + \sum_{j > 1} \Psi_{0,j} Q_{k,j} \quad (\text{Eq. 2.2})$$

2.5 Linear Static design methodology

The static design is done based on the static analysis. Static analysis studies the behaviour of the structure under static loads application. The analysis starts with the modelling of the structural members. In that line, the concrete cover, the design and verification of one horizontal (beam) and one vertical (column) structural element, both considered as representative of the other elements of their type. Footings are also analysed and verified in order to study the case of joints at the footing.

2.5.1 Concrete cover and durability

Concrete cover is most importantly a measure to protect structural reinforcements against environmental actions (table A7 of the annex). The durability of a structure depends on how long the later can be protected from external factors like environmental actions and others but also the capacity of the structure to perform its function throughout its working life without severe damage. Concrete cover is defined in Eurocode 2 as the distance between the surface of the reinforcement closest to the nearest concrete surface and the nearest concrete surface (Figure 2.1). The nominal cover is defined as, according to EN 1992-1-1_E_2004, a minimum cover, C_{min} , plus an allowance in design for deviation, ΔC_{dev} .

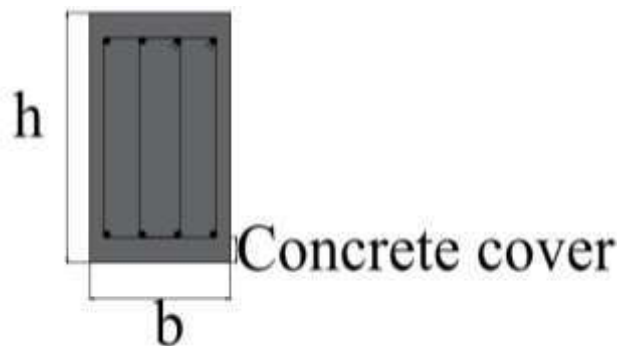


Figure 2.1. Concrete cover

$$C_{nom} = C_{min} + \Delta C_{dev} \quad (\text{Eq. 2.3})$$

With:

ΔC : The allowance in design for deviation with a recommended value of 10 mm

C_{min} : Is the minimum concrete cover

The minimum concrete cover is computed as shown in Eq 3.10.

$$C_{min} = (C_{min,b}; C_{min,dur} + \Delta C_{dur,\gamma} - \Delta C_{dur,st} - \Delta C_{dur,add}; 10mm) \quad (\text{Eq. 2.4})$$

Where:

C_{min} : Is the minimum cover due to bond requirement, equal to the diameter of the bars or the equivalent diameter in the case of bundled bars

ΔC_{dur} : Is the additive safety element with a recommended value of 0 mm

ΔC_{dur} : Reduction of minimum cover for use of stainless steel

$\Delta C_{dur\ add}$: Is the add reduction of minimum cover for use of additional protection

C_{min} : Is the minimum cover due to environmental conditions.

2.5.2 Horizontal structural element design

The horizontal structural element to be designed, in this section is a beam. The latter is designed under Ultimate Limit State (ULS) and Serviceability Limit State (SLS). The modelling and design are done with the use of the software SAP 2000 V21. Materials, section properties, loads, loads combinations, restrains and constrains and other design parameters are defined and assigned to the beam to obtain the solicitation parameters and curves. The envelop curve is then obtained for each solicitation parameter.

2.5.2.1 Ultimate Limit State design

Under ULS, the beam will be verified for bending moment and shear force solicitations as there are no axial forces on the beam.

a. Bending moment design

Design for bending moment is done with the envelope curve of the bending moment solicitation parameter. Provisions given by Eurocode 2 recommend moment reduction at the support as shown in Figure 2.2 (Djeukoua Nathou, G. L. 2019). For continuous beams, the value depends on the connection between the beam and the support.

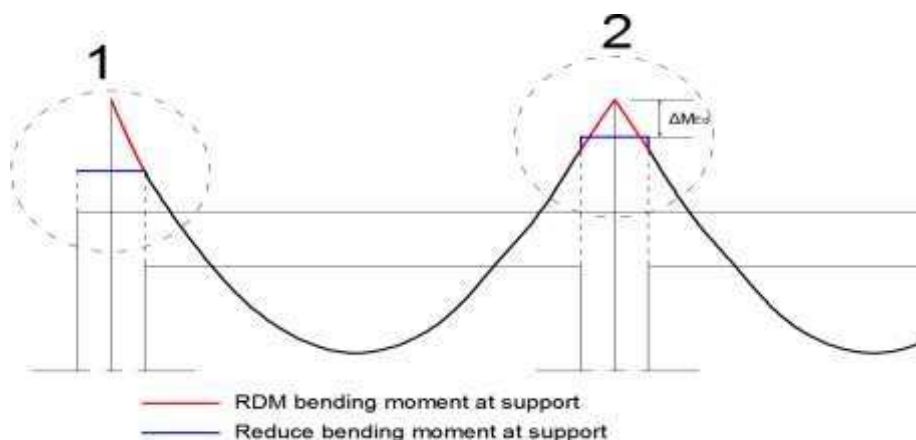


Figure 2.2. Moment reduction at supports (Djeukoua Nathou, G. L. 2019).

Where a beam is monolithic with its supports, the critical design moment at the support should be taken as that at the face of the support. As presented in the Figure 2.2 (1). If instead, the beam is continuous over a support (Figure 2.2(2)) the analysis is done considering that the support does not provide no rotational restraint. The amount of this reduction is given by equation 2.5:

$$\Delta M_{Ed} = F_{Ed,t} / 8 \quad (\text{Eq. 2.5})$$

Where:

t : Is the breadth of the support

F_{Ed} , Is the design of the support

The curve used for design is obtained by doing a shift of the moment curve a distance of a_i in the worst direction as it is illustrated in Figure 2.3 (Djeukoua Nathou, G. L. 2019), accounting for the additional tensile force.

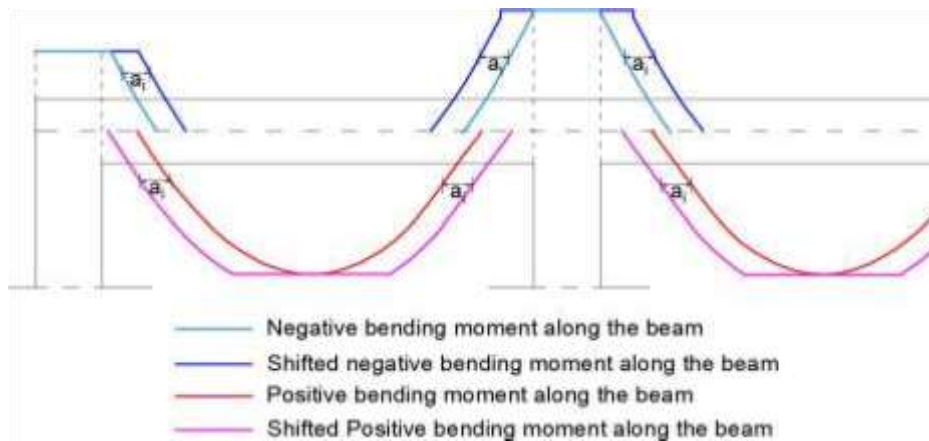


Figure 2.3. Shifting of the moment curve (Djeukoua Nathou, G. L. 2019).

a_i is computed as in equation 2.6;

$$a_i = (\cot\vartheta - \cot\alpha) / 2 \quad (\text{Eq. 2.6})$$

Where:

z : Is the inner lever arm

ϑ : Angle of concrete compression strut to the beam axis

α : Is the angle between shear reinforcement and the beam axis perpendicular to the shear force. The quantity of longitudinal reinforcements is then determined with values of bending moment obtained in the shifted curve.

Longitudinal steel reinforcement

The section of the beam is a rectangular one. The longitudinal steel reinforcement is computed using Eq. 2.7.

$$A_s = \frac{M_{Ed}}{0.9d \cdot f_{yd}} \quad (\text{Eq. 2.7})$$

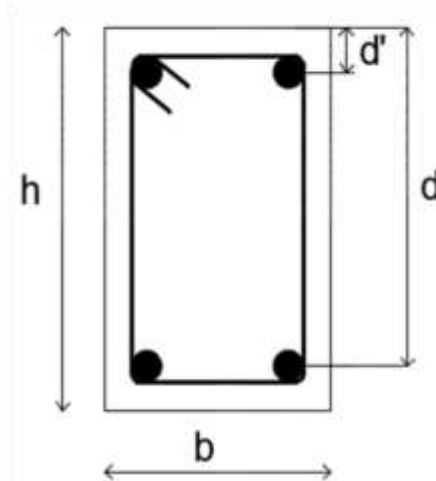


Figure 2.4. Example of transversal beam section with longitudinal reinforcements
The provisions of the Eurocode 2 to be verified by the beam cross section for minimum and maximum reinforcement areas are given in Eq. 2.8 and Eq. 2.9.

$$A_{s,min} = \max\left(0.26 \frac{j_{ctm}}{f_{yk}} b_t d; 0.0013 b_t d\right) \quad (\text{Eq. 2.8})$$

$$A_s = 0.004 A_c \quad (\text{Eq. 2.9})$$

Where:

b_t : Is the mean width of the tension zone

d : is the effective depth of the section

j_{ctm} : Tensile strength of the concrete

Verification of the steel reinforcement

We compute the number of reinforcement bars needed and the corresponding area of reinforcement. The section is verified, using the position of the neutral axis inside the section, by calculating the resisting bending moment of the section.

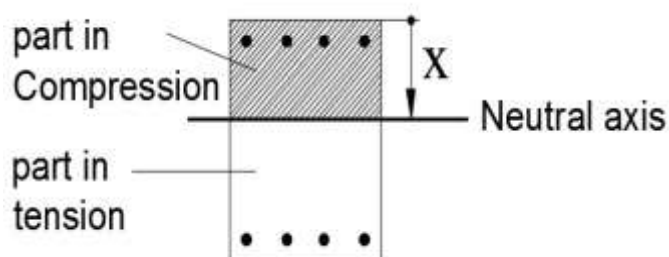


Figure 2.5. Neutral axis position in the beam section

Equation 2.10 below is the computation of the neutral axis position.

$$x = \frac{d}{2\beta_2} - \sqrt{\left(\frac{d}{2\beta_2}\right)^2 - \frac{M_{Ed}}{\beta_1\beta_2 \cdot b \cdot f_{cd}}} \quad (\text{Eq. 2.10})$$

Where:

d : Effective depth of the section b : Width of the section

f_{cd} : Design concrete compressive strength

β_1 and β_2 : Correction factor equal to 0.81 and 0.41 respectively

We then calculate the resisting moment using equation 2.11:

$$M_{Rd} = A_{s,real} \cdot f_{yd} \cdot (d - \beta_2 \cdot x) \quad (\text{Eq. 2.11})$$

With;

$A_{s,real}$: Effective area of the steel section

f_{yd} : Design yielding strength of the steel

b. Shear verification

The beam element needs to resist shear forces. Transversal steel reinforcement is therefore needed inside the beam. These reinforcements are called stirrups and can be determined from the minimum of V_{rds} and $V_{rd,max}$ given in Eq 2.13 and Eq 2.14. Whether shear reinforcement is needed or not is agreed on, on comparison of the acting shear, V_{Ed} , with the shear resistance of the members without shear reinforcements, $V_{Rd,C}$.

$$V_{Rd,C} = \{ [C_{Rd,C} k (100 \rho_l f_{ck})^3 + k_1 \sigma_{cp}] b_w d; (V_{min} + k_1 \sigma_{cp}) b_w d \} \quad (\text{Eq. 2.12})$$

With;

$V_{Rd,C}$: is the characteristic strength of the reinforcement

d : is the effective depth of the section

b_w : is the smallest width of the cross section in the tensile area

$$\sigma_{cp} = \frac{N_{Ed}}{b_w d} < 0.2 f_{ck} \quad [N/mm^2]$$

N_{Ed} : Axial force of the cross section due to loading or prestressing

$b_w d$: Concrete cross-sectional area

$$k = 1 + \sqrt{\frac{200}{d}} \leq 2.0 \quad \text{With } d \text{ in mm}$$

$$\rho_l = \frac{A_{st}}{b_w d} \leq 0.02$$

Minimum shear reinforcement is provided where, according to the provision above, no shear reinforce is required.

$$V_{Rd,C} = \alpha_{cw} b_w z v_1 f_{cd} / (\cot \vartheta + \tan \vartheta) \quad (\text{Eq. 2.13})$$

$$V_{Rd,S} = \frac{A_{sw}}{s} z f_{ywd} \cot \vartheta \quad (\text{Eq. 2.14})$$

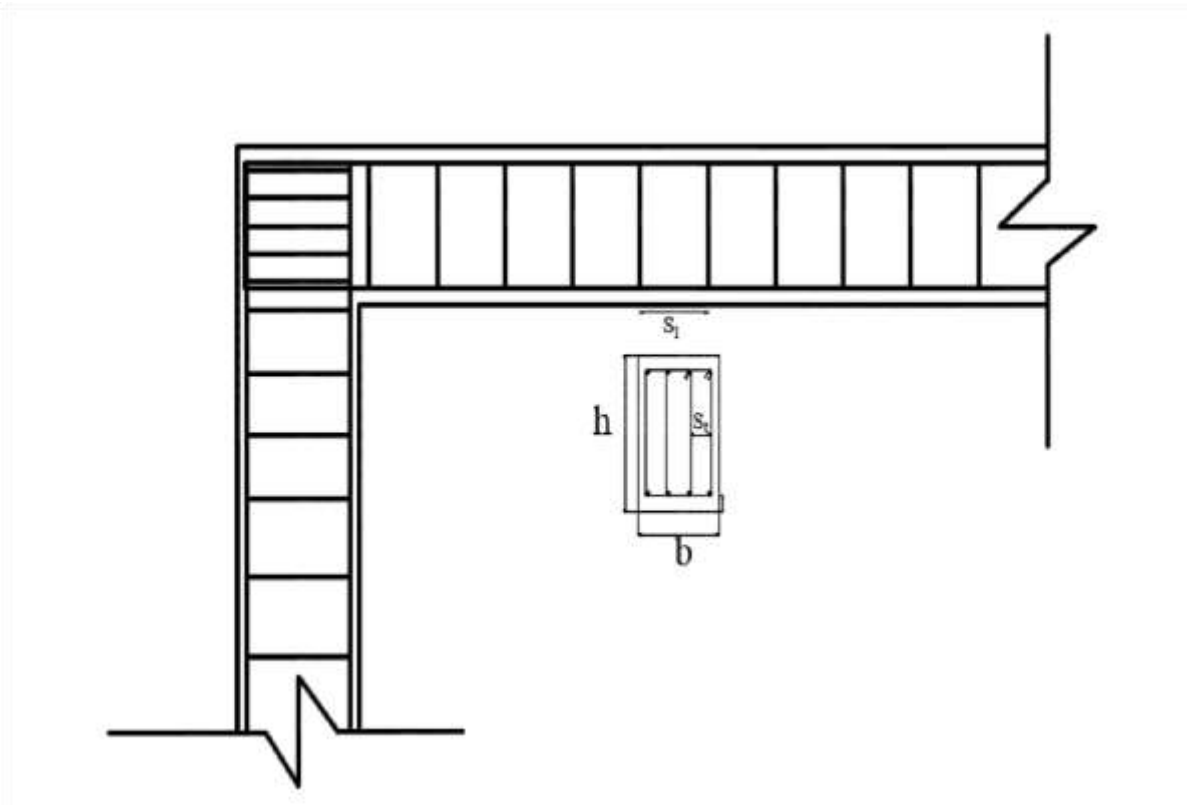


Figure 2.6. Maximum longitudinal spacing and transversal spacing of the legs

$$s_l = 0.75(1 + \cot \alpha) \quad (\text{Eq. 2.15})$$

$$s_t = 0.75d \leq 600 \text{ mm} \quad (\text{Eq. 2.15})$$

$$\rho_{w, \min} = (0.08 \sqrt{f_{ck}}) / f_{yk} \quad (\text{Eq. 2.16})$$

Where the minimum reinforcement ratio is given by; $\rho_w = A_{sw} / (s \cdot b_w \cdot \sin \alpha)$

2.5.2.2 Serviceability Limit State

The parameters of interest in this section are the stress limitations, the crack and the deflection control. Only the stress limitation for the structural elements is presented in this work. The rare combination mentioned earlier in the previous sections, is the combination used for the stress verification because it permits to avoid inelastic deformation of the reinforcement and longitudinal cracks in concrete. Long-term and short-term effects are accounted for by the modular ratio, on which depends the stress value.

$$n_0 = \frac{E_s}{E_c} \quad (\text{Eq. 2.17})$$

$$n_\infty = n_0(1 + \varphi_L \times \rho_\infty) \quad (\text{Eq. 2.18})$$

Where $\phi_L = 0.55$ for shrinkage of concrete and the parameter $\rho_\infty = 2 \div 2.5$. For an uncracked concrete section, the neutral axis is computed using equation 2.19:

$$x = \frac{-n(A'_s + A_s) + \sqrt{[n(A'_s + A_s)]^2 + 2bn(A'_s d' + A_s)}}{b} \quad (\text{Eq. 2.19})$$

Where A'_s and A_s are the upper and lower steel reinforcement inside the section respectively. b , d' and d , are the geometrical characteristics of the section presented in the Figure 2.7.

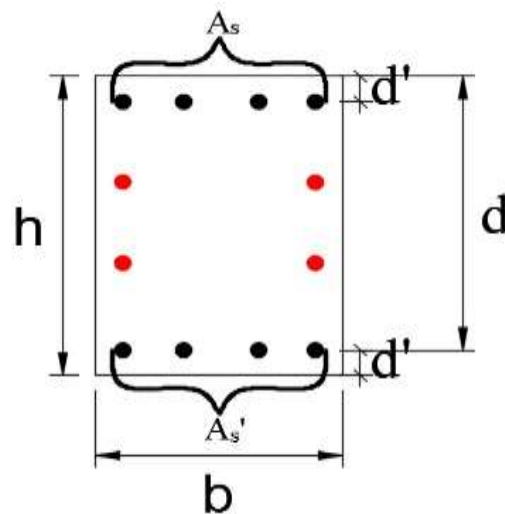


Figure 2.7. Geometric characteristics of a transversal beam section

The moment of inertia of the uncracked section is given by equation 2.20:

$$J_{cr} = \frac{bx^3}{3} + nA_s(d - x)^2 + nA'_s(x - c)^2 \quad (\text{Eq.2.20})$$

The stresses in the concrete and steel can now be computed using Eq. 21 and Eq. 22.

$$\sigma_s = \frac{M_{Ed}(d-x)}{J_{cr}} \times n_{zz} \quad (\text{Eq. 2.21})$$

$$\sigma_c = \frac{M_{Ed} \cdot x}{J_{cr}} \quad (\text{Eq. 2.22})$$

The verifications of these stresses, as provided by Eurocode 2, are given in equations 2.23 and 2.24 below.

$$\sigma_c \leq k_1 * f_{ck} \quad (\text{Eq. 2.23})$$

$$\sigma_s \leq k_3 * f_{yk} \quad (\text{Eq. 2.24})$$

With $k_1 = 0.6$ and $k_3 = 0.8$

2.5.3 Vertical structural element design

Before the vertical structural element could be designed, the entire structure has to be modelled on SAP2000 V21. Similar to the beam, different load arrangements and combinations are assigned to the column to obtain the envelope curve that represents the worst case of loading the column could be subjected to, throughout the structure's working life. Only ULS is considered in the case of the column and the verifications done for axial force, bending moment and shear force. The procedure for shear force verification for the column is the same as that of the beam. As such, the procedure will not be detailed anymore, but the detailing will be presented.

2.5.3.1 Bending moment-axial force verification

For a column line, from the ground floor to the roof, the envelope curve is derived. Shear forces put aside, each column at each level is subjected to moment and axial force; these solicitations are obtained from the respective envelope curves. Each couple of points, M-N (moment-axial force) should belong to the section M-N interaction diagram.

The interaction is a diagram representing all the limit situations deterministic of the section failure and is computed through the determination of points, which will be plotted to obtain the curve. Points lying within the diagram are respectful of the design criteria otherwise failure occurs. When considering a rectangular section as shown in Figure 2.8, the computation of the points is done as presented in the subsequent sections.

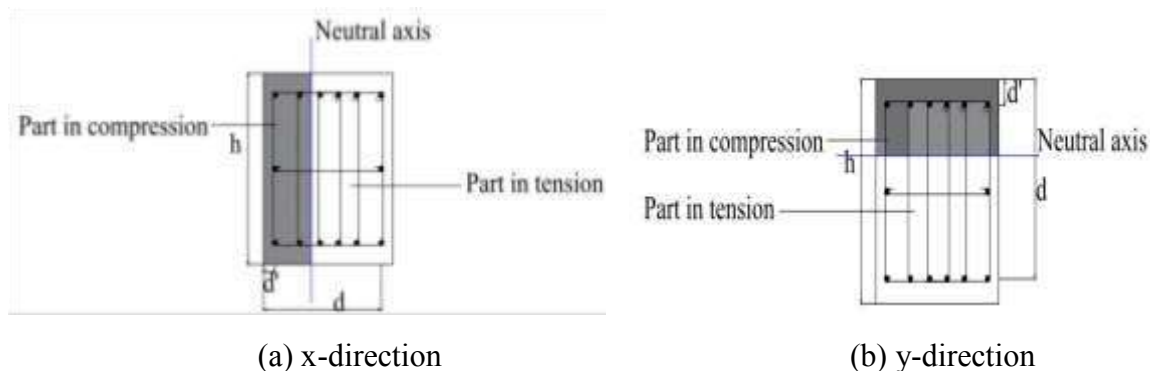


Figure 2.8. M-N diagram computation of a rectangular column section in both loading directions

a. First point

At this point, the section is completely subjected to tension, thus, the concrete is not reacting (Concrete does not work under tension). We impose $\varepsilon_s = \varepsilon_{su}$, $\varepsilon_s' = \varepsilon_{syd}$. The stress inside the element corresponds to the design yielding strength of the steel reinforcement and the limit axial force and bending moment are obtained from Eq. 2.25 and Eq. 2.26.

$$N_{Rd} = f_{yd} \cdot A_s + f_{yd} \cdot A'_s \quad (\text{Eq. 2.25})$$

$$M_{Rd} = f_{yd} \cdot A_s \cdot \left(\frac{h}{2} - d'\right) - f_{yd} \cdot A'_s \cdot \left(\frac{h}{2} - d'\right) \quad (\text{Eq. 2.26})$$

b. Second point

At the second point, the section is completely subjected to tension. We impose that; the strains, $\varepsilon_s = \varepsilon_{su}$, $\varepsilon_c = 0$. The upper steel yielding condition is verified. If the steel has not yielded, then ε_s' is determined. Eq. 2.25 and Eq. 2.26 are used for the computation of the axial force and the bending moment.

c. Third point

Here failure is due to concrete and the lower reinforcements have yielded. We assume $\varepsilon_s \geq \varepsilon_{syd}$, $\varepsilon_c = \varepsilon_{cu2}$ and the position of the neutral axis is determined. Yielding condition of the upper steel reinforcement is verified. If the steel is yielded or not is determined by determining ε_s' in order to determine the corresponding stress. The axial force and bending moment corresponding to the third point are computed thus:

$$N_{Rd} = -\beta_1 \cdot b \cdot x \cdot f_{cd} + f_{yd} \cdot A_s - f_{yd} \cdot A'_s \quad (\text{Eq. 2.27})$$

$$M_{Rd} = f_{yd} \cdot A'_s \cdot \left(\frac{h}{2} - d'\right) + f_{yd} \cdot A_s \cdot \left(\frac{h}{2} - d'\right) + \beta_1 \cdot b \cdot x \cdot f_{cd} \left(\frac{h}{2} - \beta_2 \cdot x\right) \quad (\text{Eq. 2.28})$$

d. Fourth point

We impose that the failure is due to concrete and the lower reinforcement reaches exactly $\varepsilon_s = \varepsilon_{syd}$. Likewise, we determine the neutral axis position and the strain ε_s' . Eq 3.34 and Eq 3.35 are used to compute the fourth point.

e. Fifth point

We impose that $\varepsilon_s = 0$ and failure is due to concrete. The lower reinforcement is considered to have yielded and the position of the neutral axis is the same as that of the effective depth.

$$N_{Rd} = -\beta_1 \cdot b \cdot x \cdot f_{cd} - f_{yd} \cdot A'_s \quad (\text{Eq. 2.29})$$

$$M_{Rd} = f_{yd} \cdot A'_s \cdot \left(\frac{h}{2} - d'\right) + \beta_1 \cdot b \cdot d \cdot f_{cd} \left(\frac{h}{2} - \beta_2 \cdot x\right) \quad (\text{Eq. 2.30})$$

f. Sixth point

We impose that concrete is uniformly compressed and assume the strain $\varepsilon_s = \varepsilon_c \geq \varepsilon_{c2}$. Axial force and bending moment are computed as below.

$$N_{Rd} = -b \cdot h \cdot f_{cd} - f_{ywd} \cdot A'_s - f_{yd} \cdot A_s \quad (\text{Eq. 2.31})$$

$$M_{Rd} = f_{yd} \cdot A'_s \cdot \left(\frac{h}{2} - d'\right) - f_{yd} \cdot A_s \cdot \left(\frac{h}{2} - d'\right) \quad (\text{Eq.2.32})$$

An example of a M-N interaction diagram is shown in Figure 2.9 below. The figure shows the M-N diagram in red for positive and negative loading directions with the couple of points (solicitation M_{Ed} and N_{Ed}), in blue, which lie within it, thereby respecting the design criteria. Provisions of Eurocode with regards to the steel reinforcement of the column

Recommend that

$$A_{s,min} = \max\left(\frac{0.10N_{Ed}}{f_{yd}}; 0.002A_c\right) \quad (\text{Eq. 2.33})$$

$$A_s = 0.04A_c \quad (\text{Eq. 2.34})$$

Where

N_{Ed} : Design axial compression force

f_{yd} : Design yield strength of the longitudinal reinforcement

For joint reinforcements,

$$A_s = 0.09sb_{ch} \frac{f'_c}{f_{yh}} \quad (\text{Eq. 2.35})$$

And not less than;

$$A_{sh} = 0.3sb_{ch} \left(\frac{A_g}{A_{ch}} - 1\right) \frac{f'_c}{f_{yh}} \quad (\text{Eq. 2.36})$$

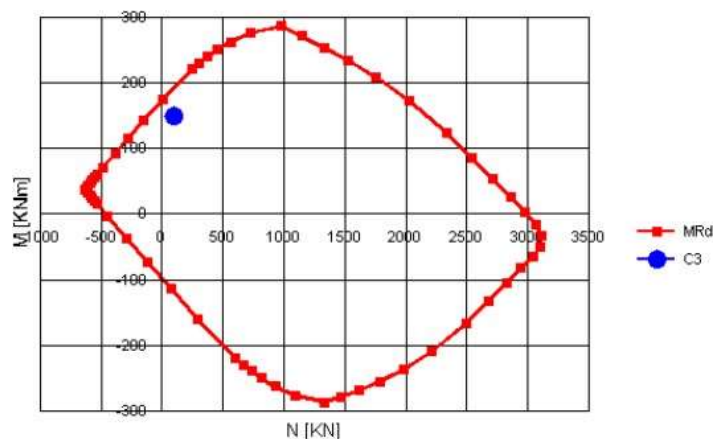


Figure 2.9. Example of M-N diagram (D'Antino et al., 2016)

2.5.3.2 Shear verification

Just like the beam, the procedure goes same. Provisions given by the Eurocode 2 requires a minimum diameter of 6mm or one quarter of the maximum diameter of the longitudinal bars. The maximum spacing of the transverse reinforcement is given by the equation 2.37.

$$S_{cl} = \min (20\phi_l; 400mm) \quad (\text{Eq. 2.37})$$

Where:

ϕ_l : Minimum diameter of the longitudinal bars

b: Lesser dimension of the column

The factor of 0.6 is used to reduce the maximum spacing in sections within a distance equal to the larger dimension of the column bars.

2.5.3.3 Slenderness verification

The need for slenderness verification arises from whether or not second order effects are to be accounted for. Eurocode 2 recommendations are outlined below:

$$\lambda_{lim} = 20 \cdot A \cdot B \cdot C / \sqrt{n} \quad (\text{Eq. 2.38})$$

With:

$$A = \frac{1}{1+0.2\varphi_{ef}} \quad (\varphi_{ef}: \text{ is the effective creep ratio; If not known, } A=0.7)$$

$$B = \sqrt{1 + 2\omega} \quad (\omega = A_s f_{yd} / A_c f_{cd}: \text{ mechanical reinforcement ratio})$$

$$C = 1.7 - r_m \quad (r_m = M_{01} / M_{02}: \text{ the moment ratio; equal to 1 for unbraced system})$$

$$n = N_{Ed} / A_c f_{cd}: \text{ relative normal force}$$

The expression in Eq 3.44 is the one used for the estimation of slenderness.

$$\lambda = l_0 / i \quad (\text{Eq. 2.39})$$

Where:

i : The gyration radius of the uncracked concrete

l_0 : Effective length of the element ($l_0 = 0.7l$)

$$i = \sqrt{\frac{I}{A}} \quad (\text{Eq. 2.40})$$

I : Moment of inertia and A is the area of the section.

2.5.4 Footing design

This is the structural element that lies directly on the ground surface. It is in charge of correctly distributing the charge from the super structure onto the ground without any failure. Classified broadly into two broad main classes (shallow and deep foundation), its design is based on the soil characteristics: the density ρ , the Elastic modulus E , and Poisson ratio ν , which are determined by geotechnical laboratory tests and shear modulus G , shear wave velocity V_s , oedometric modulus E_c of the soil are obtained from empirical formulae as shown in equations (2.41), (2.42), (2.43) respectively

$$G = 1 + \frac{E}{2(1 + \nu)} \quad (\text{Eq 2.41})$$

$$V_s = \sqrt{\frac{G}{\rho}} \quad (\text{Eq 2.42})$$

$$E_c = \frac{(1 - \sigma)E}{(1 + \sigma)(1 - 2\sigma)} \quad (\text{Eq 2.43})$$

The above characteristics are useful in determining the allowable bearing capacity of the soil using equation (2.44). From there, the cross-sectional area of the foundation is determined using equation (2.45). The breadth and length of the footing are chosen using a trial and error method in such a way that the line of action of the resultant of the axial load from the column or wall passes through the centroid of the section.

$$q_a = \frac{q_f}{n} = \frac{K_s/40}{n} \quad (\text{Eq 2.44})$$

$$A = \frac{DD(\text{structure} + \text{footing} + \text{surchage}) + LL(\text{on column or wall})}{q_a} \quad (\text{Eq 2.45})$$

With

$K_s = 4\gamma V_s$, represents the subgrade coefficient

n : represents the safety factor ($n=4$).

DD: dead load

LL: live load

2.6 Modal analysis methodology

This analysis is used to determine the natural frequencies, periods of vibration and modes of deformation of the building. For regular buildings, the first two modes of vibrations are translational and the third is torsional. The natural periods of vibrations are compared with the fundamental period obtained from the spectral analysis.

2.6.1 Fundamental period of vibration

The fundamental period of a building is an inherent property which depends on the structure's characteristics. For its determination, expressions based on empirical formulae as that proposed by Ec8 for buildings with height of up to 40m in equation 2.46.

$$T_1 = C_t H^{\frac{3}{4}} \quad \text{Eq 2.46}$$

Where

C_t : is a coefficient that depends on the moment resisting type of the structure.

H : is the total height of the building above the foundations in meters

2.6.2 Vibration modes

The vibration modes of the structure are obtained from SAP 2000 after the simulation is launched with the calculated sections gotten from linear analysis. The most important are the first three modes, which should count for at least 80% of mass participation of the structure.

2.7 Pushover analysis methodology

This is a nonlinear static analysis method that consists of applying a gradually increasing lateral force on the building in order to predict the structure's behaviour under nonlinear force as the seismic load. Using this method, the failure regions (regions where the capacity resistance are lower than the seismic capacity demands) are easily identified. The results obtained from this analysis are presented as capacity curves which relates the base shear force and the displacement at the top of the building. The representative form of the curve for the hinge formation is as shown in Figure 2.10. It is divided into five main regions:

- Region A- B: represent a linear and elastic behaviour of the structure.
- Region B- C is characterised by a nonlinear phase corresponding to the development of plastic hinges.

- Region C- D is characterised by a sudden drop in the moment resisting capacity of the structure.
- Region D – E is characterised by a further drop in the resisting capacity of the structure.
- Region E – F is characterised by a major and complete loss in the moment resisting capacity of the structure.
- Point IO (immediate occupancy) represents a point of light damage and no permanent drift; the structure retains its original strength and stiffness.
- Point LS (life safety), represents a point of moderate damage and little permanent drift; the structure might be beyond economic repair and the damage affects non-structural members.
- Point CP (collapse prevention): represents a point of severe damage and there is large displacement of structural members; the structure is close to collapse.

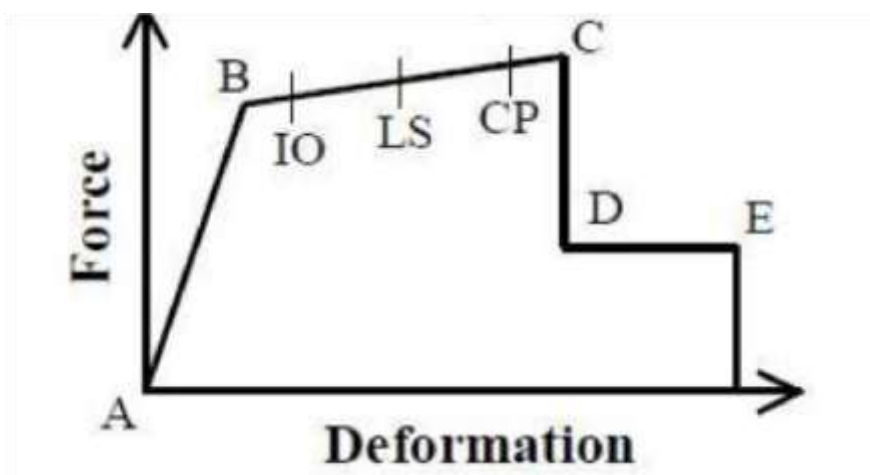


Figure 2.10. Force- Deformation for hinge formation

SAP2000 has a code colour representative of these various points as it is shown in Figure 2.11

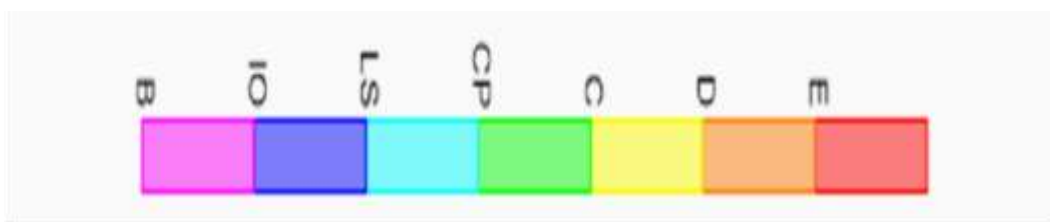


Figure 2.11. Colour codification for performance identification in SAP 2000

This analysis method is a practice procedure that estimates the structural capacity of buildings in the post-elastic range and enhances the lateral force procedure into the non-linear

regime. Pushover analysis is conducted with constant gravity loads and monotonically increasing lateral loading applied on the masses of the structural model until the displacement of interest is reached. In this thesis, base shear - roof displacement relationship is used as representative of force and displacement (see Figure 2.12).

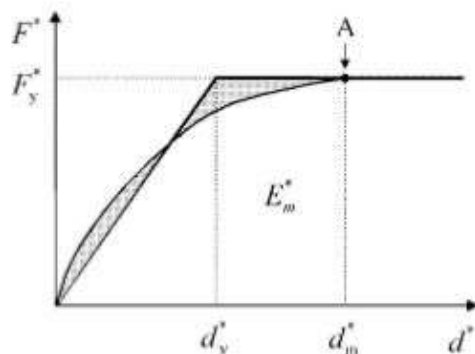


Figure 2.12. Pushover curve and bilinear idealisation scheme (P. Fajfar et al. 2004)

2.8 Soil structure interaction Analysis

Since the soil is a heterogeneous milieu, the real ground properties have to be considered when modelling the structure. In this part, we will consider a more real case, where the soil type and interactions between the soil and the foundation will be taken in to consideration, and the foundation modelled before determining the frequencies of the structure and the pushover analysis performed to study the storey displacements. The of soil subgrade modulus for different soil types is shown in figure 2.13 (subgrade modulus for different soil types by Forni, sd).

Nature du sol	C (t/m ³)
1 terrain légèrement tourbeux et marécageux	500- 1 000
2 terrain essentiellement tourbeux et marécageux	1 000- 1 500
3 sable fin	1 000- 1 500
4 remblais d'humus, sable et gravier	1 000- 2 000
5 sol argileux détrempé	2 000- 3 000
6 sol argileux humide	4 000- 5 000
7 sol argileux sec	6 000- 8 000
8 sol argileux très sec	10 000
9 terrain compacté contenant de l'humus du sable et peu de pierres	8 000-10 000
10 même nature que ci-dessus avec beaucoup de pierres	10 000-12 000
11 gravier fin et beaucoup de sable fin	8 000-10 000
12 gravier moyen et sable fin	10 000-12 000
13 gravier moyen et sable grossier	12 000-15 000
14 gros gravier et sable grossier	15 000-20 000
15 gros gravier et peu de sable	15 000-20 000
16 gros gravier et peu de sable mais très compacté	20 000-25 000

Figure 2.13. Subgrade modulus for different soil types (Forni, sd)

Conclusion

The various steps through which the accomplishment of this thesis have been presented in the above chapter. As a matter of facts, the structure was analysed and design according to the various design codes aforementioned. Analysis was performed using the structural analysis software SAP 2000 version 22 while the design was done manually with the aid of the analytic formulas provided by the European design codes (European standard), using Excel. The case study will be presented, analysed and designed following the aforementioned steps. For the modelling of the structure, we'll first work with fixed supports in our footings without considering the soil types, then we will take into consideration the soil-structure interaction and remodel the building, using springs to characterise our soil interactions at the level of the footings, then perform another pushover analysis. This will help us compare the results of the pushover analysis and other behaviours of the structure in the two cases. In the next chapter, results of the static and dynamic design are presented and interpreted.

Chapter 3. RESULTS

Introduction

The various procedures mentioned in the previous chapters were performed to determine the geometric characteristics of the different structural elements namely; beams, columns and footings. The case study, which is a six-storey building, is presented including its characteristics and design principles considered for its analysis and design. The solicitation parameters (moments, shear forces and axial forces) as well as the stresses in the constitutive materials are determined after the static analysis is performed. These data give indication on the choice of the characteristics (geometric and mechanical) of the structural elements (beams and columns and footings in this study). The structural elements, once they are designed, can now be used to model the entire structure on SAP2000 where the linear dynamic and non-linear static analyses (pushover analyses) will be performed to get the different behaviours of the structure to a particular ground force. From here, the soil structure interaction will also be considered and the foundation will be modelled and pushover analysis performed.

3.1 General presentation of the site

Here, we present the study area through its location, geology, relief, climate, hydrology, population and socio-economic activities.

3.1.1 Geographic location

Yaoundé is the political capital of Cameroon and chief town of the Centre region; situated at latitude 3.87° ($3^{\circ}50'$) North and longitude 11.52° ($11^{\circ}31'$) East at an elevation of 760 metres above sea level. Located 300km from the Atlantic Ocean and surrounded by 7 hills, Yaoundé belongs to the Mfoundi division of the Centre region and measures a total surface area of 183km^2 (18300ha).

3.1.2 Geology

The bedrock in Yaoundé is mainly composed of gneiss. This rock is neither porous nor soluble, but it is its discontinuities (faults, diaclases) that give fissure permeability to the formation. The hydrogeology is characterized by continuous aquifers, approximately exploitable overlying water bearing fissures or fracture aquifers in the bedrock; these types of aquifers are superimposed or isolated.

3.1.3 Relief

Concerning the relief, the land rises gently in escarpments from the south-western coastal plain before joining the Adamawa Plateau via depressions and granite massifs. The field is characterised by rolling, forested hills, the tallest of which have bare, rocky tops.

3.1.4 Climate

Yaoundé features a tropical wet and dry climate, with record high temperatures of 36°C, an average of 23.8°C and a record low temperature of 14°C. Primarily due to the altitude, temperatures are not as high as would have been expected for a city located near the equator. The town of Yaoundé features a lengthy rainy season covering a nine-month span between March and November. However, there is a noticeable decrease in precipitation within the rainy season, observed during the months of July and August, giving the city the appearance of having two rainy and two dry seasons. The average precipitation is 1650mm of rain per year and average humidity is 80%.

3.1.5 Hydrology

The hydrographic network of Yaoundé is very dense and composed permanent rivers such as the Mfoundi river which crosses the city from North to South, a few creeks and lakes. Yaoundé is part of the western sector of the Southern Cameroon Plateau. The area is characterized by gentle rolling chains of hills, and numerous valleys and wetlands; this varied physical landscape permits a combination of streams, hydromorphic soils and a great variety of plants and Fauna.

3.1.6 Population and

Yaoundé has a total population estimated at 3.8 million in 2019. The city of Yaoundé being a cosmopolitan city, there is a considerable portion of population coming from several other region of the country (west, far north etc.).

3.1.7 Socio-economic activities

Most of Yaoundé's economy is centred around the administrative structure of the civil services and the diplomatic services. Due to these, Yaoundé has a higher standard of living and security than the rest of Cameroon. However, Yaoundé is a tertiary city and there are a few industries: breweries, sawmills, carpentry, tobacco, paper mills, machinery and building materials.

3.2 Presentation of the project

Our case study is a building constructed for administrative purposes in the National Advanced School of Public Works in Yaounde. Though not yet occupied, its external finishing has been made with allucobon (see figure 3.1). The building is found on the left when you enter from the school main gate just before you go up to the basketball court and directly behind it we have the block I which is found the school disciplinary office. This edifice can be said to be the most beautiful structure in the campus as it is the centre of attraction of every road user passing on the

Elig-effa – Mini-firm Street. The building comprises of offices, conference rooms, store rooms, and toilets. It has two main stair cases (one at each extreme) and one special stair case at the fifth floor which gives access to the conference room on the sixth floor. There is just one lift case in the building comprising of two lifters



Figure 3.1. Administrative building in the NASPW Yaounde

The new administrative building of the NASPW Yaounde is made up of three reinforced concrete building block frames (block A, block B and block C) each separated by a rupture joint. Blocks A and B are made up of six-storeys for office use while block C consists of 6 storeys and contains an emergency staircase. The formwork view is shown in figure 3.2.

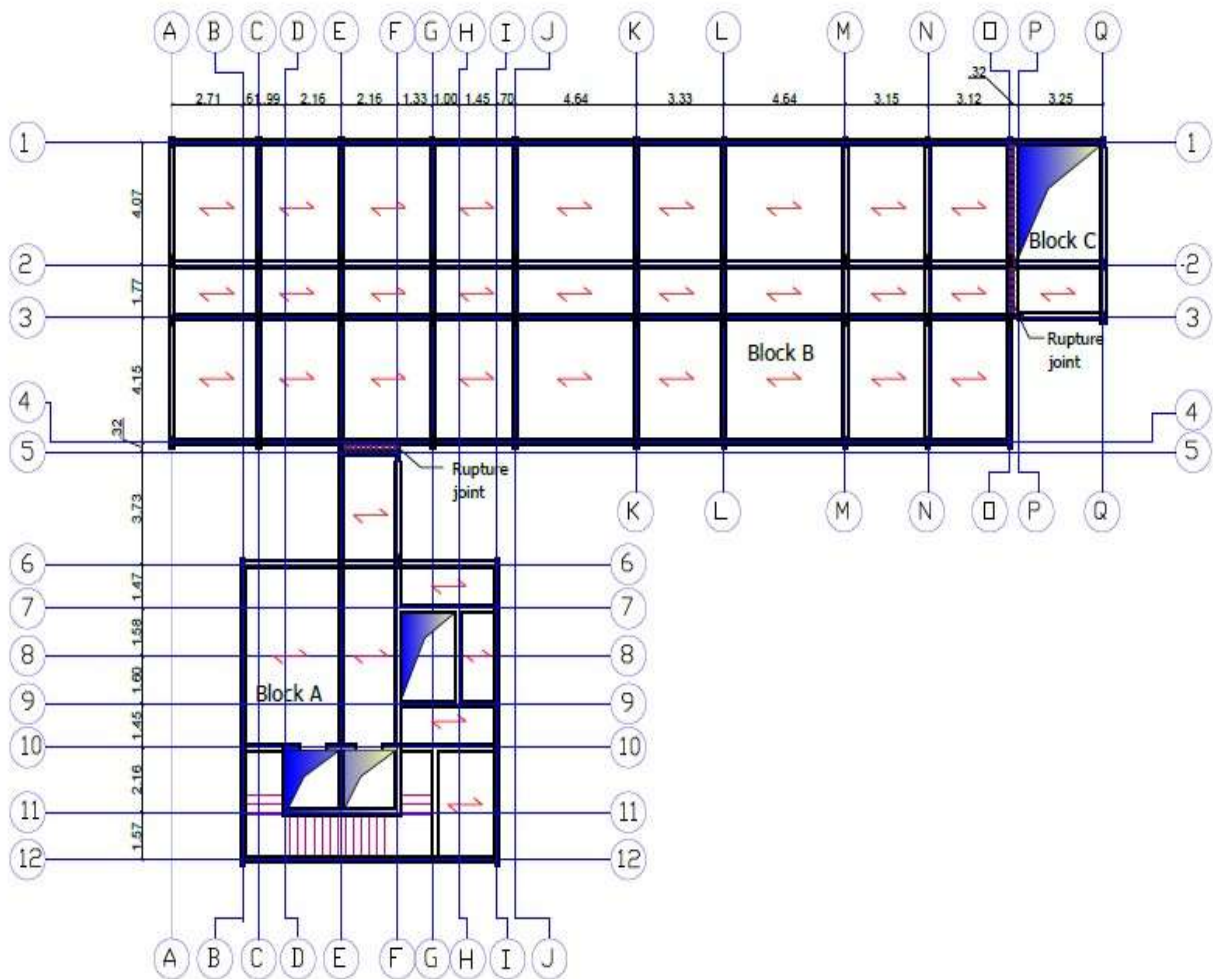


Figure 3.2. Formwork plan of the building

Since the different building blocks are separated by rupture joints, they can be studied separately. In the case of our studies we will be working on Block B. It is a rectangular floor, with its length being 32.18m and the width 10.19m. The slab is assumed to be a reinforced concrete slab with hollow blocks of thickness 20cm. The height of every floor is 3.2m making a total height of 19.2m for the building. The building is regular in plan and irregular in elevation. The formwork plan and a cut sections of building block B are shown in figure 3.3, figure 3.4 and figure 3.5 respectively. Beams on the same floor do not have the same design. They have the same sections but not the same influence areas, and this is the case in either directions (x-direction and y-direction).

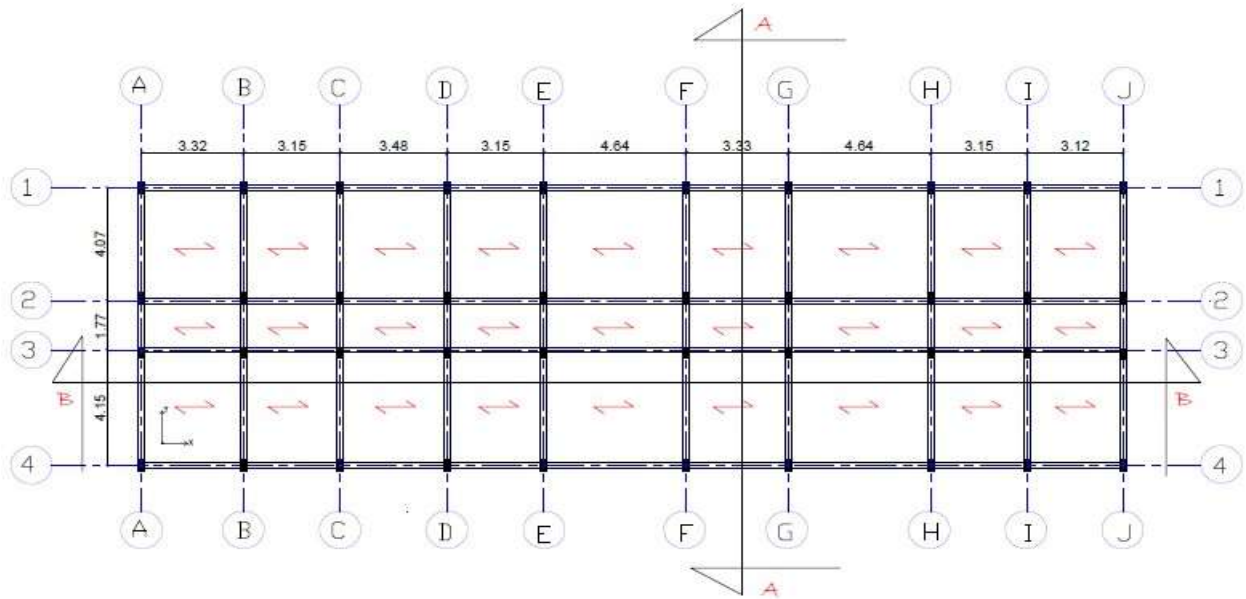


Figure 3.3. Formwork plan of block B

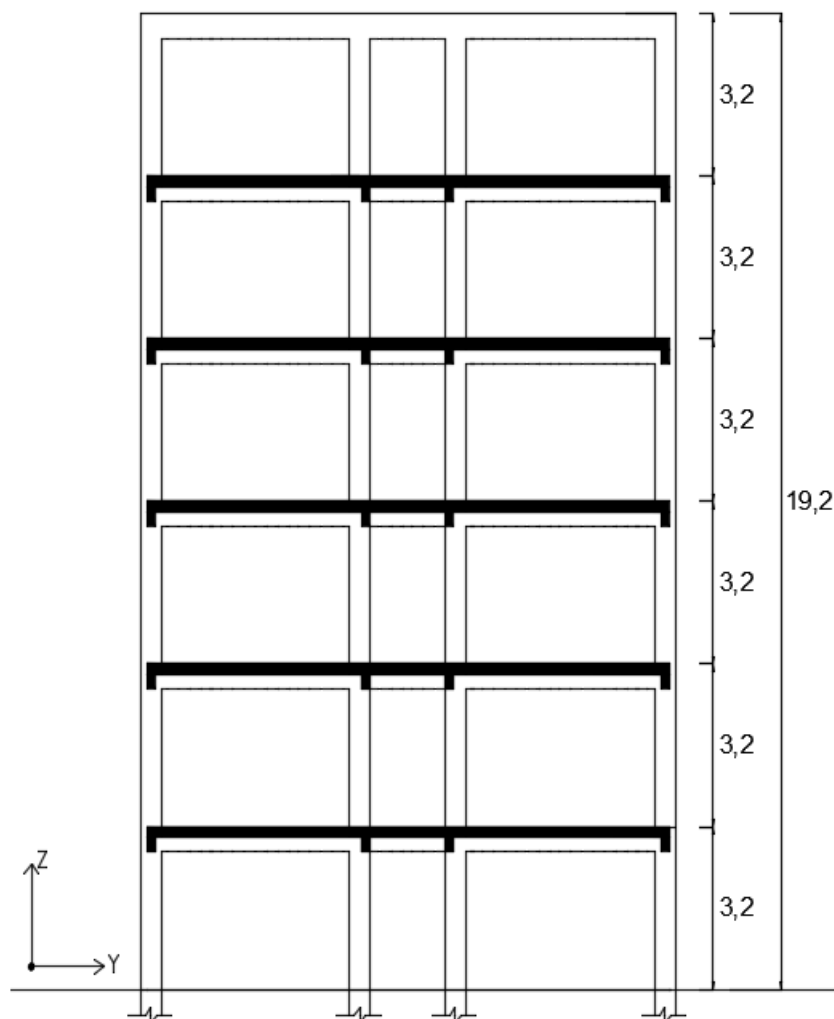


Figure 3.4. Section A-A of block B

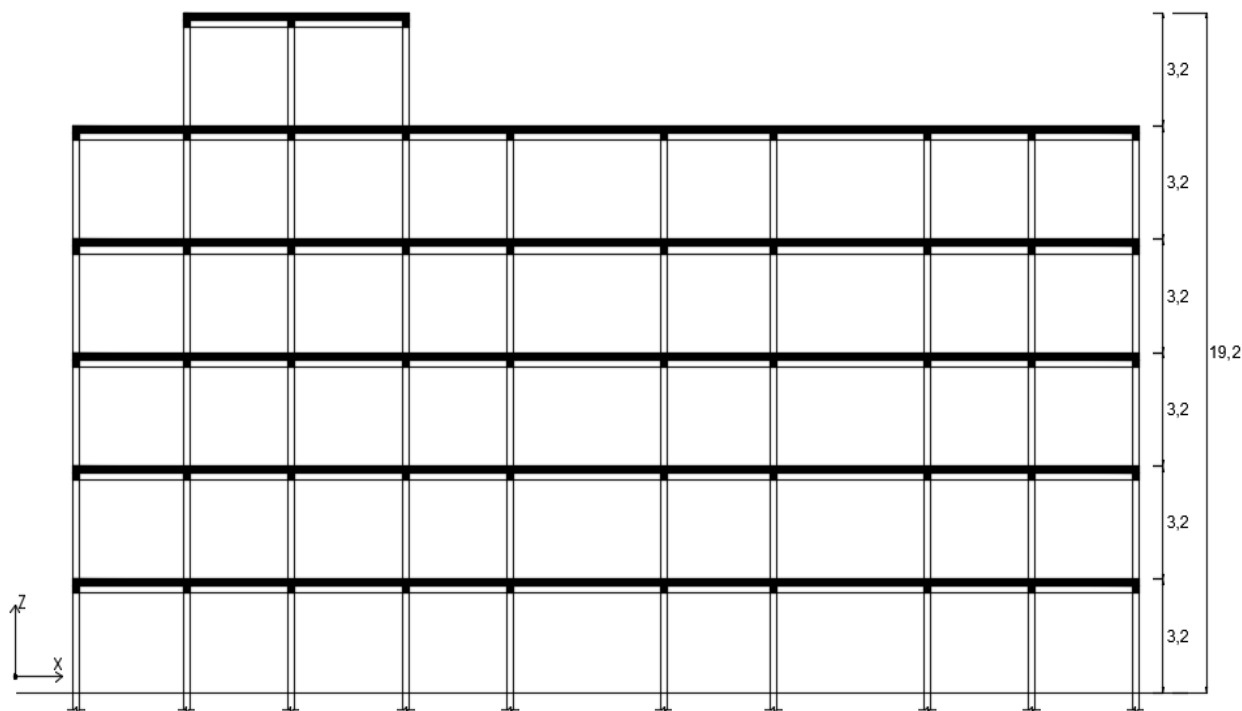


Figure 3.5. Section B-B of block B

3.3 Presentation of data collected

The Data collected on site were mainly geotechnical (soil type) and structural (which has to do with the materials used in the construction).

3.3.1 Geotechnical data

The ground type condition considered for this study is that of compacted ground containing sand humus and few stones.

3.3.2 Material properties

The concrete class chosen is C25/30 and the longitudinal steel reinforcement is FE400. We consider a characteristic yield strength of 235 MPa for the transversal reinforcement. Table 3.1 below shows the main characteristics of concrete and Table 3.2 that of steel used as reinforcement for linear analysis and design of the structure.

Table 3.1. Concrete characteristics.

Property	Value	Unit	Definition
Class	C25/30	-	Concrete class

R_{ck}	30	MPa	Characteristic cubic compressive strength
f_{ck}	25	MPa	Characteristic compressive strength of concrete at 28 days
$f_{cm} = f_{ck} + 8$	33	MPa	Mean value of concrete cylinder compressive strength
γ_c	1.5	-	Partial factor for concrete
$f_{ctm} = 0.3 \times (f_{ck})^{\frac{2}{3}}$	2.56	MPa	Mean value of axial tensile strength of concrete
$f_{ctd} = 0.7 \times \frac{f_{ctm}}{\gamma_c}$	1.2	MPa	Design resistance in traction
$E_{cm} = 22000 \times \left(\frac{f_{cm}}{10}\right)^{0.3}$	31476	MPa	Secant modulus of elasticity
ν	0.2	-	Poisson's ratio
G	13115	MPa	Shear modulus
γ	25	kN/m ³	Specific weight of the concrete

Table 3.2. Longitudinal reinforcement characteristics

Property	Value	Unit	Definition
Class	FE400	-	Steel class
f_{yk}	400	MPa	Characteristic yield strength
γ_s	1.15	-	Partial safety factor for steel
γ	78.5	MPa	Specific weight of the steel
ν	0.3	-	Poisson's ratio

3.4 Actions on the building and load combinations

The building is subjected to vertical (gravity) loads. The loads are either permanent or variable and are combined in various combinations in order to study the various effects and to determine the unfavorable (worst loading case) situation.

3.4.1 Permanent action

There are two categories of permanent loads acting on the structure which are the permanent structural loads and the permanent non-structural loads. Both are presented in Table 3.3 and Table 3.4 below.

Table 3.3. Structural loads of building

Nature	Description	Value	Unit
G _{1k}	Hollow block slab (16+4 cm)	2.85	kN/m ²

Table 3.4. Non-structural loads of the building

Nature	Description	Value	Unit
G _{2k}	Tiles	0.44	kN/m ²
G _{2k}	Cement coating(1.5 cm thick)	0.33	kN/m ²
G _{2k}	Partition wall (15 cm thick)	1.35	kN/m ²
G _{2k}	Alucobond	0.08	kN/m ²
Total G_{2k}		2.2	kN/m²

3.4.2 Variable actions and load combinations

The building, because of its function is classified as category B building for which the imposed load is in the range 2.0 to 3.0 kN/m². In this work we consider an imposed load of 2.5 kN/m².

3.4.3 Load combinations

The load combination in the equation below provides for the verification of the structure at Ultimate Limit State.

$$1.35G_k + 1.5Q_k \quad (\text{Eq. 3.1})$$

$$G_k = G_{1k} + G_{2k} \quad (\text{Eq. 3.2})$$

For non-reversible Serviceability Limit State (SLS), the verification is done using the following equation.

$$G_k + Q_k \quad (\text{Eq.3.3})$$

3.5 Linear Static design

Static design is done for vertical static actions on the building. This implies considering only permanent and imposed loads. The procedure goes by selecting one horizontal and one vertical element of the structure for their respective designs.

3.5.1 Durability and concrete cover to reinforcement

Considering a concrete structural class S4 and the exposure class XC1 together with the provisions of the Eurocode 2 outlined in section 2.2.1, the concrete cover obtained is given by:

$$C_{min} = \max(16; 15; 10) = 16mm$$

$$\text{From Eq. 2.3, } C_{nom} = 16 + 10 = 26mm$$

. We will consider a minimum concrete cover of 30mm in the following design situations.

3.5.2 Horizontal structural component

3.5.2.1 Preliminary design

The principal and secondary beams constitute the horizontal structural elements. Principal beams are those which support the slab and transfer the loads to the columns. Since the different building blocks are separated by rupture joints, they can be studied separately. So our work is focused on block B since it contains the beam selected for the studies as seen on Figure 3.6.

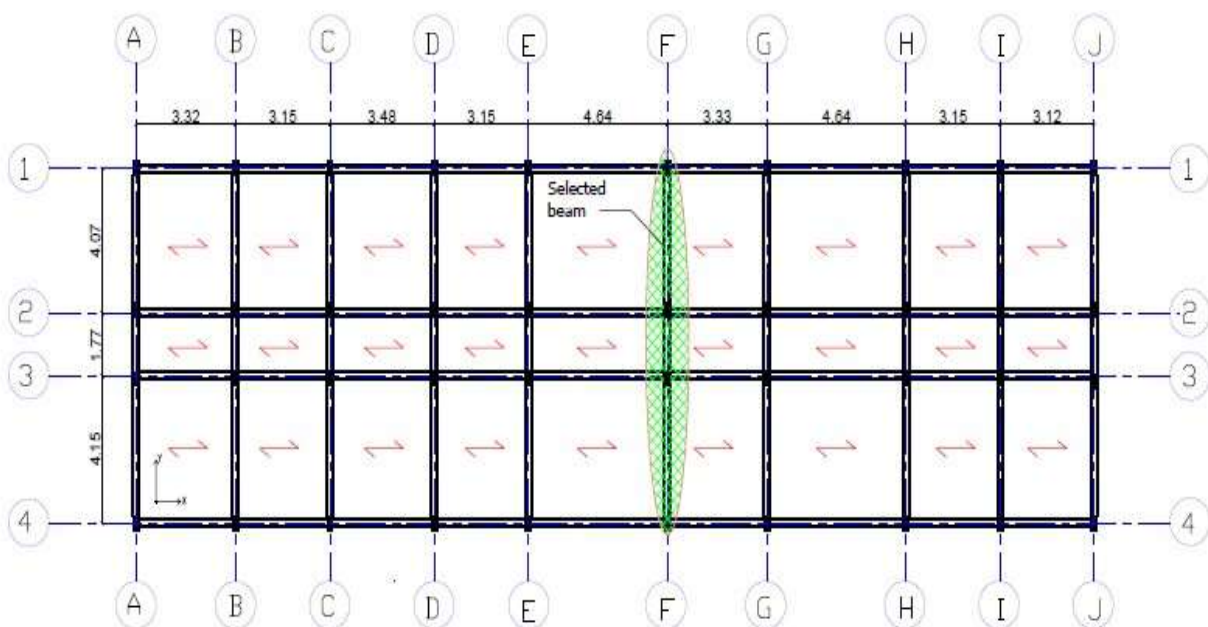


Figure 3.6. Selected beam for design

The dimensions b (width) and h (depth) are the geometric characteristics of the beam section. On the site the values measured are $b=200\text{ mm}$ and $h=500\text{ mm}$ as represented in figure 3.7.

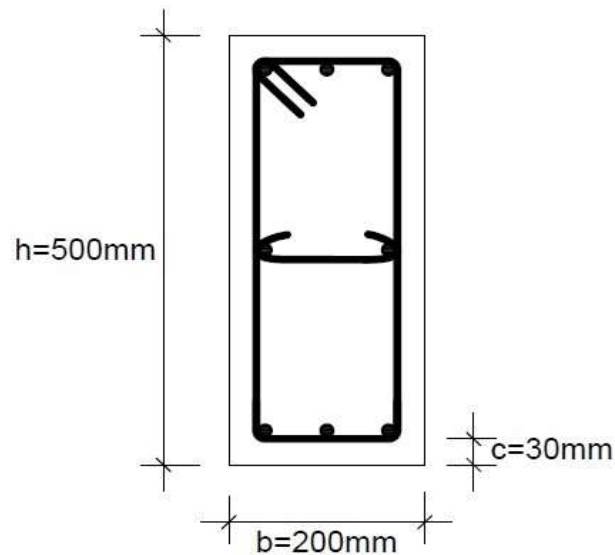


Figure 3.7. Dimensions of the beam section

For the design of the above horizontal element, ten (10) load arrangements are considered from which design solicitation parameters are determined. The load arrangements are shown in Figure 3.8.

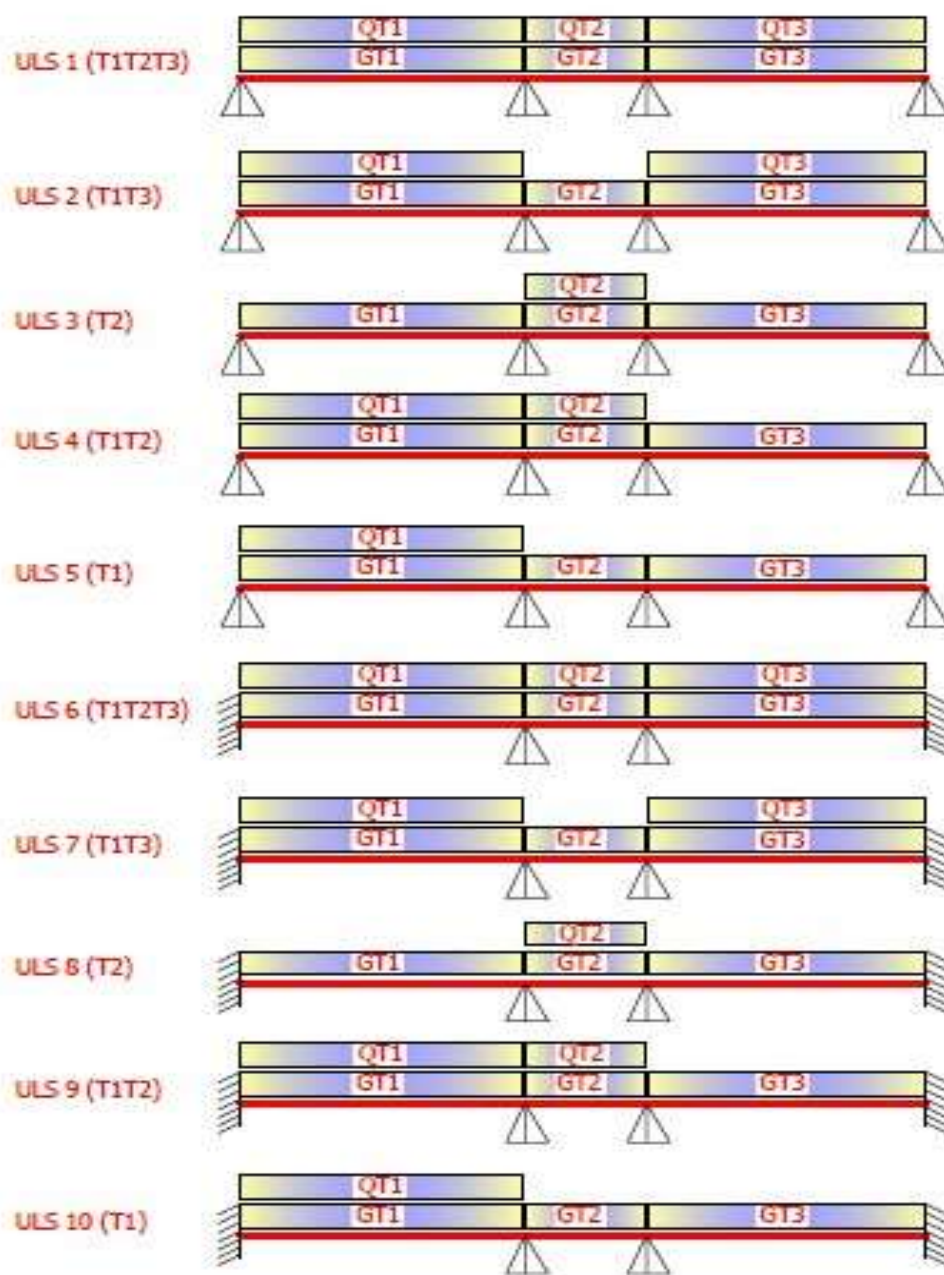


Figure 3.8. Load combinations at ULS

Henceforth, we proceed the modelling and the design of the horizontal structural element with the use of SAP 2000 and Excel. End supports of the beam are modelled with simple support for maximum positive bending moment at mid-spans and fixed supports for maximum negative bending moment. The static scheme of the studied beam considering simple supports is shown on figure 3.9, while that for the fixed supports is shown on figure 3.10

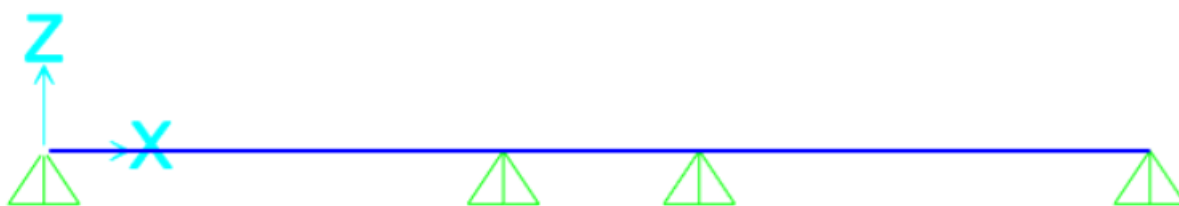


Figure 3.9. Beam model with simple supports

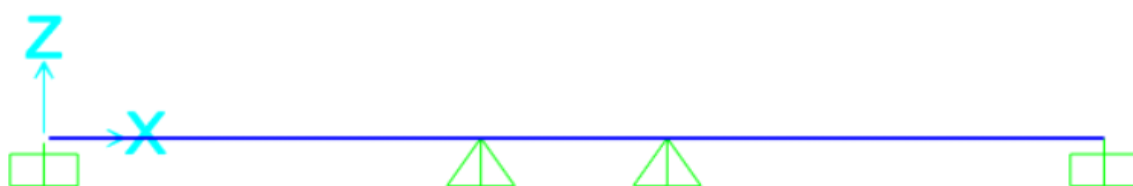


Figure 3.10. Beam model with fixed supports

3.5.2.2 Ultimate Limit State

The curves in figure 3.11 and figure 3.12 show the solicitations for bending moment and shear forces respectively for the beam obtained from the results of the analysis performed in SAP software.

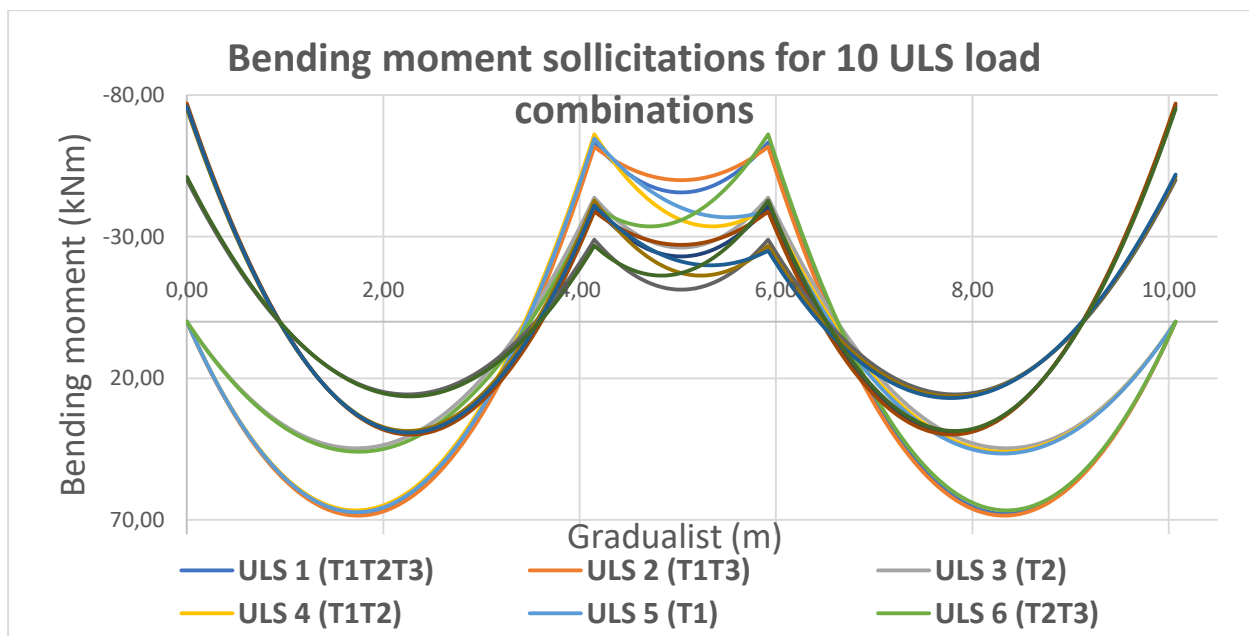


Figure 3.11. Bending moment solicitation curves of the beam

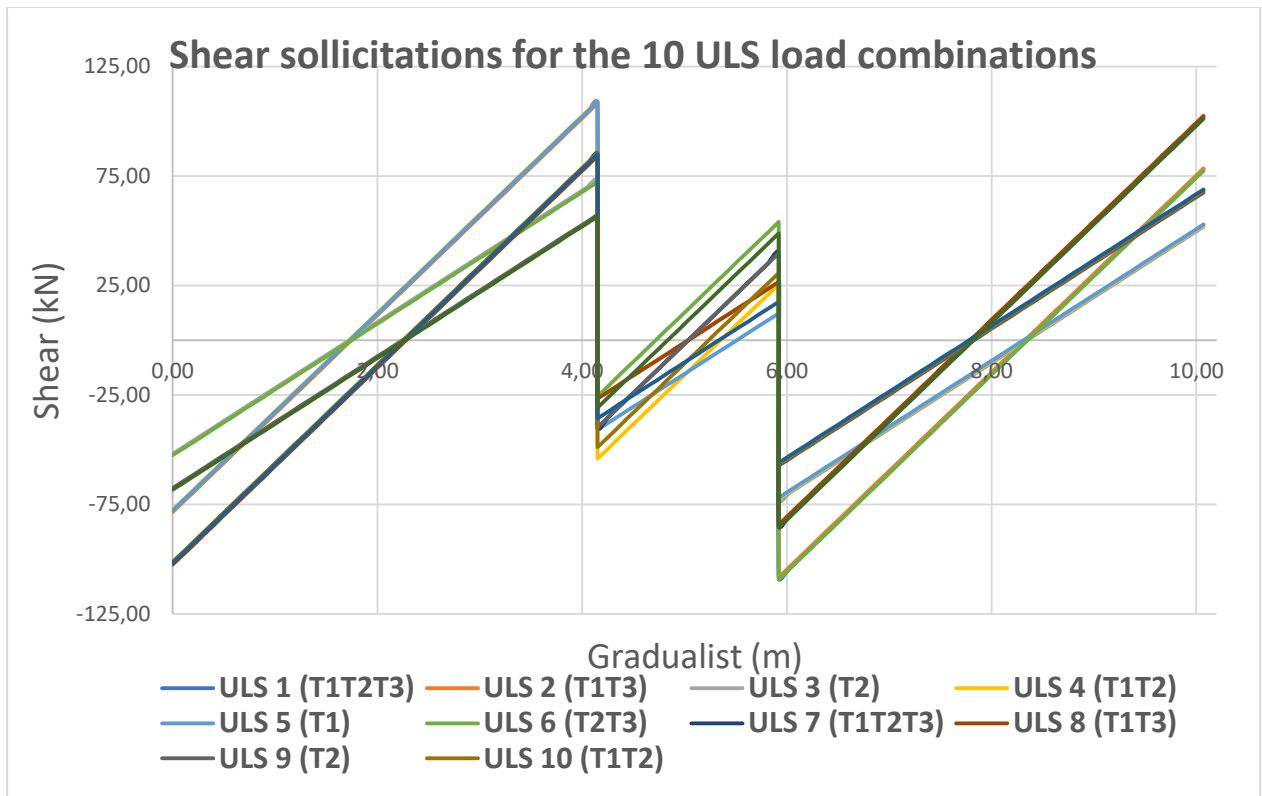


Figure 3.12. Shear solicitation curves on the beam

We obtain the envelope curve (which is the maximum of positive values and the minimum for negative values from all the combinations) of both bending moment and shear forces from the above curves as represented in figure 3.13 and figure 3.14 respectively;

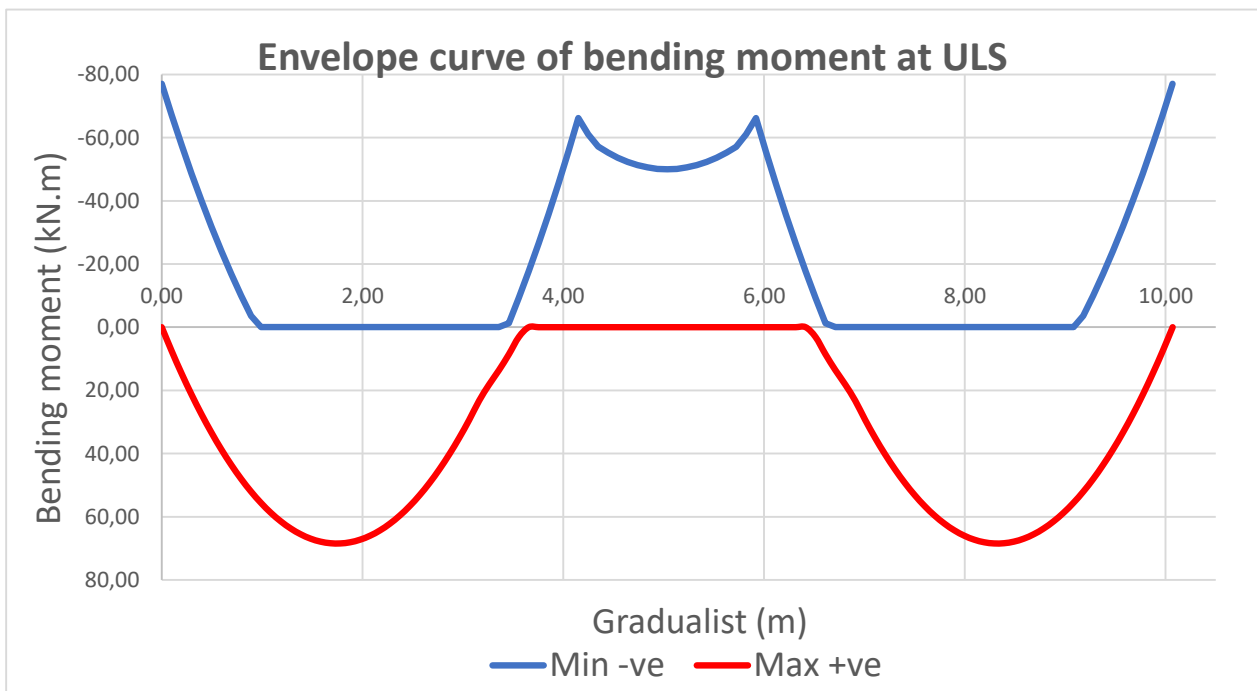


Figure 3.13. Envelope curve for bending moment

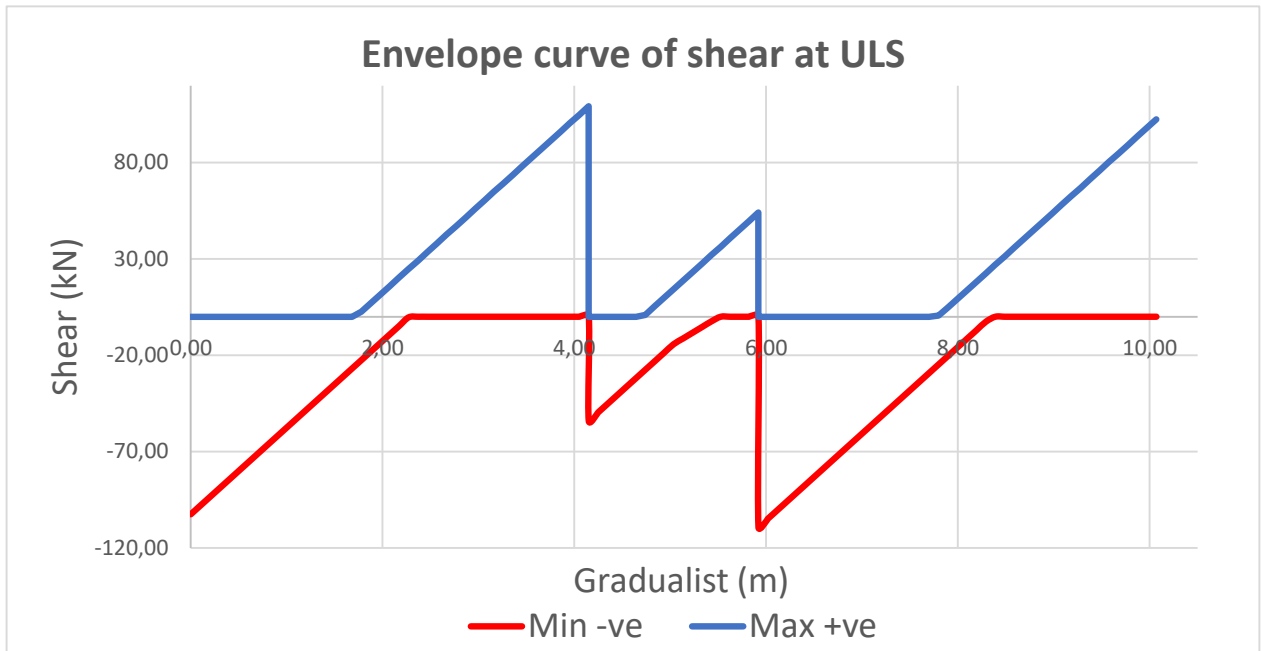


Figure 3.14. Envelope curve for shear solicitation

The steel reinforcements are computed using Eq. 2.7. The verifications are performed for the detailing of the horizontal structural element using equations 2.11 and 2.14. Finally, the steel section is verified for a beam section of $200 \times 500 \text{ mm}$. In Figure 3.15 are the reinforcements obtained from the previous computations.

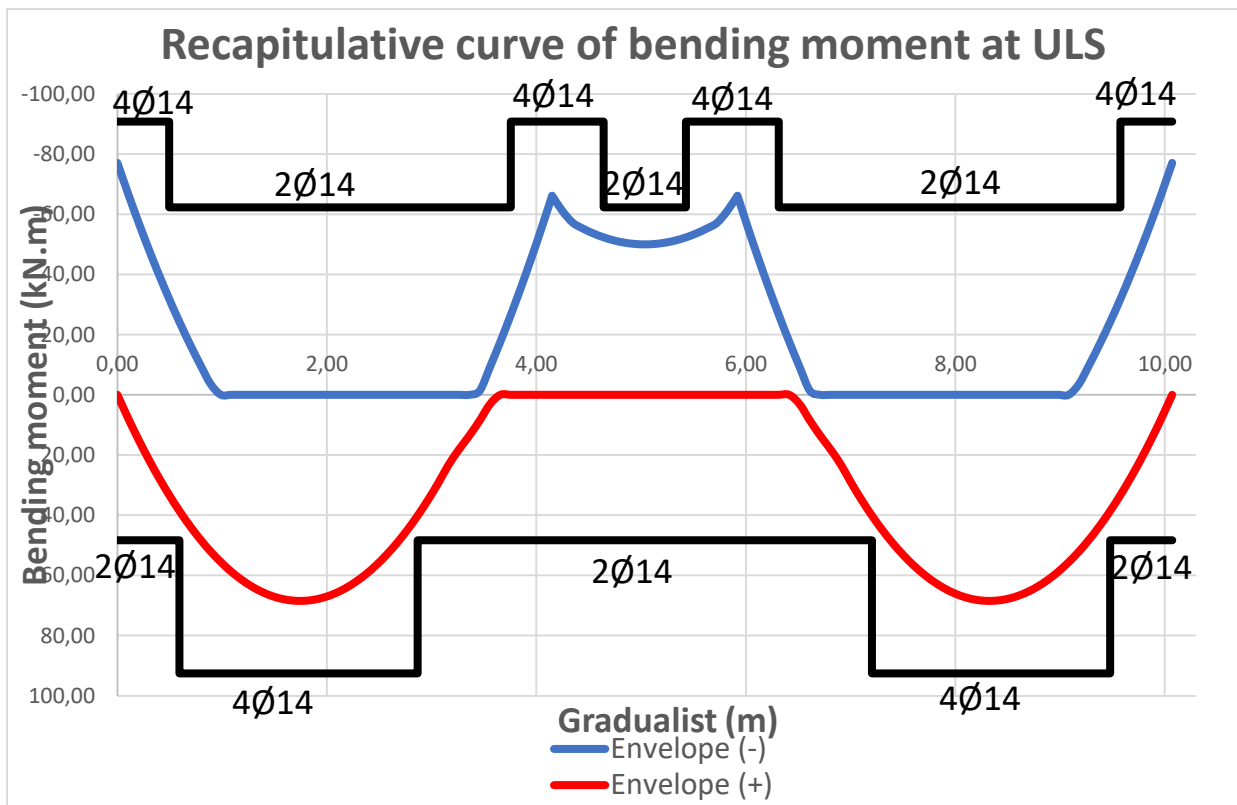


Figure 3.15. Recapitulative curve for bending moment verification of the beam

Figure 3.16 presents the spacing of the transversal reinforcements for shear resistance. The later is computed through the Eurocode 2 provisions expressed in section 2.2.2.1 (b), which presents equations used to obtain the stirrups. We consider diameter of 6 mm for shear resisting mechanism.

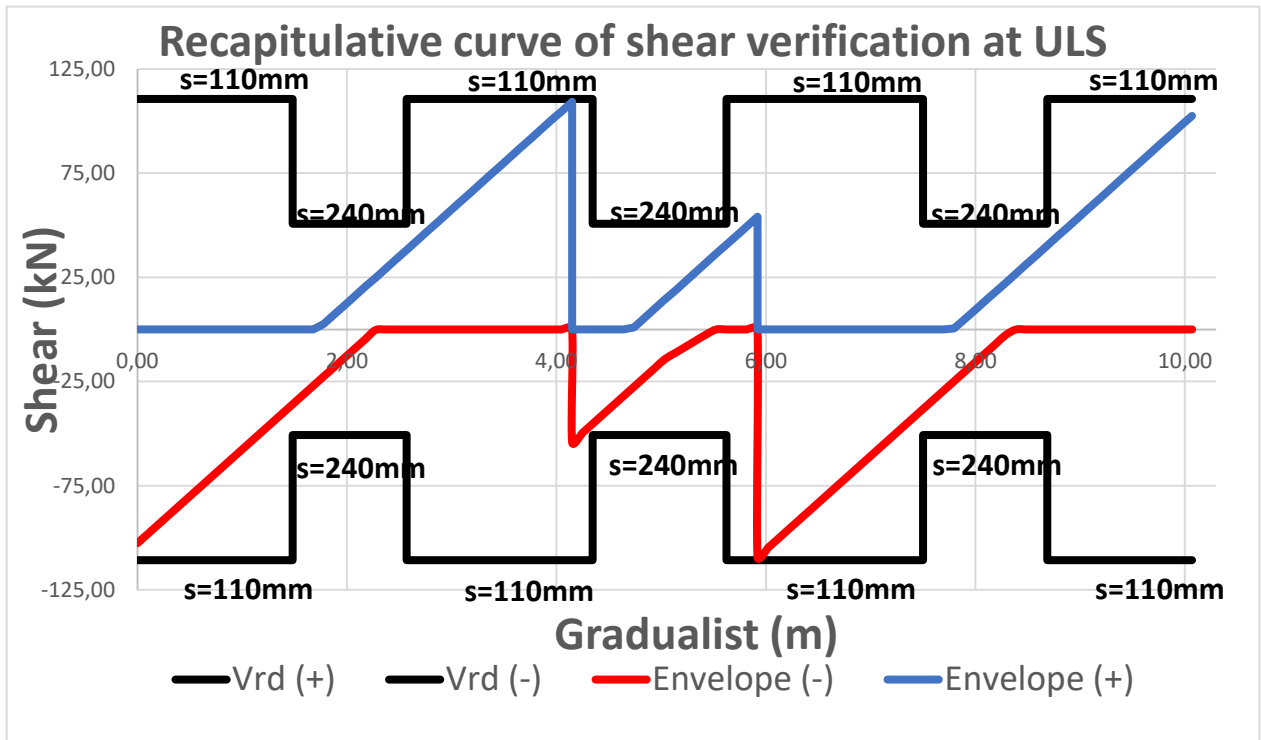


Figure 3.16. Recapitulative curve for shear verification of the beam

3.5.2.3 Stress limitation in serviceability limit state

For the same 15 load arrangements of the beam, we obtain the solicitation curves for SLS by using the SLS load combination in equation 3.3 shown in Figure 3.17.

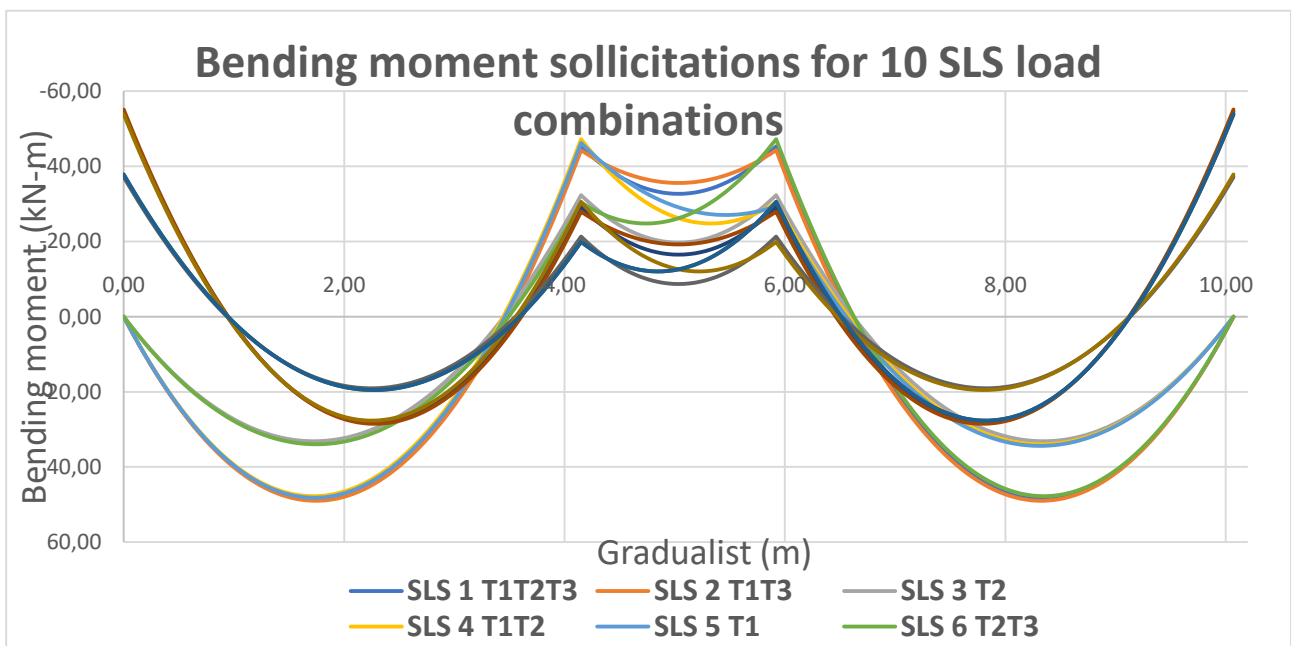


Figure 3.17. Bending moment solicitation curves for the beam at SLS

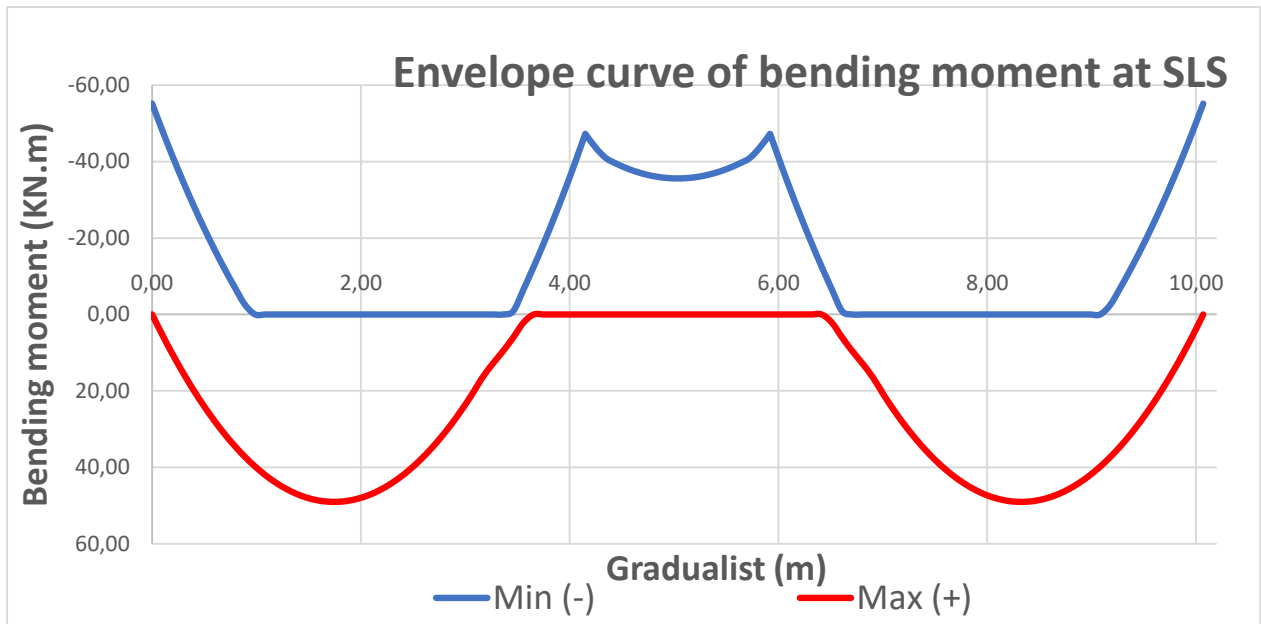


Figure 3.18. Envelope curve for bending moment at SLS

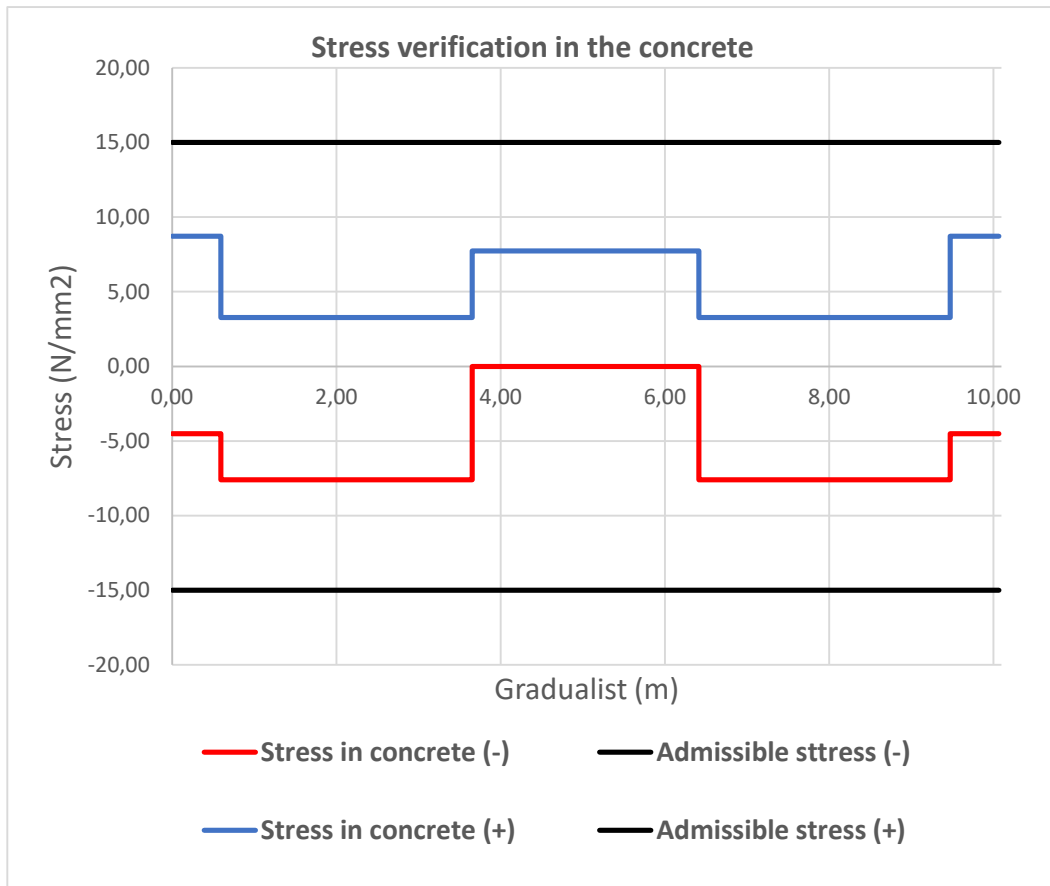
Likewise the solicitation curves for bending moment at ULS, an envelope curve, as shown in Figure 3.18, is obtained from the solicitation curves for SLS.

The stresses in concrete and in the reinforcing steel are respectively obtained as expressed in equations 2.21 and 2.22 reminded here.

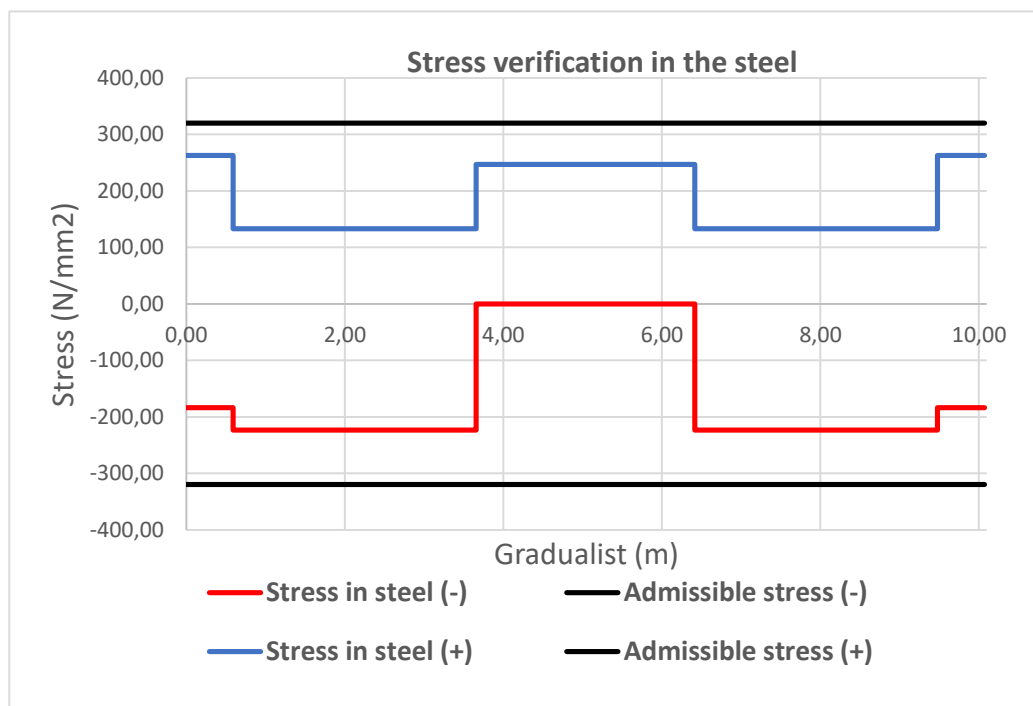
$$\sigma_s = \frac{M_{Ed}(d - x)}{J_{cr}} \times n_{\infty}$$

$$\sigma_c = \frac{M_{Ed} \cdot x}{J_{cr}}$$

The values obtained are compared to the limit values of stress in both concrete and steel respectively according to equations 2.23 and 2.24. The values of k_1 and k_3 are given by the Eurocode provisions as 0.6 and 0.8 respectively. The admissible stress and the actual stresses are compared in the subsequent figure. Figure 3.19 shows the respective curves for the stress verification in both concrete (a) and steel (b).



(a) Stress verification in concrete



(b) Stress verification in steel

Figure 3.19. Recapitulative curve of the stress verification of the beam

Figure 3.20 shows the reinforcement details of the studied beam. Due to the large height of the beams, constructive reinforcements are placed, which were not calculated based on sollicitations. They just help in the confinement of the concrete section thereby limiting the occurrence of cracks.

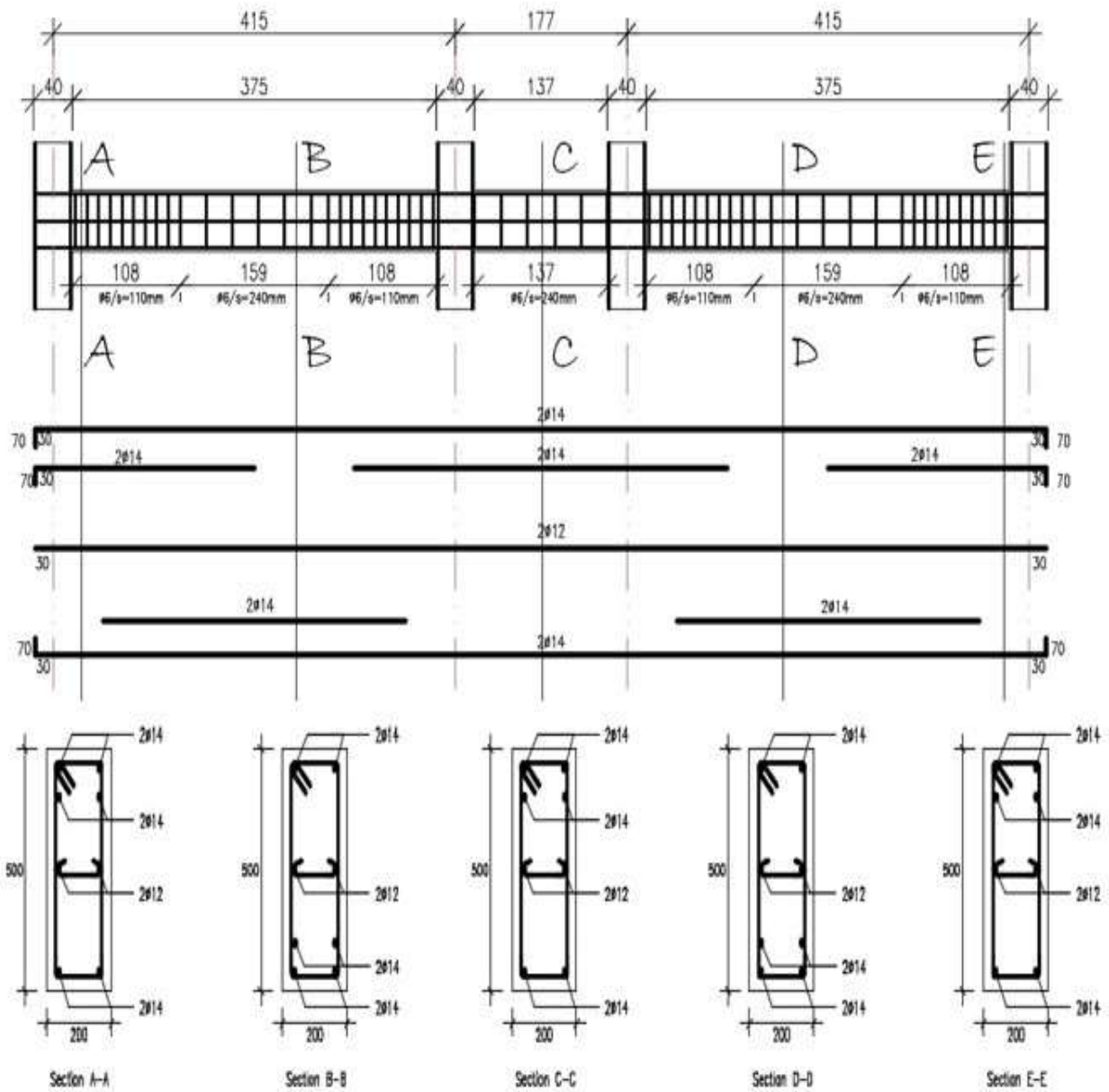


Figure 3.20. Recapitulation of beam detailing

3.5.3 Vertical structural elements

The vertical structural elements of the structure are composed only of the columns. Then one of them will be considered for the design. The column chosen for the design is the column corresponding to row F2 presented in figure 3.21.

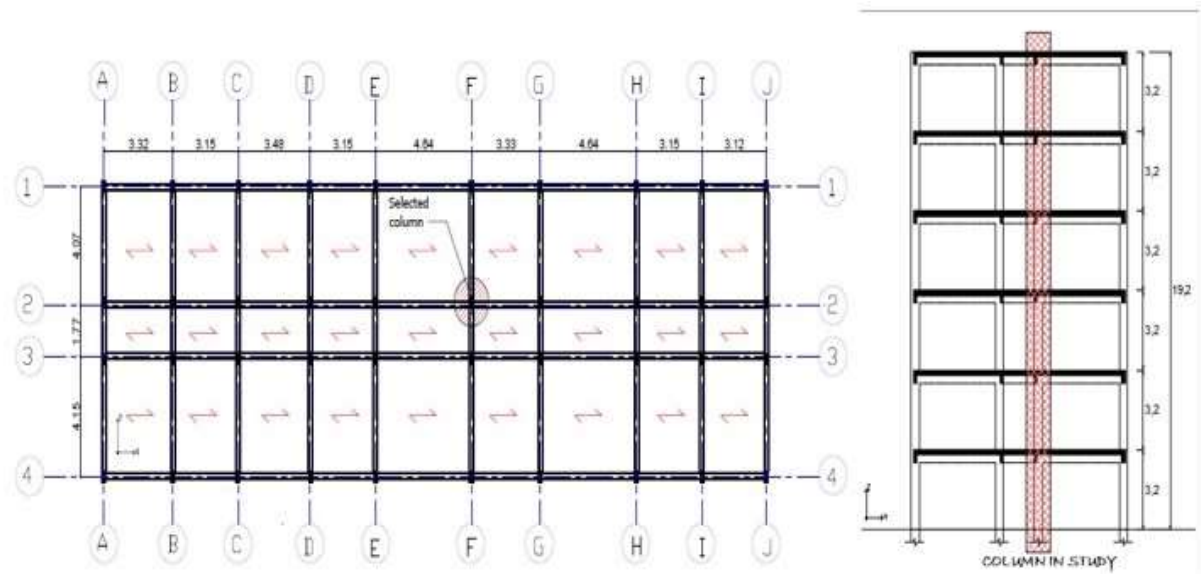


Figure 3.21. Choice of the studied column

The design of the column is done by the 3D modeling of the structure with fixed base. The vertical elements as well as the horizontal elements are modelled as frame elements.

The combination of the principal beams loads arrangements and the secondary beams loads arrangements leads to seven (07) load arrangements for the columns.

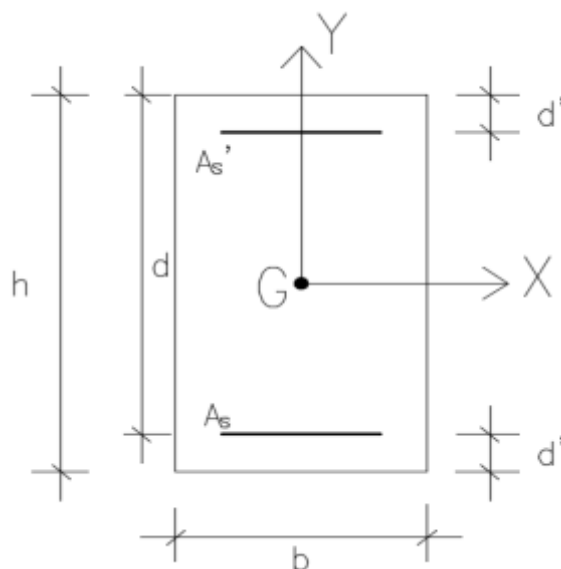


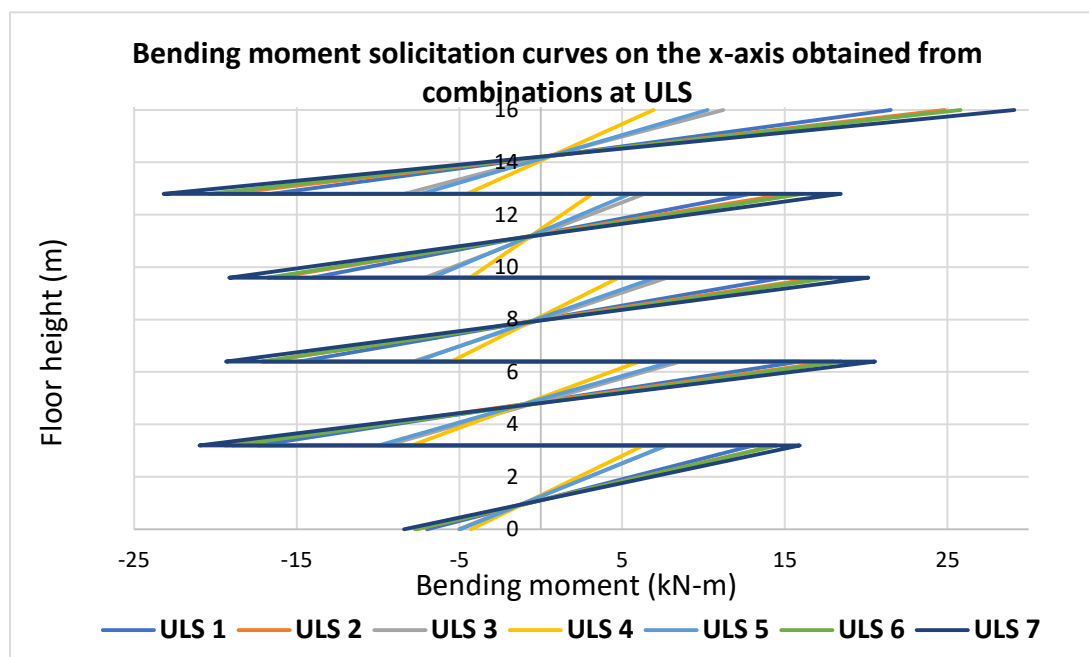
Figure 3.22. Dimensions of the beam section

3.5.3.1 Preliminary design

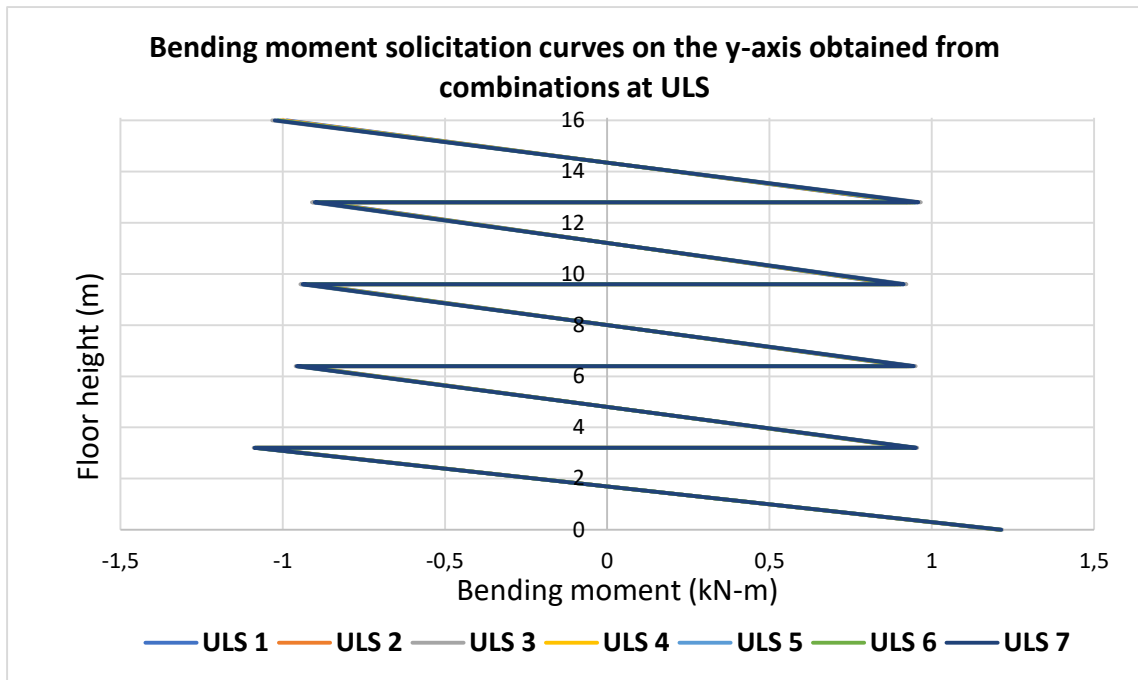
The dimensions b (width) and h (depth) are the geometric characteristics of the column section. On the site the values measured are $b=200\text{ mm}$ and $h=400\text{ mm}$ as represented in figure 3.22. This section of column goes from the first to the last floor.

3.5.3.2 Bending moment-axial force design verification

The load combinations considered for the principal and secondary beams of the building generate the following solicitation curves for bending moment presented in Figure 3.23 and axial force presented in Figure 3.24.



(a) Bending moment solicitation curves in the x-direction



(b) Bending moment solicitation in the y-direction

Figure 3.23. Bending moment solicitation curves on the columns

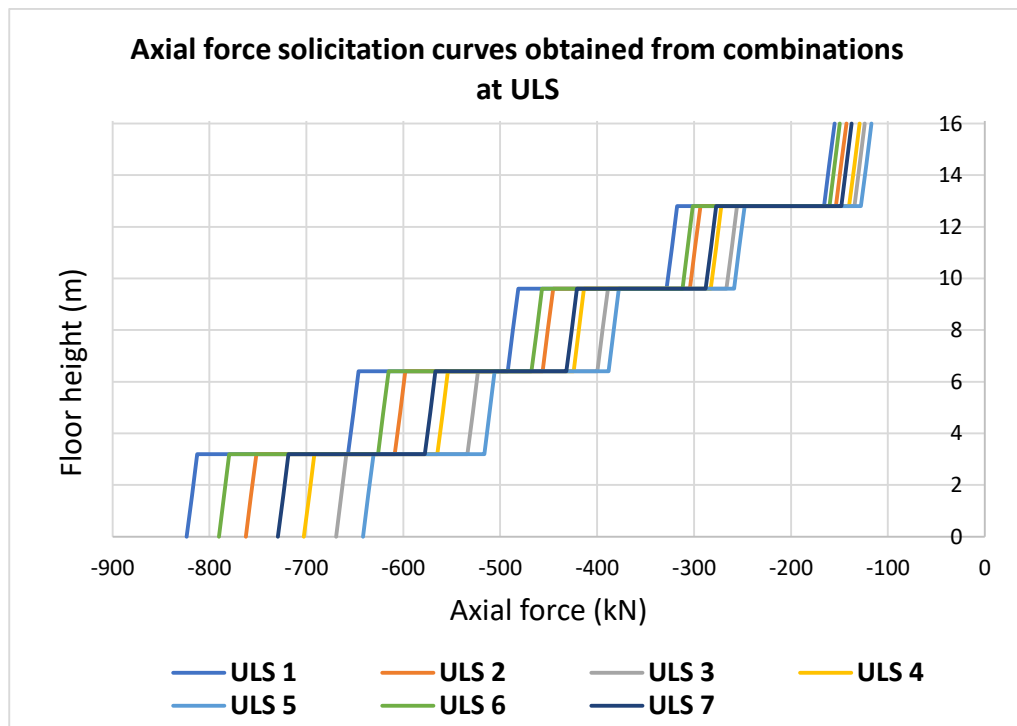
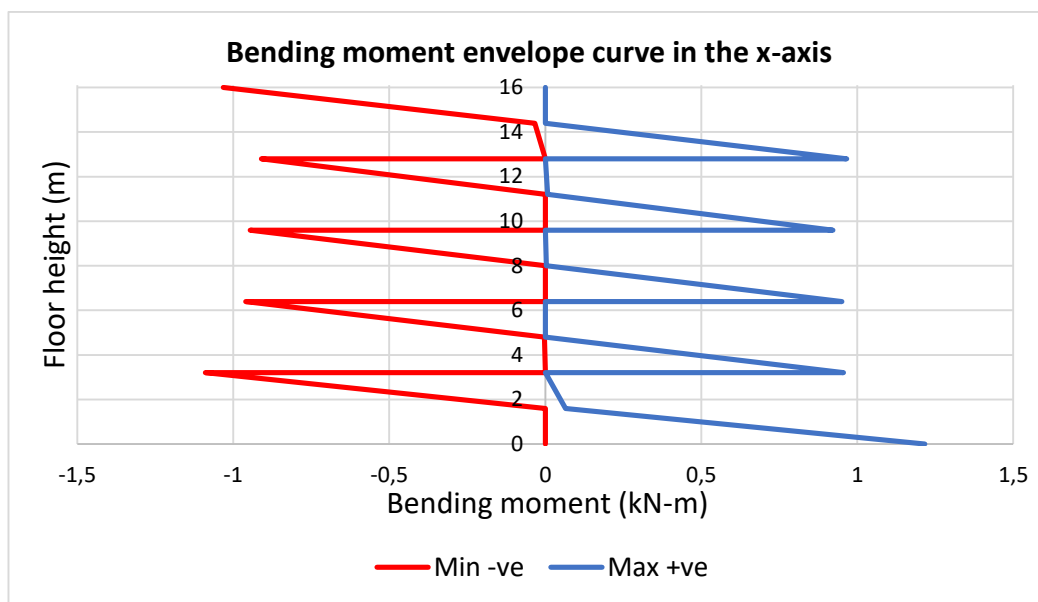


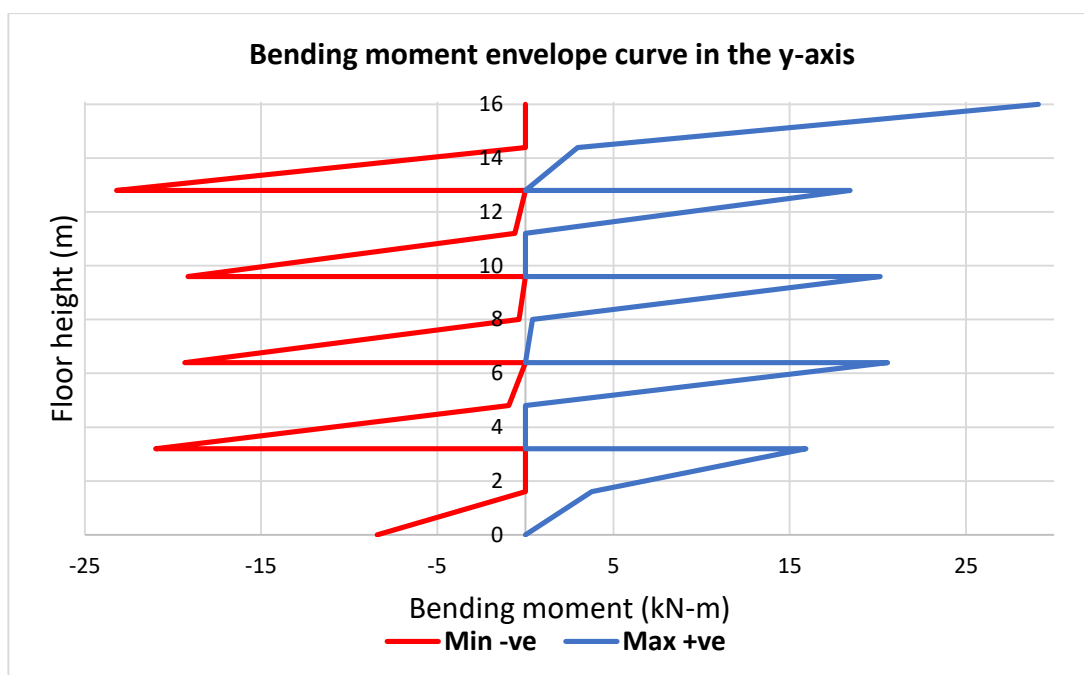
Figure 3.24. Axial load solicitation curve on the column

Similarly to the beam design, the maximum of the positive values and the minimum of the negative values are extracted from the curves in figure 3.23 and figure 3.24 above to obtain the

envelope curve for both bending moment and axial forces respectively. The envelope curves are presented in figure 3.25 and figure 3.26.



(a) Bending moment envelope curve on the x-axis



(b) Bending moment envelope curve on the y-axis

Figure 3.25. Envelope curve of bending moment on the column

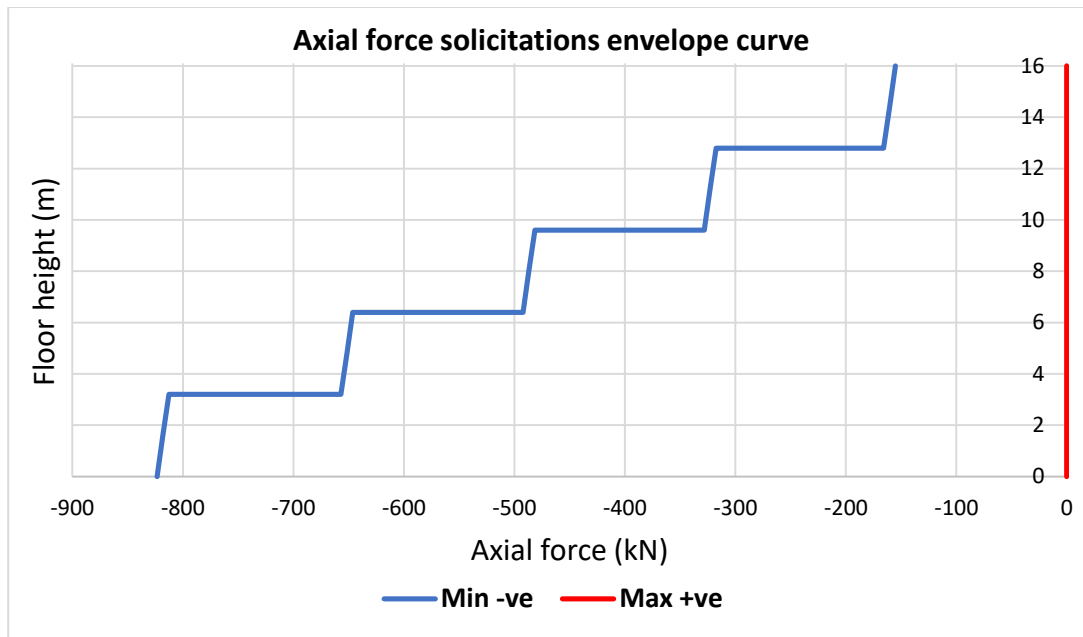


Figure 3.26. Envelope curve of axial load on column

The column verification can be assessed by calculating moment-axial load interaction diagram. Tension is assumed negative, whereas compression is considered positive. According to section 2.6.3.2 and equations 2.34 and 2.35 we obtain that:

$$237mm^2 \leq A_s \leq 5600 mm^2$$

Therefore, we select 4 Ø14 ($A_s = 616 mm^2$) and a covering $c = 30 mm$. This column section can be verified by calculating moment-axial load interaction diagram in both X and Y directions. Tension is assumed negative, whereas compression is considered positive. The M-N diagram for the columns are presented in figure 3.27 and figure 3.28 for x-direction and y-direction respectively.

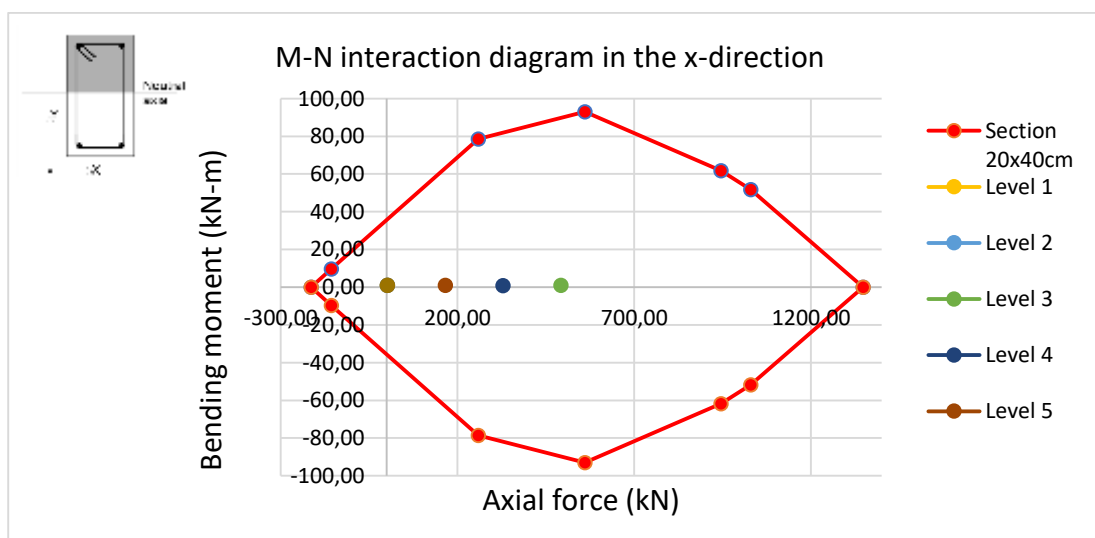


Figure 3.27. Interaction diagram of the column F2 in the x-direction

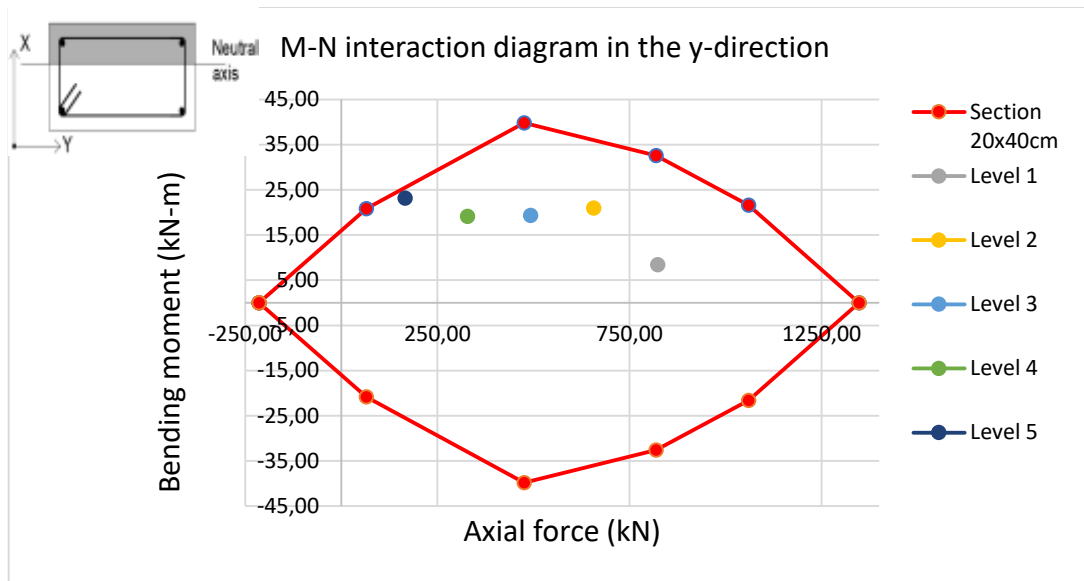
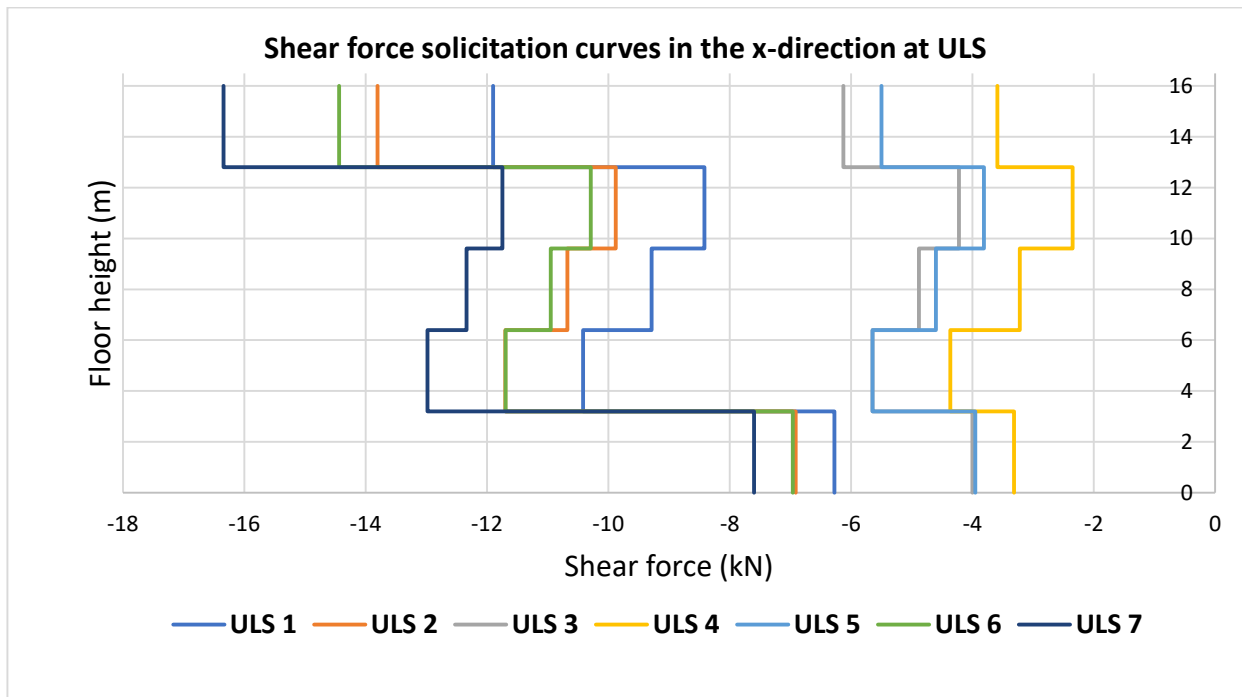


Figure 3.28. Interaction diagram of the column F2 in the y-direction

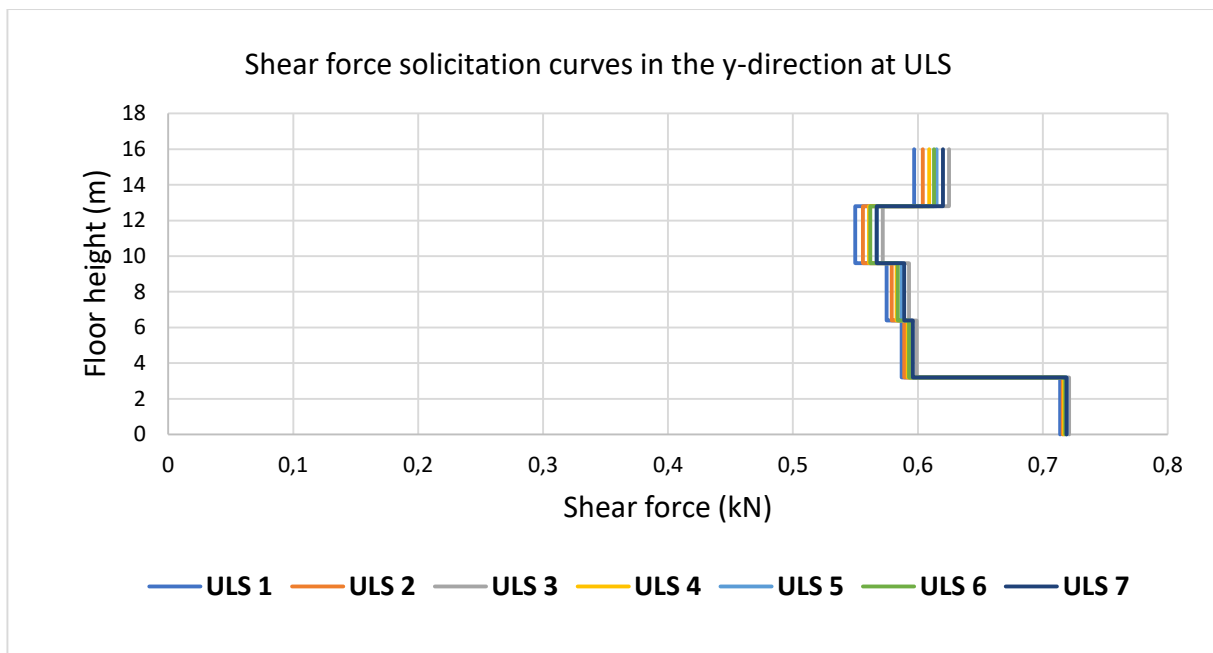
From the construction of the interaction diagram of the column, it is possible to observe that the acting forces on the element fell inside the diagram and, therefore, the column is able to withstand them.

3.5.3.3 Shear verification

The solicitation curves for shear from the load arrangements are obtained for both x and y directions as presented in Figure 3.29.



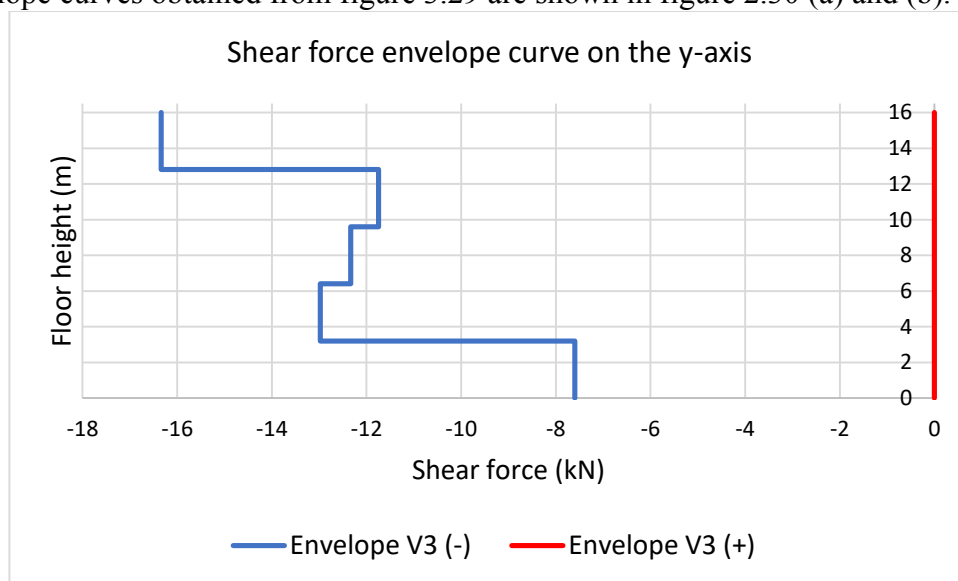
(a) Shear force solicitation curves in the x-direction



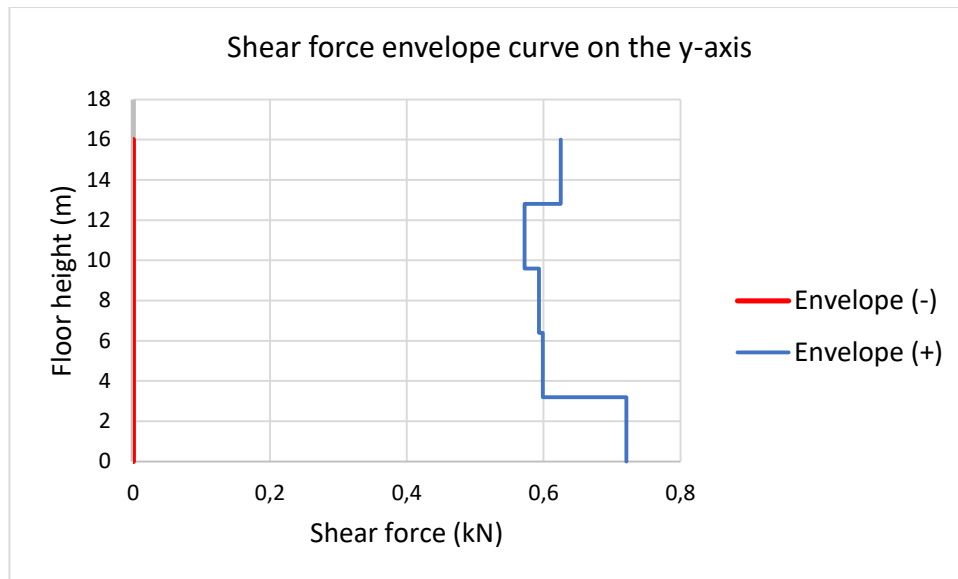
(b) Shear force solicitation curves in the y-direction

Figure 3.29. Shear force solicitation curve on the column

The envelope curves obtained from figure 3.29 are shown in figure 2.30 (a) and (b).



(a) Shear force envelope curve in the y-axis



(b) Shear force envelope curve on the y-axis

Figure 3.30. Shear force envelope on the column

Applying the procedure presented in the section 2.6.2.2. (b), we observe that the shear resistance of the section without shear reinforcement ($V_{rd,c} = 44.3\text{kN}$) is greater than the maximum shear solicitation on the column. So we can apply the maximum spacing. If we consider a diameter of 6mm as stirrups, the maximum spacing of the transverse reinforcement is given by:

$$S_{cl,max} = \min(280; 200; 400) = 200\text{mm}$$

So, we obtain a spacing of the shear reinforcement of:

- 12 cm within 0.4 m above and below the beam
- 20 cm along the rest of the column section

3.5.3.4 Slenderness verification

Following the procedure presented on the section 2.6.3.4, the different parameters are evaluated and presented in table 3.6.

Table 3.5. Parameter for the computation of λ_{lim}

A	B	C	n
0.7	1.38	1.7	0.73

The limit value of the slenderness obtained is: $\lambda_{lim} = 27.99$

The slenderness of an element is evaluate using the equation 2.46:

$$\lambda = l_o/i$$

The application of the equation 2.47 permits to evaluate the gyration radius of the section and we obtain: $i = 0.115 \text{ m}$

For a column height of 3.2m, we have the slenderness $\lambda = 19.48 < \lambda_{lim}$. So the slenderness is verified for the column. Figure 3.31 shows the details of the designed column.

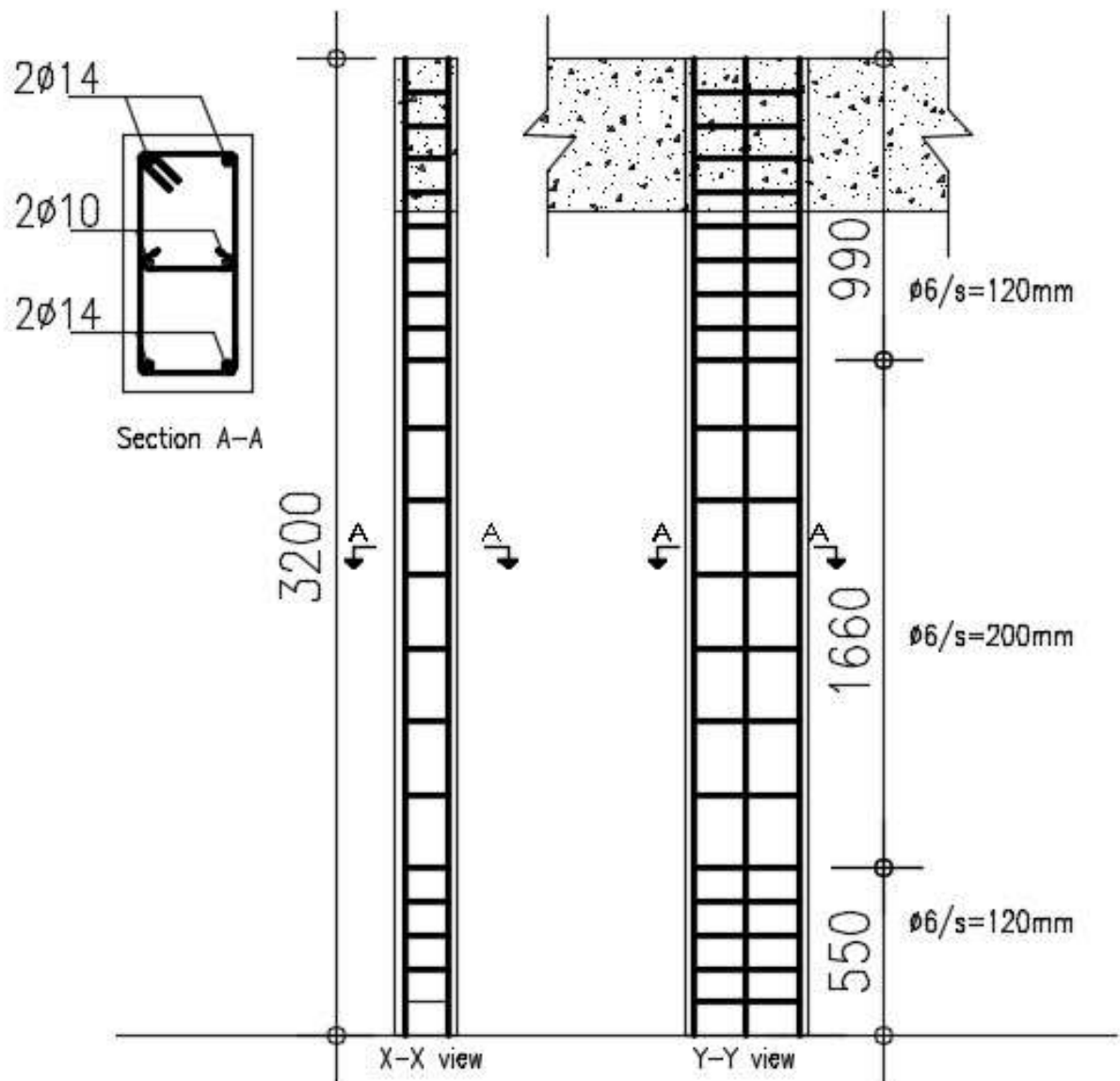


Figure 3.31. Recapitulative of the column detailing

The reinforcement detailing for the entire frame studied is given in figure 3.32

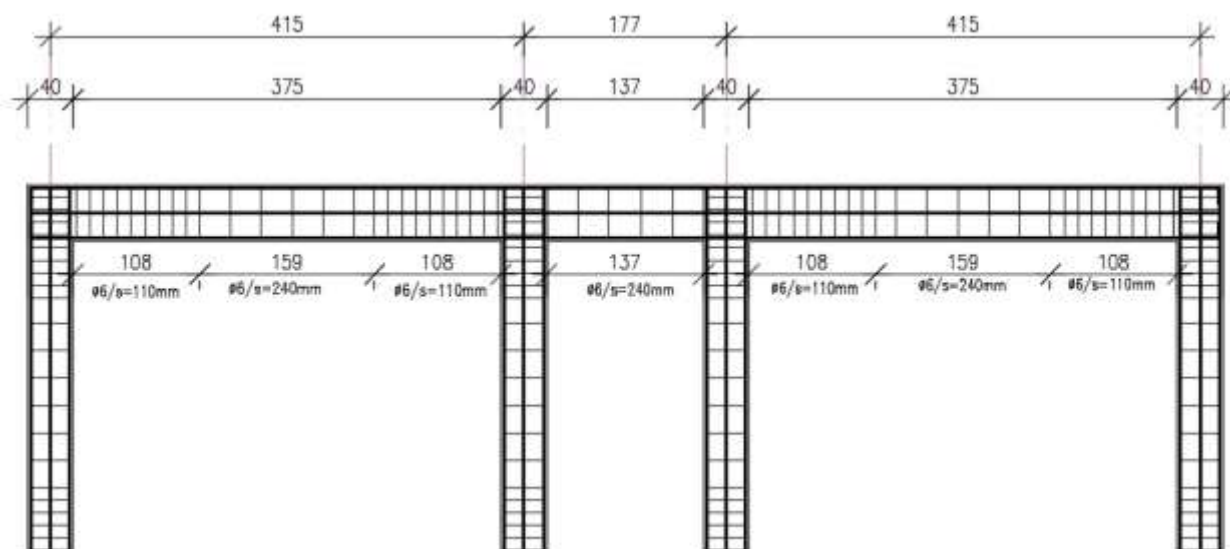


Figure 3.32. Reinforcement detail for studied frame

3.5.4 Footing design

The geotechnical test results for the foundation soil not being available, a value of admissible stress of soil of 0.3 MPa is assumed. The axial loads arriving the top of foundation from the columns are varying along axis 5; this variation causes an overlap of the footing (pad foundation) all through the axis line. For this reason, a strip foundation is opted and using equation (2.45), the results obtained are presented in Table 3.6. The model used for the design of the foundation is as shown in Figure 3.33.

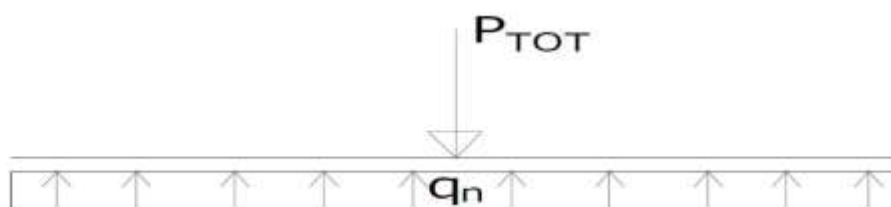


Figure 3.33. Load on footing

Table 3.6. Characterisation of foundation geometry

Entity	P_{TOT} (kN)	A (m ²)	L (m)	B (m)
Value	863	2.877	2.39	1.20

From the table above, it is drawn a conclusion that the footings will have a length of 2.39 m but is adopted a length of 2.40 m and a width of 1.20 m.

3.6 Modal analysis

SAP2000 V22, a structural analysis software integrated with the finite element method of analysis of the stability and resistance of structures, is used for the modelling and design of the case study. The slab loads are applied directly to the beams as distributed loads. In the same way is applied the loads of the walls as they are considered being carried by the slab. Beams and columns are modelled as frame elements having their connections (beam-column joints) ensured by the insertion of joints between two or more elements. To ensure rigidity of every floor above ground level, a diaphragm constraint is assigned to each node of the structure from the first to the last storey. Figure 3.34 shows a 3D structural model of the building.

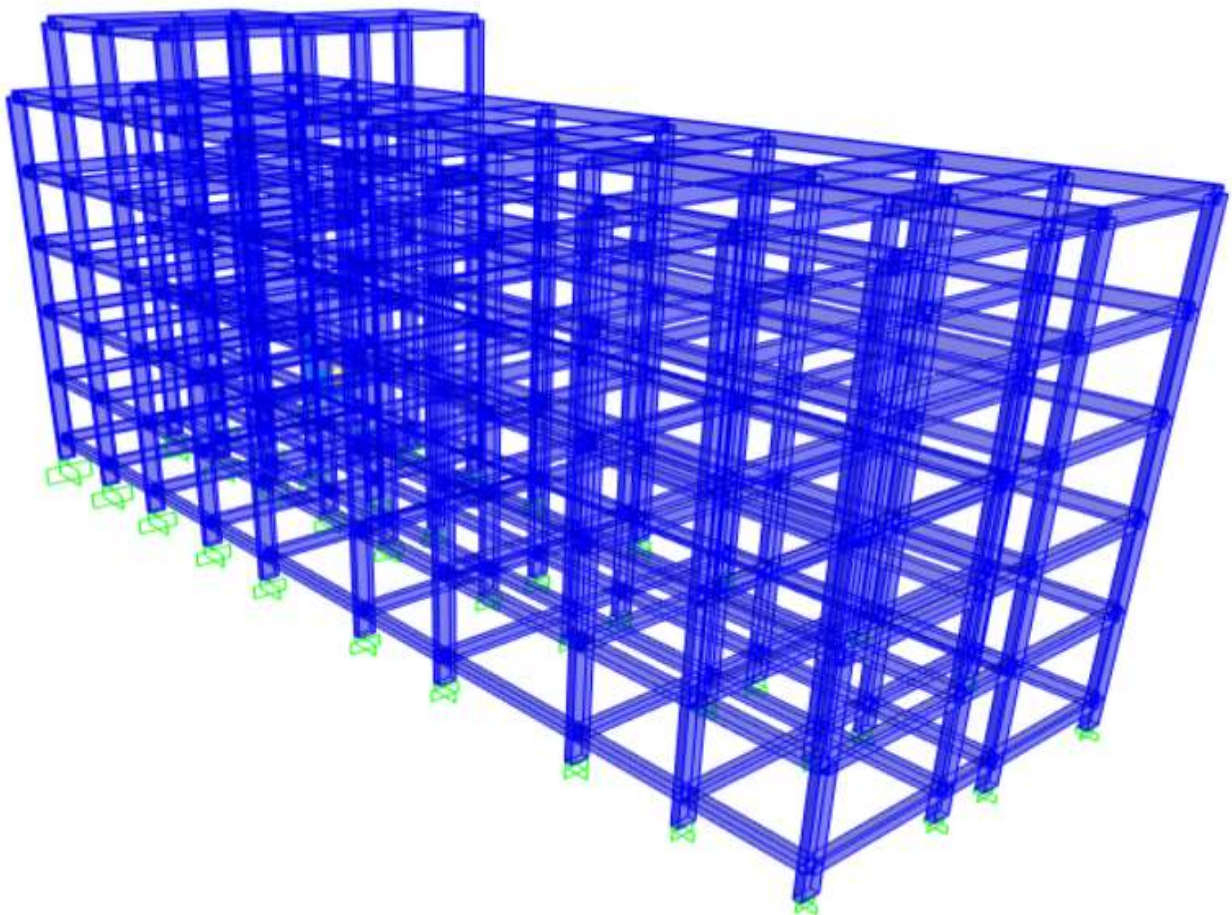


Figure 3.34. Structural model with fixed footings.

The fundamental period of vibration of the structure was determined using equation 2.41 and the results below were obtained:

$$T_1 = C_t H^{3/4} = 0.69$$

With $C_t=0.075$, for concrete frames and $H=19.20\text{m}$, the height above ground level.

With a mass participation of 100 % for the dead loads and 30% for the imposed loads, the fundamental modes of vibration obtained were respectively: translation in the x-direction, rotational-translation in the y-direction and a complete torsional mode. The period of vibration obtained in each case is: 0.73, 0.61, and 0.56 respectively. Figure 3.35, Figure 3.36 and Figure 3.37 show the respective modes of vibration.

Deformed Shape (MODAL) - Mode 1; T = 0,72591; f = 1,37758

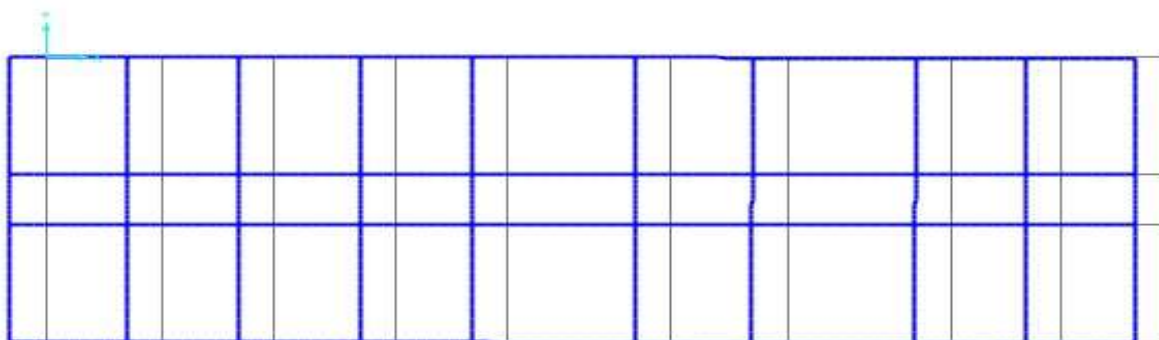


Figure 3.35. First vibrational mode, translational in the x-direction

Deformed Shape (MODAL) - Mode 2; T = 0,61057; f = 1,63781

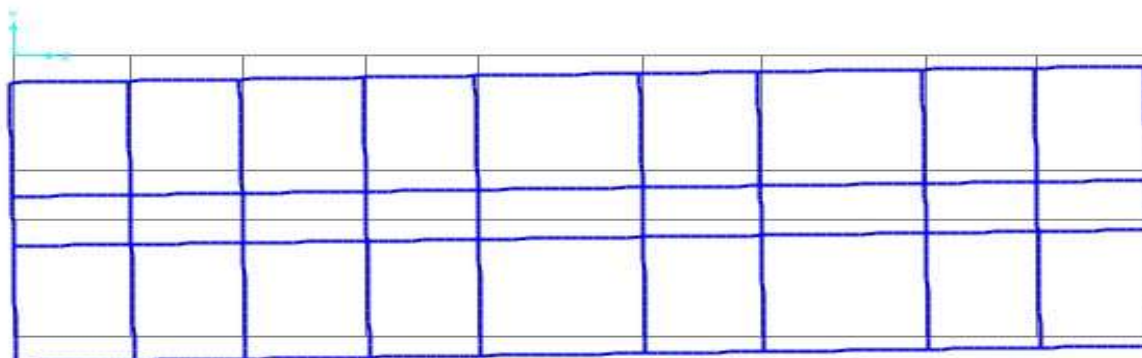


Figure 3.36. Second vibrational mode, translational-rotation in the y-direction

Deformed Shape (MODAL) - Mode 3; T = 0,55541; f = 1,80046

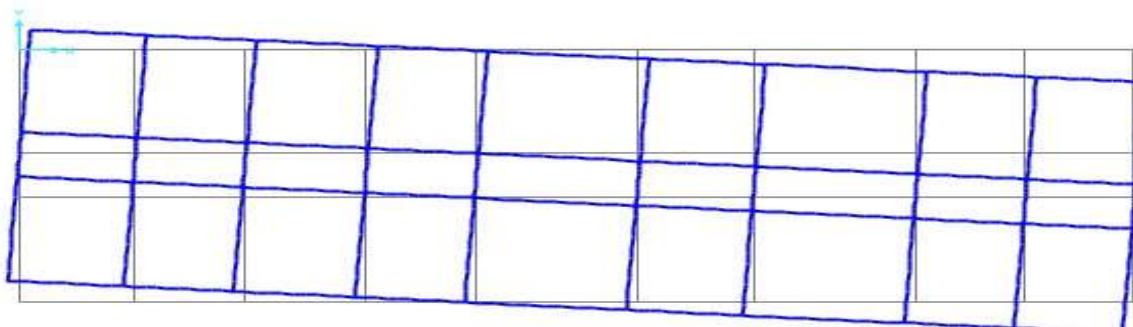


Figure 3.37. Third vibrational mode, rotational

We observe that the rotation is predominant in our structure because it is irregular due to the presence of an extrusion at the sixth upper floor. Nevertheless, we notice that the periods of oscillation in the first is below the fundamental period while the second and third modes are all below the fundamental period of our building T_1 .

3.7 Pushover analysis

A control displacement pushover analysis if performed on two external frames of the building: one in the direction OXZ and another in the direction OYZ and plastic hinges are formed as seen on figure 3.38. The base shear is plotted against the roof displacement in each case, and the results are presented in figure 3.39 and figure 3.41. As regards the failure mechanisms due to the increasing lateral force, its representations are shown in figure 3.40 and figure 3.42. Figure 3.43 and figure 3.44 reveal that the structure is ductile with a displacement of up to 35 cm before failure. The drift of each floor is equally represented in figure 3.45 and from figure 3.46, the observation made is that, the columns plasticize first with respect to the beams.

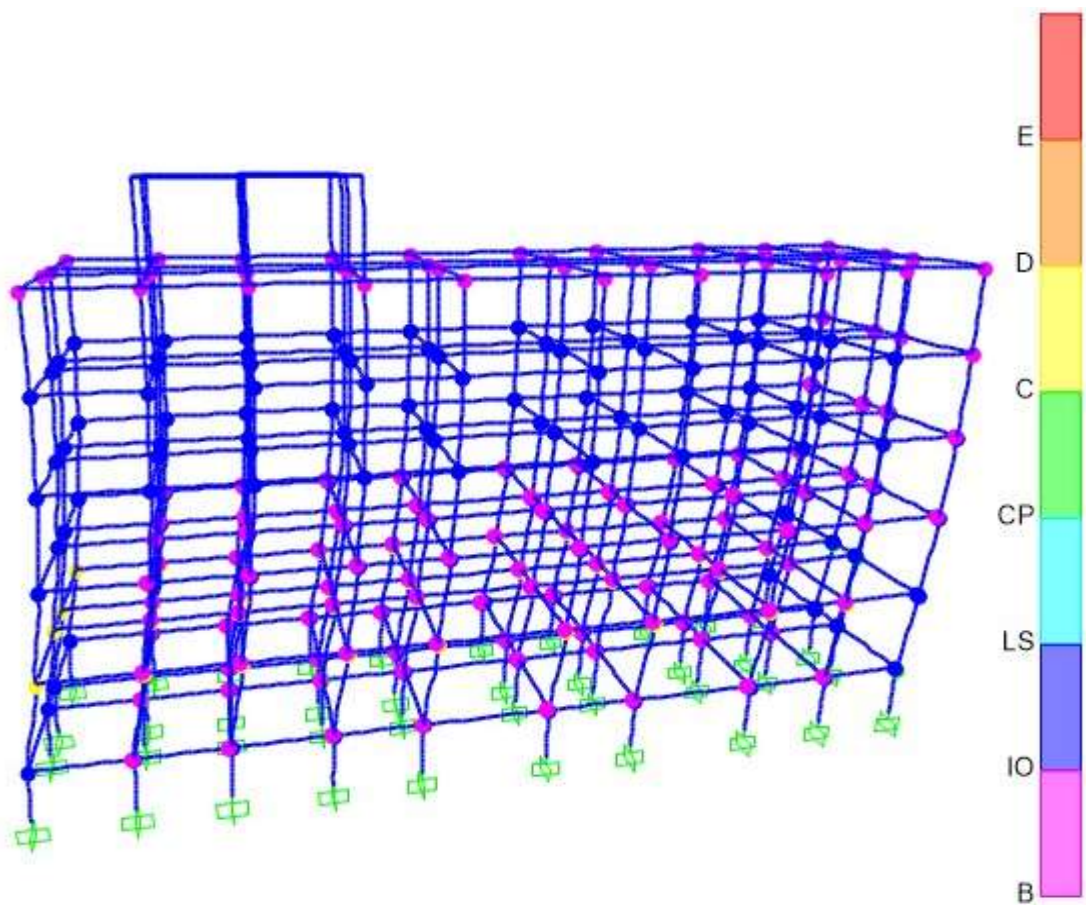


Figure 3.38. formation of plastic hinge non the entire structure

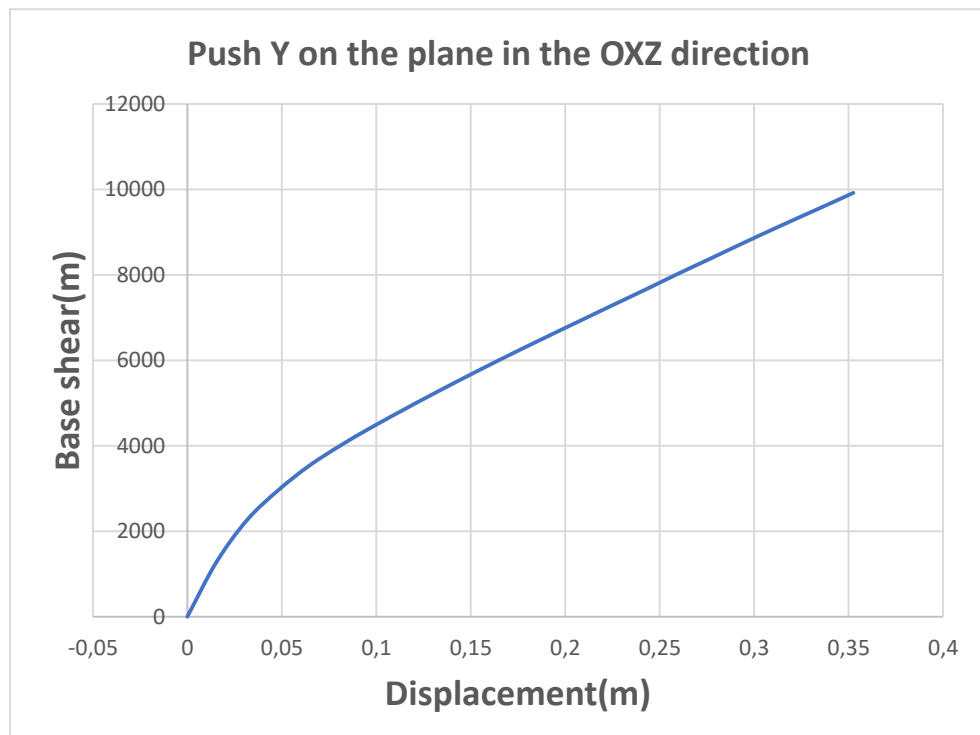


Figure 3.39. Push on frame in direction OXZ

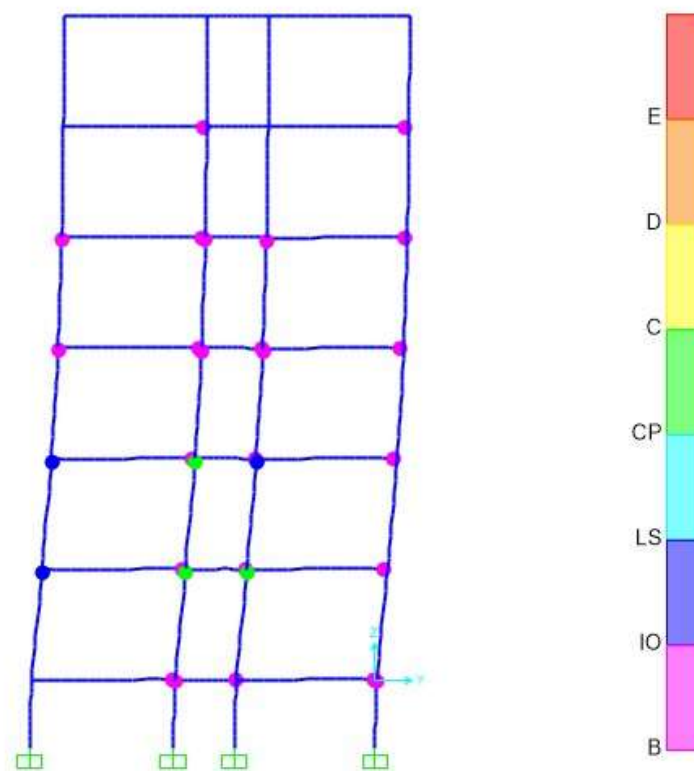


Figure 3.40. Hinge formation for push on frame in direction OXZ

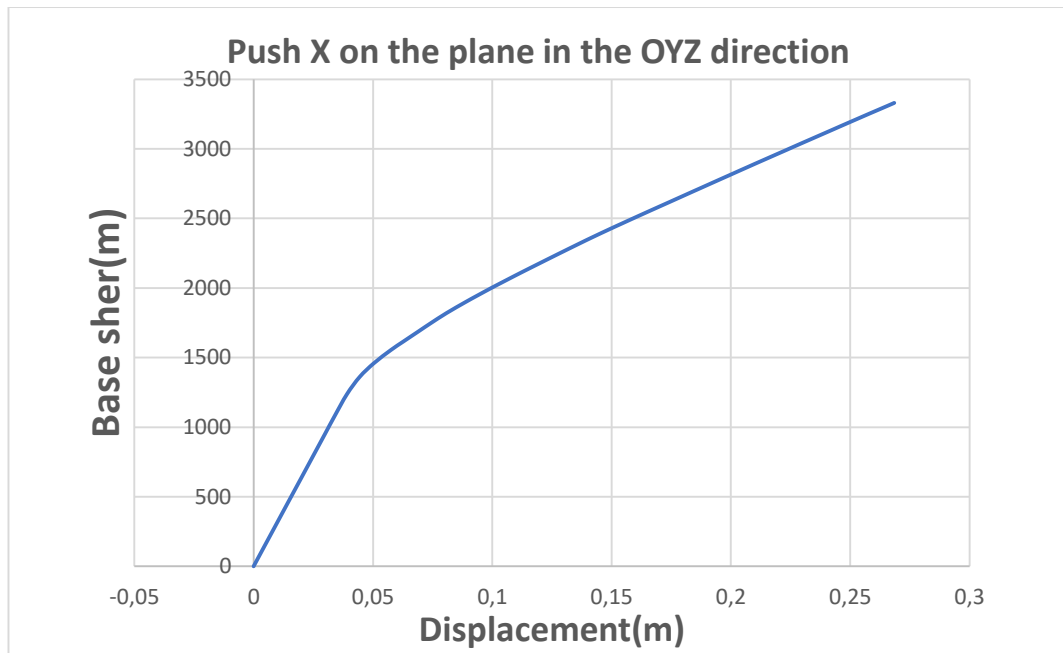


Figure 3.41. Push X on frame frame in direction OYZ

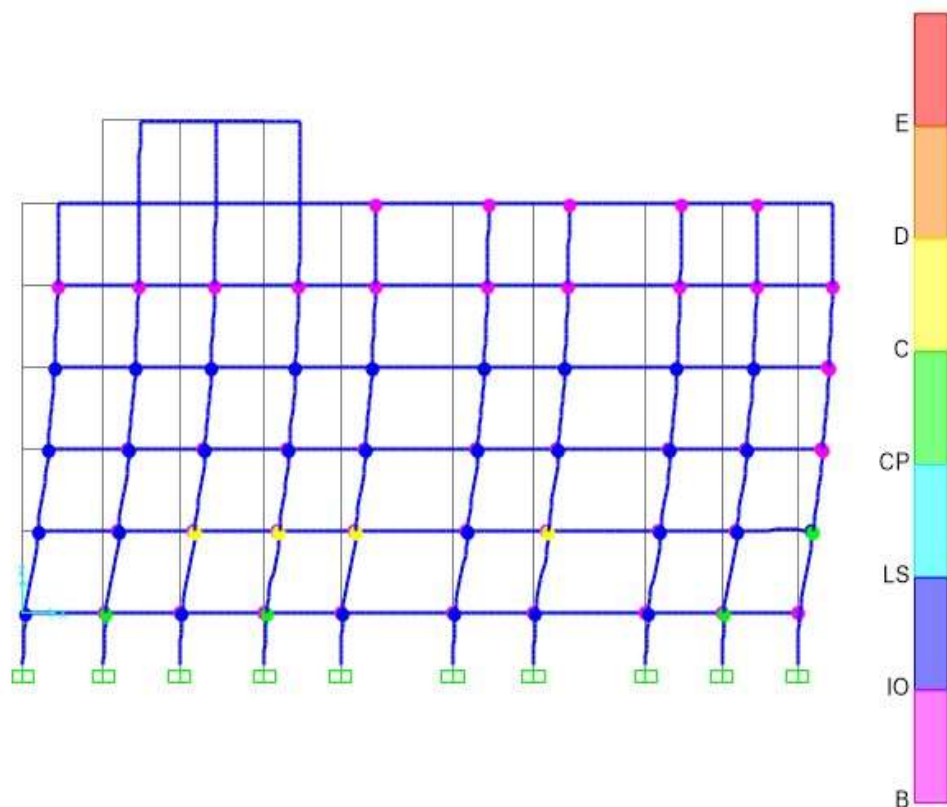


Figure 3.42. Hinge formation due to push X on frame in direction OYZ.

On application of the increasing lateral force, the lateral displacement of the each floor for the X and Y directions are presented in figure 3.42 and figure 3.43

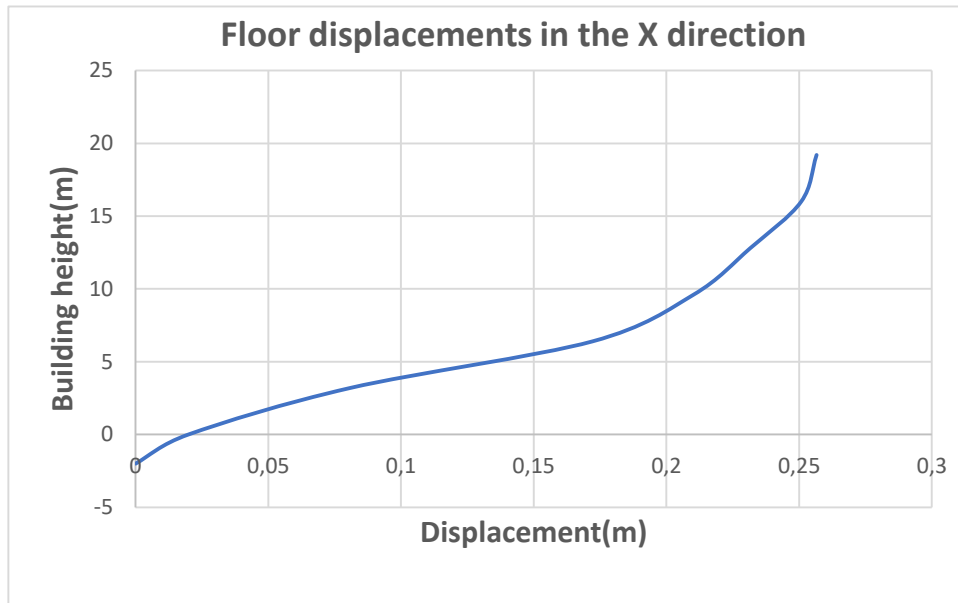


Figure 3.43. Floor displacement in the X- direction

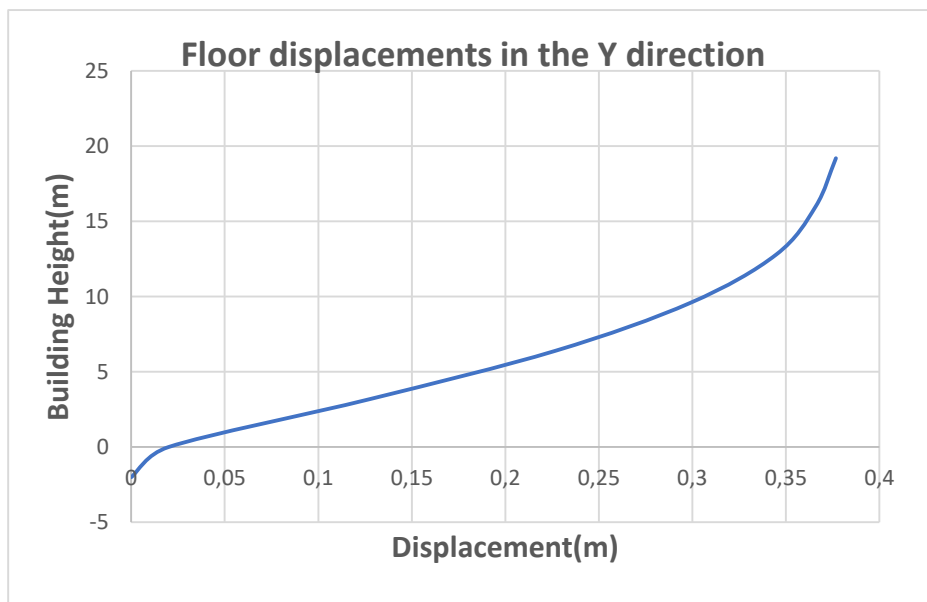


Figure 3.44. Floor displacement in the Y direction

It can be observed that the displacement before failure in the X direction (about 25 cm) is smaller than the displacement in the Y axis (about 37 cm).

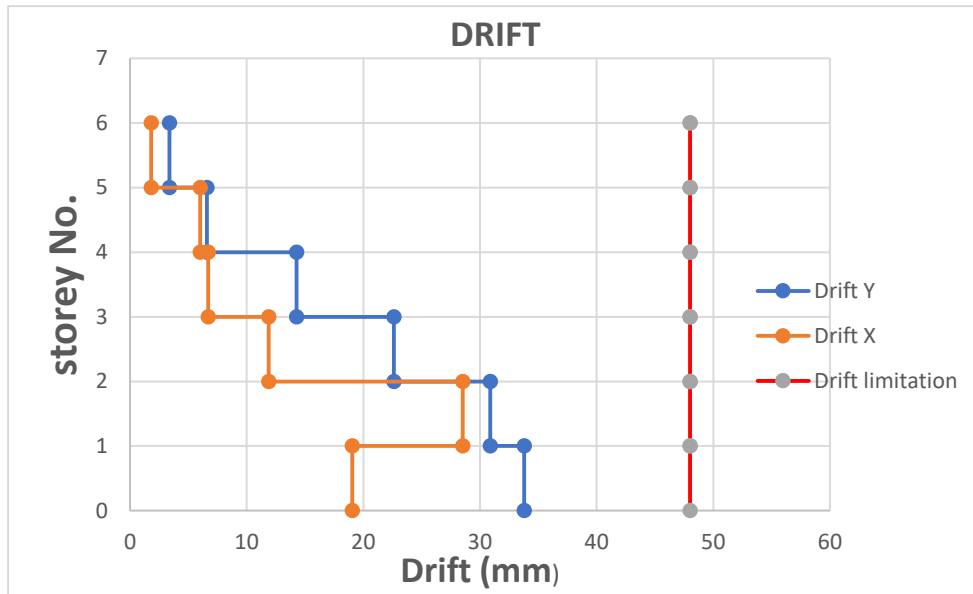


Figure 3.45. Storey drift

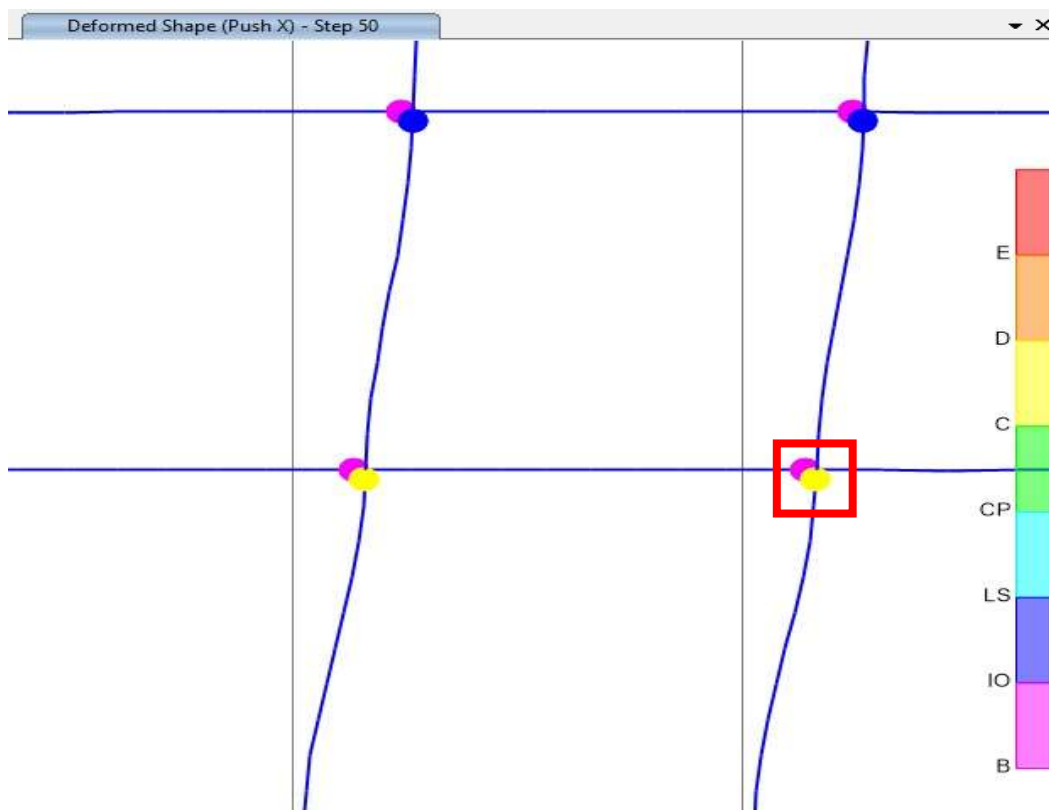


Figure 3.46. Failure mode of structure

The failure (collapse) mode of the structure is presented in figure 3.44 where we observe that the columns actually collapse before the beams under the action of a given ground force.

3.8 Analysis including soil structure interaction

In this part, we will consider a more real case, where the soil type and interactions between the soil and the foundation footing will be taken in to consideration, and the foundation modelled before determining the frequencies of the structure and the pushover analysis performed to study the storey displacements.

3.8.1 Modelling including soil structure interaction

The foundation footings are modelled as shell elements and the soil structure interaction (SSI) is considered through the application of springs on the base of the shell element and on its sides since we are going to be carrying out horizontal displacements on the building.

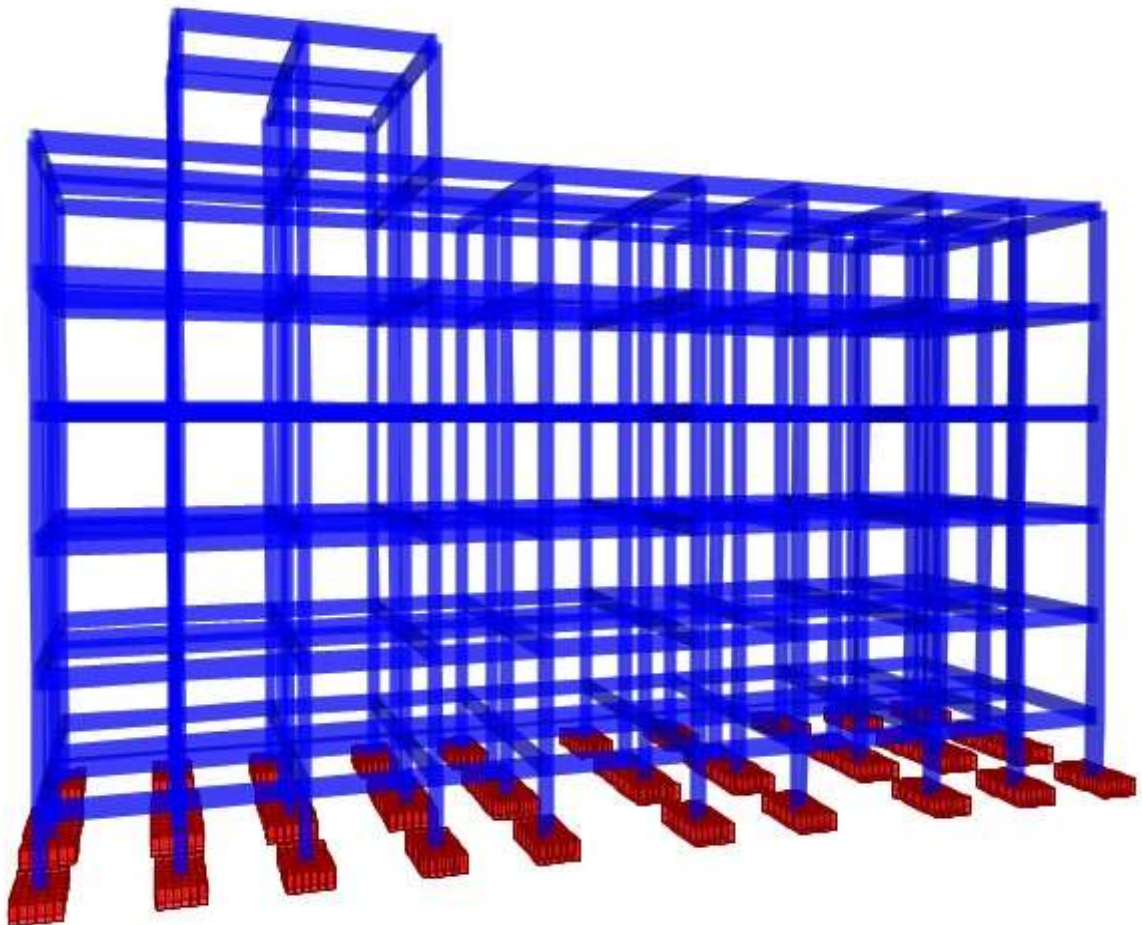


Figure 3.47. Building model considering SSI

3.8.2 Time period for soil structure interaction

The first three modes of oscillation are respectively perfect translation in the x-direction with a period $T_1 = 1.203s$ as seen in **figure 3.48**, followed by a rotational translation in the y-direction with a period $T_2 = 0.814s$ as seen in **figure 3.49**, and finally a perfect rotation about the z-axis with a period $T_3 = 0.736$ as seen in **figure 3.50**

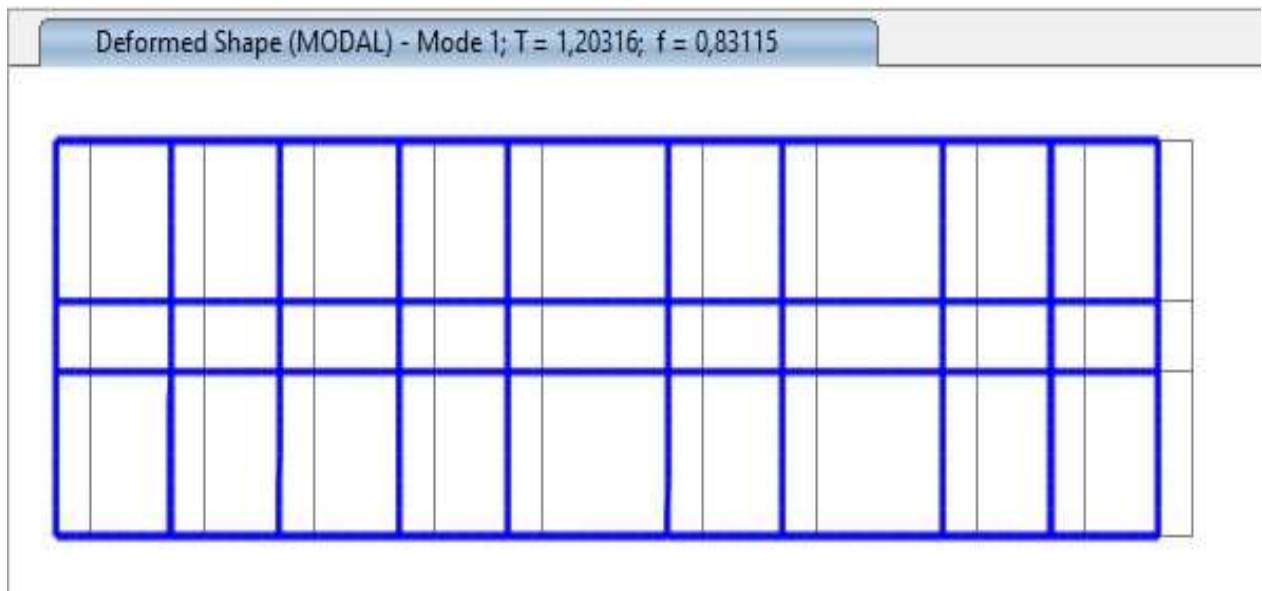


Figure 3.48. First mode of vibration considering SSI

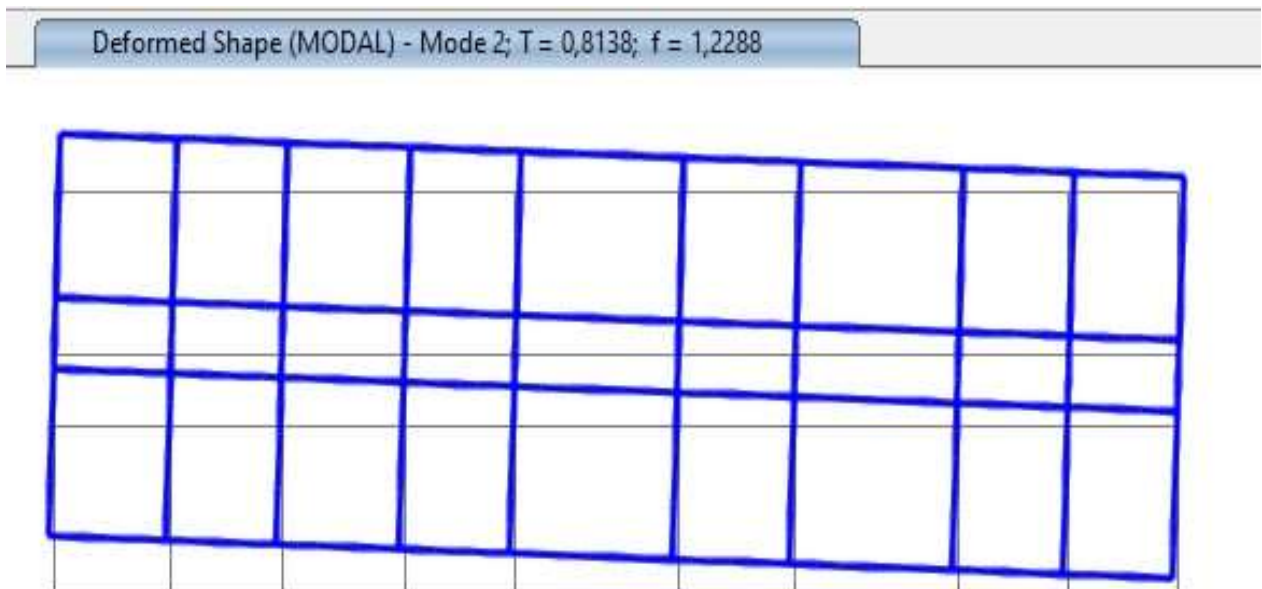


Figure 3.49. Second mode of vibration considering SSI

Deformed Shape (MODAL) - Mode 3; T = 0,73635; f = 1,35804

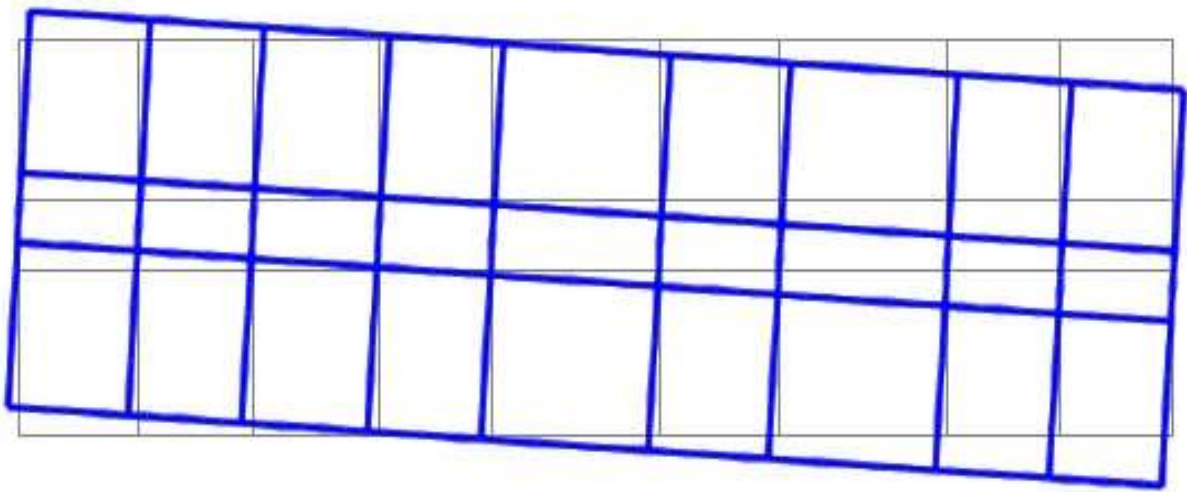


Figure 3.50. Third mode of vibration considering SSI

3.8.3 Pushover curves for soil structure interaction

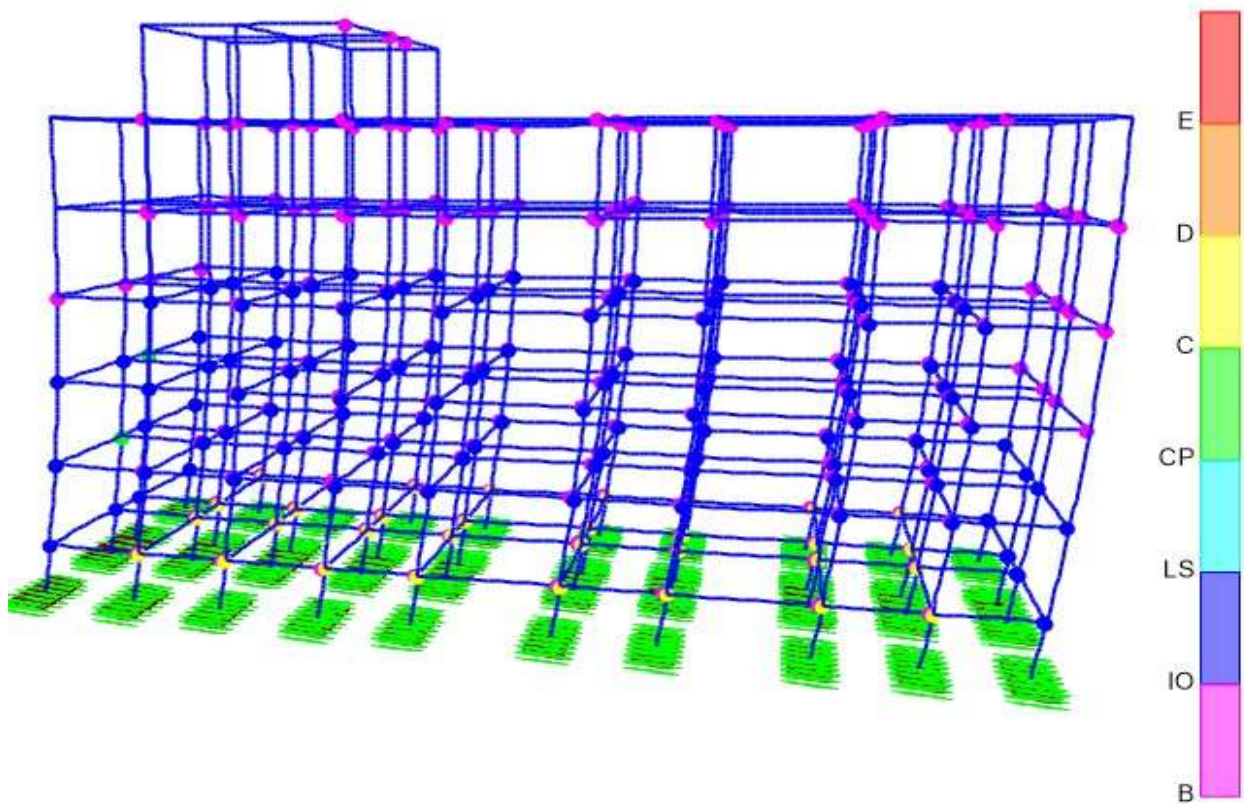


Figure 3.51. Formation of plastic hinges after considering SSI

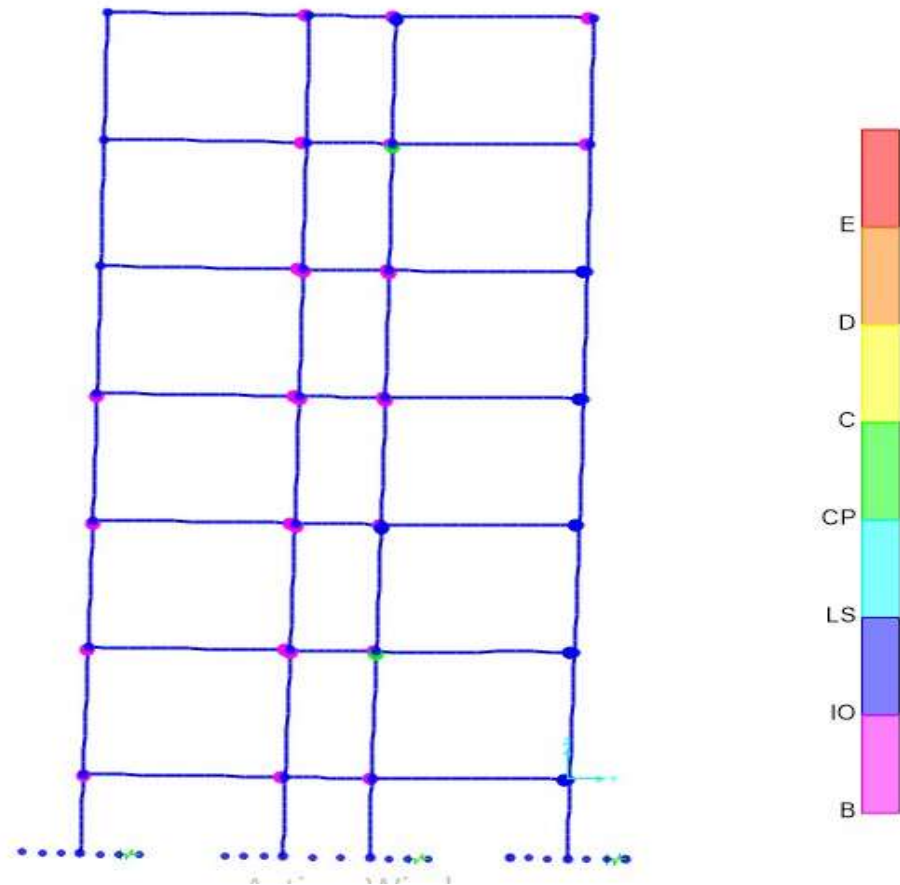


Figure 3.52. Hinge formation in Y-direction considering SSI

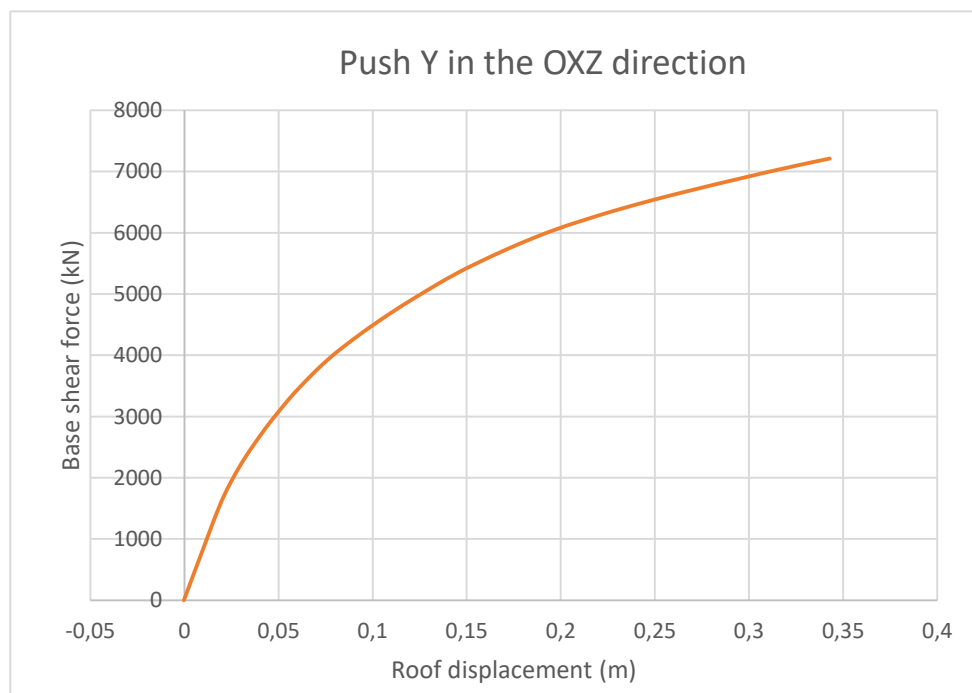


Figure 3.53. Pushover curve for push Y considering SSI

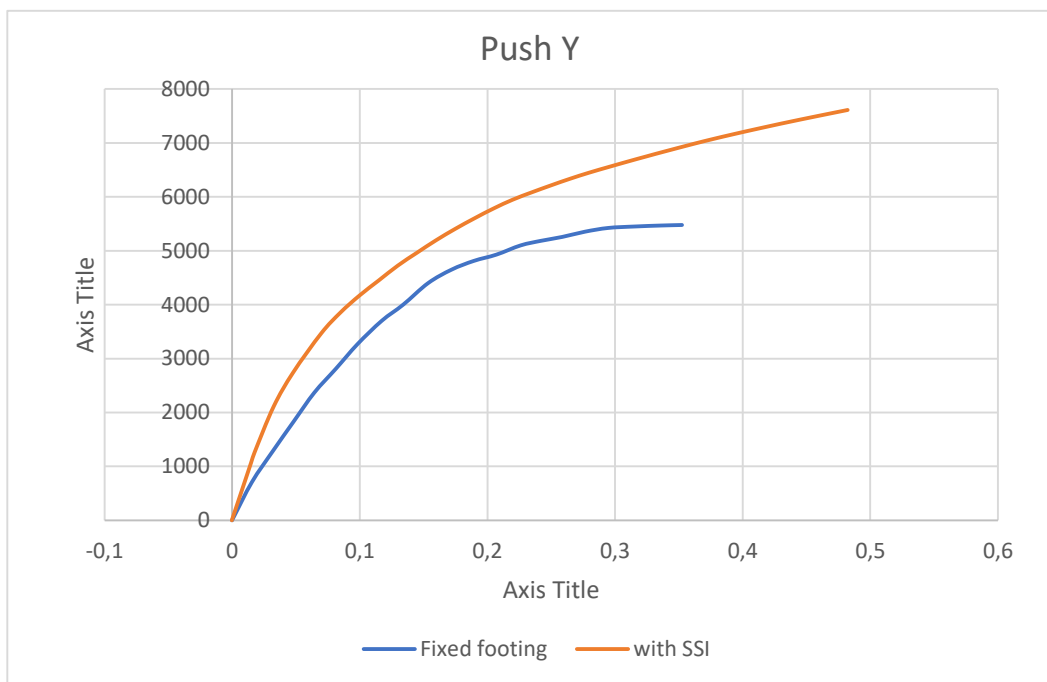


Figure 3.54. Comparison for push Y

Here we notice that there is a higher force at the base for the case where we consider SSI. This is due to the increased periods of vibration.

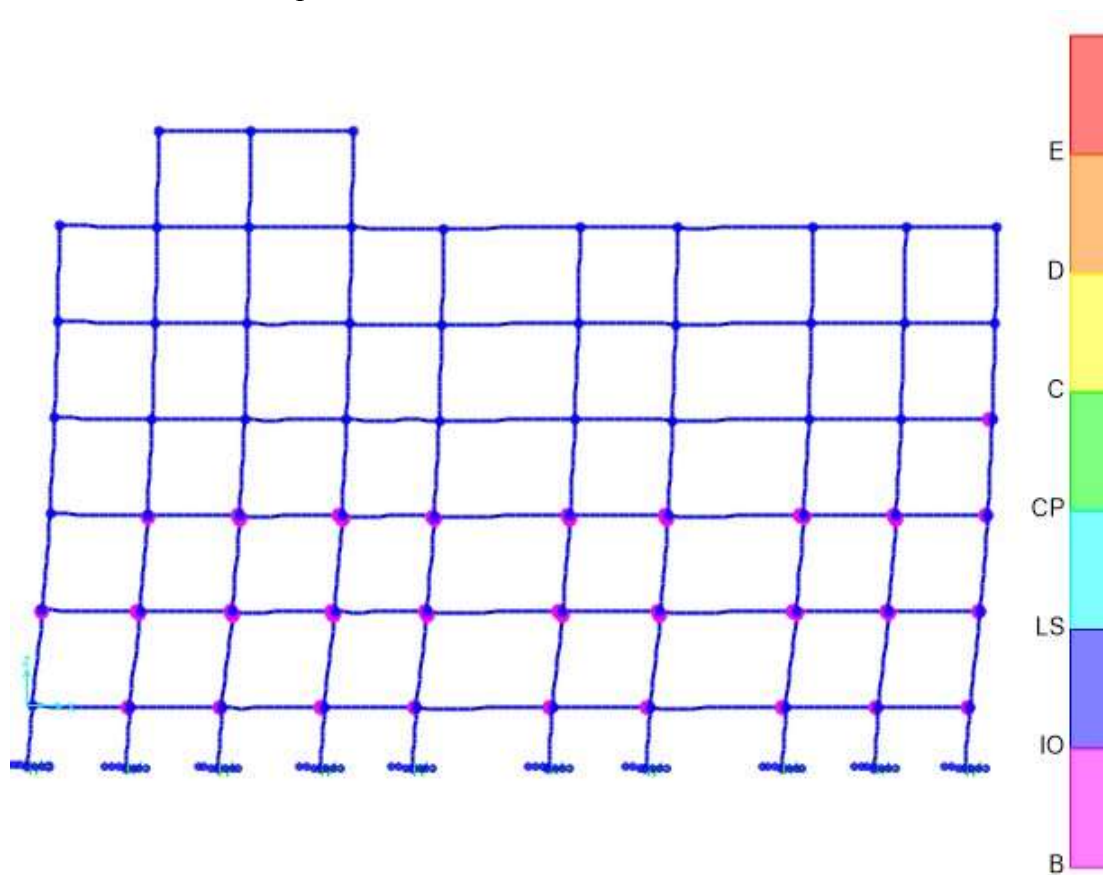


Figure 3.55. Hinge formation in x-direction considering SSI

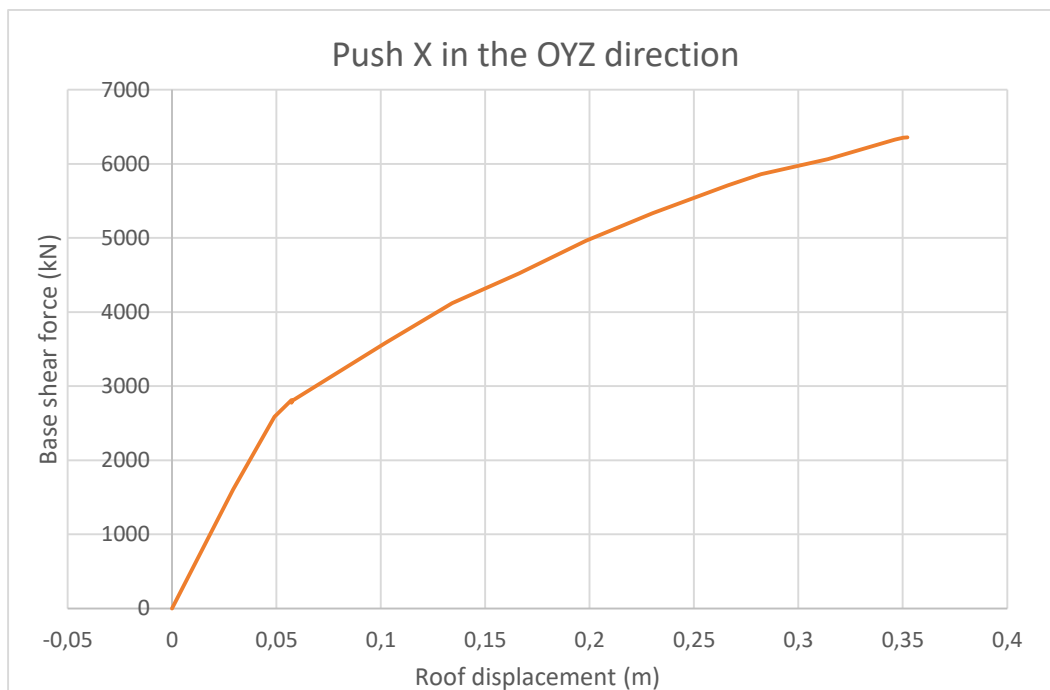


Figure 3.56. Pushover curve for push X considering SSI

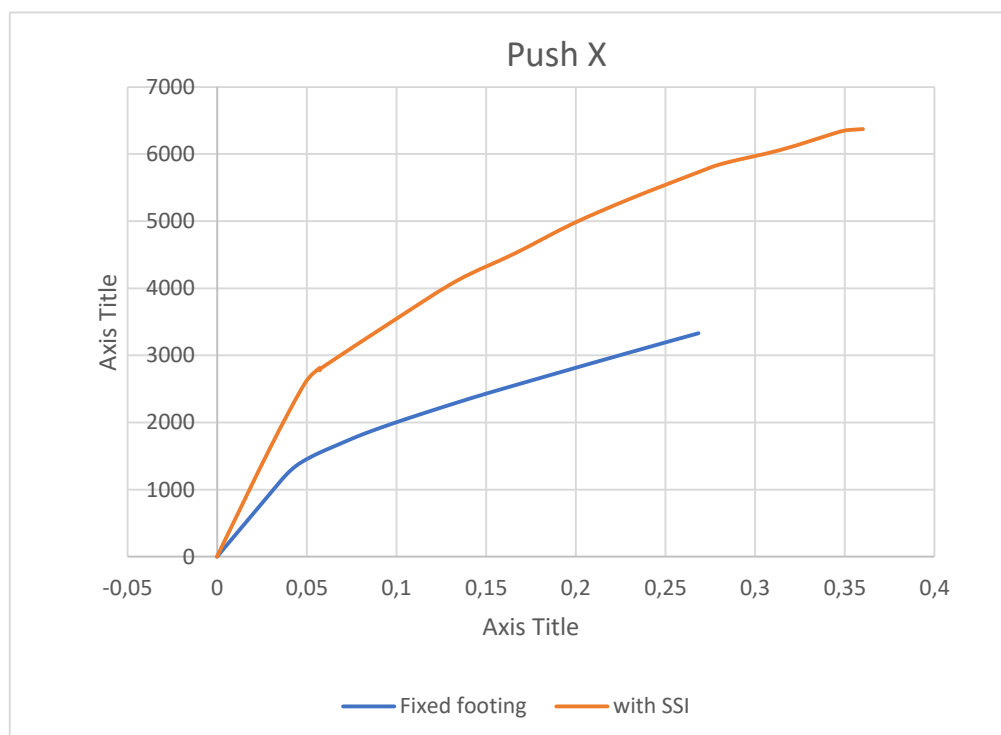


Figure 3.57. Comparison for push X

Similarly as in the y-direction, here we equally notice that there is a higher force at the base for the case where we consider SSI which is still due to the increased periods of vibration.

3.8.4 Storey displacement for soil structure interaction

On application of the increasing lateral force, the lateral displacement of the each floor for the X and Y directions are presented in figure 3.58 and figure 3.59.

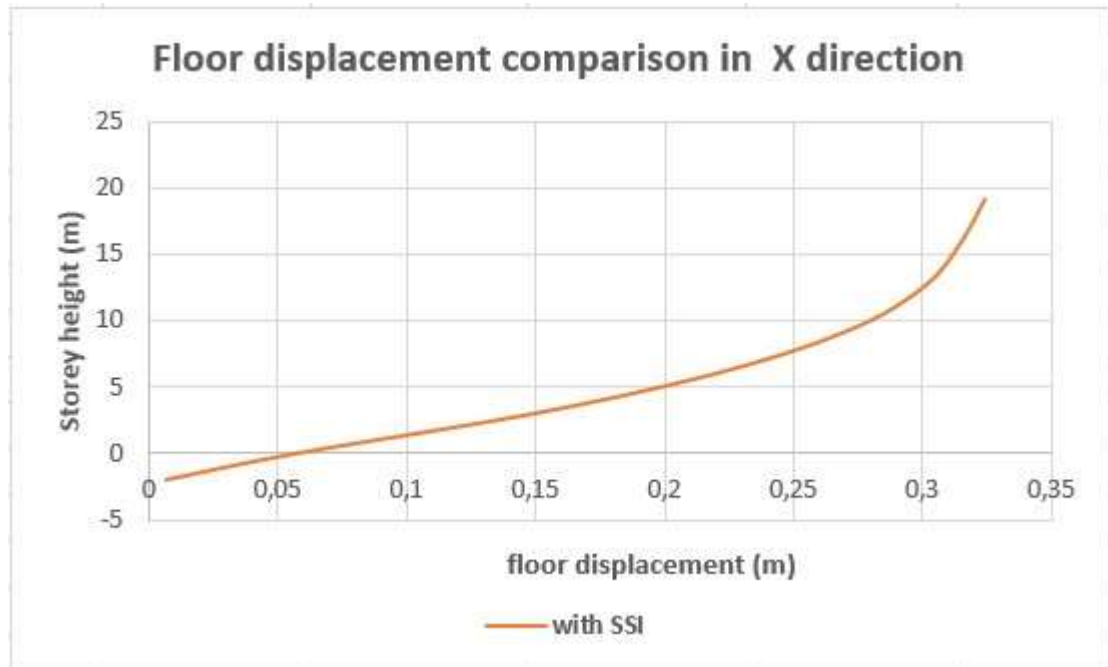


Figure 3.58. Floor displacement in x-direction considering SSI

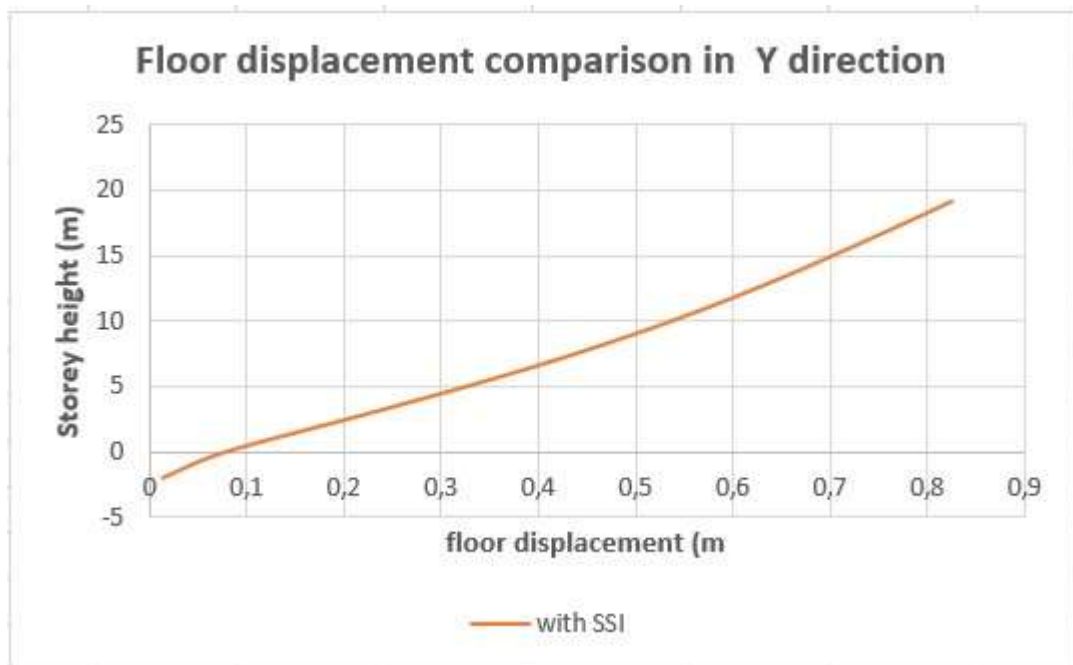


Figure 3.59. Floor displacement in y-direction considering SSI

It can be observed that the displacement before failure in the Y direction (about 12 cm) is greater than the displacement in the X axis (about 8 cm).

The respective comparisons between the storey displacements are given in figure 5.60 and in figure 5.61 for the x and y-directions, where we notice that the displacements are higher when we consider SSI than for fixed footings. This was earlier explained in the literature review under effects of SSI on buildings

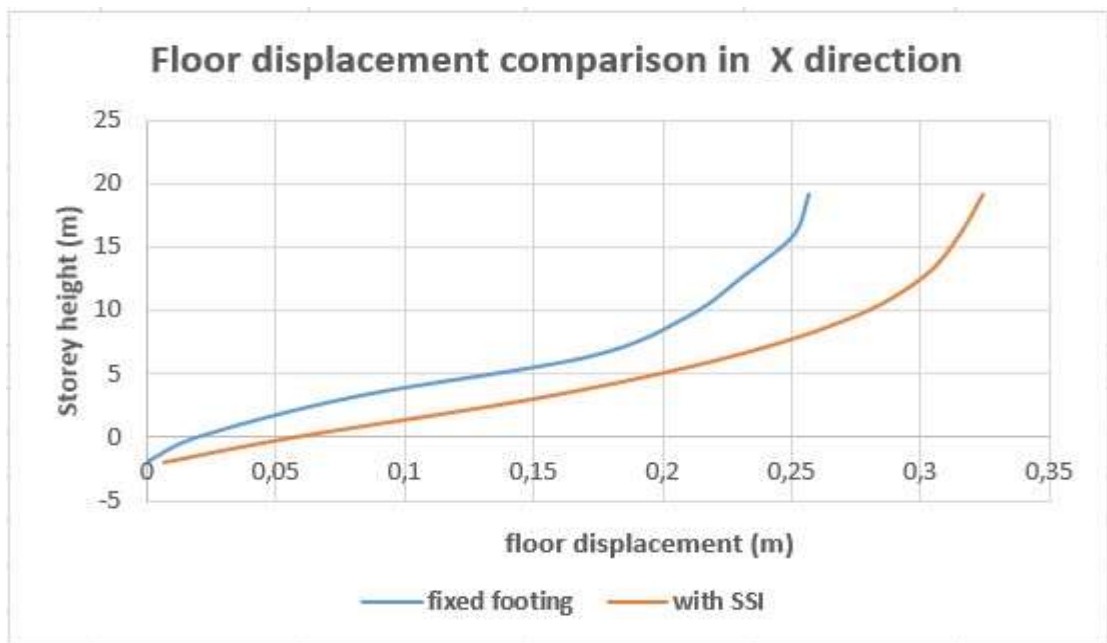


Figure 3.60. Floor displacement comparison in the x-direction

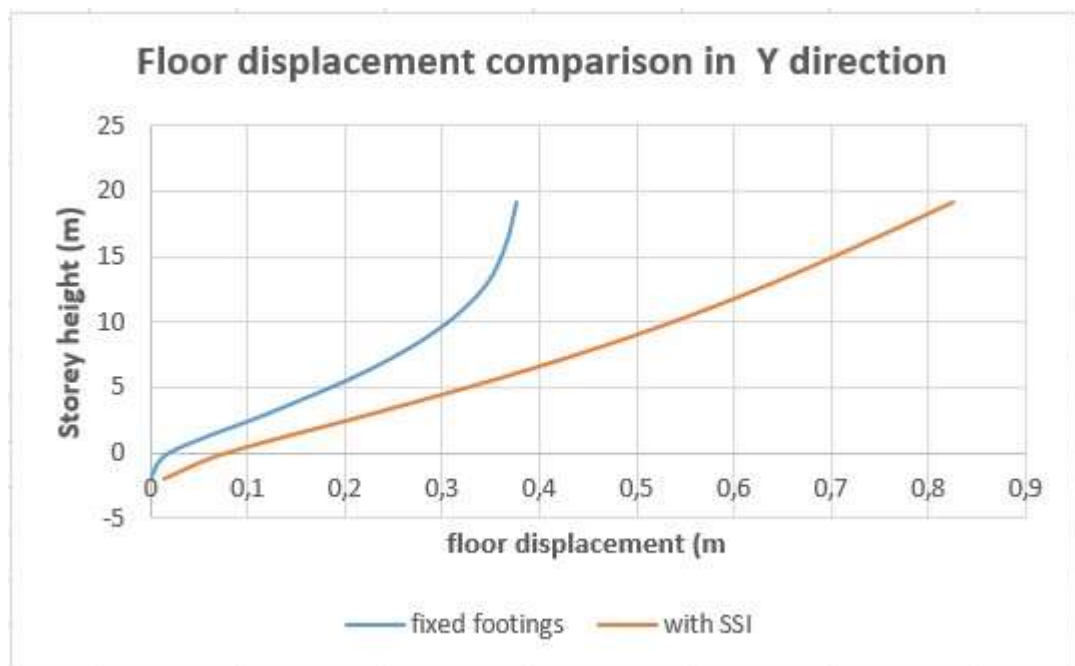


Figure 3.61. Floor displacement comparison in the y-direction

3.8.5 Storey drift considering soil structure interaction

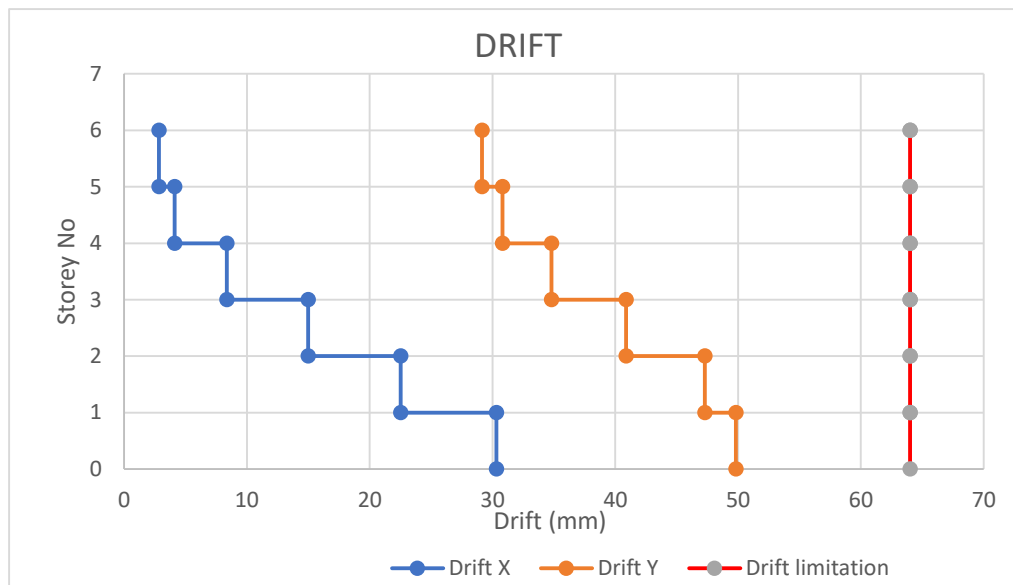


Figure 3.62. Storey drift considering SSI

3.8.6 Failure mode of the structure

Still after considering the SSI, the failure (collapse) mechanism of the structure as presented in figure 3.63 is seen to be one in which the beams actually collapse before the columns, and is a very good failure mechanism for the performance based methodology.

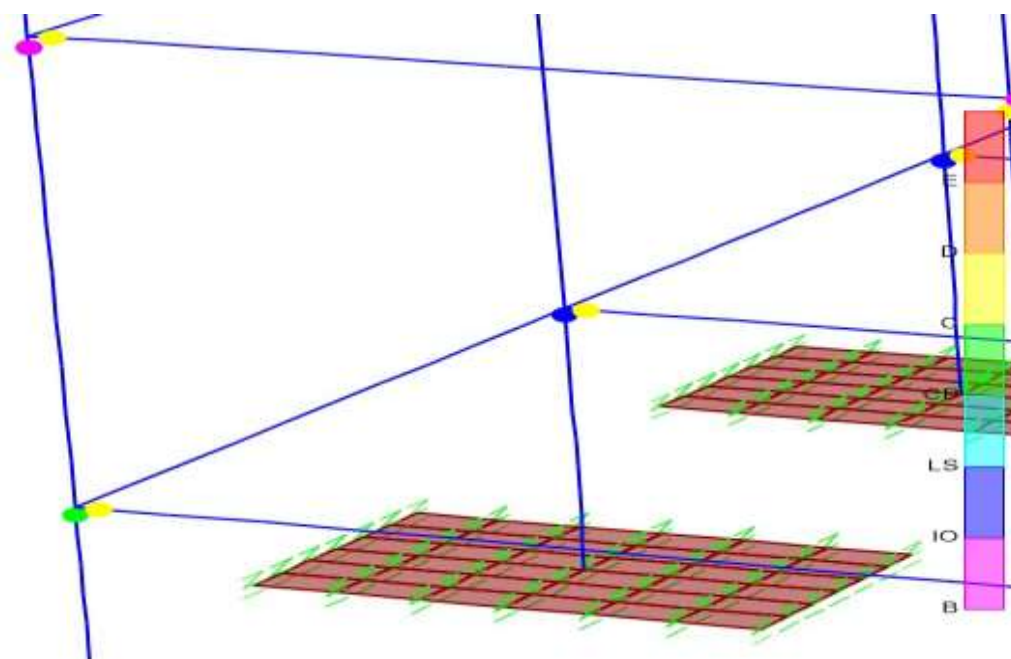


Figure 3.63. Failure mode after considering SSI

Conclusion

In this chapter was presented the case study of this work. An identification of the structural system, the architectural plans. A reassessment of the structure was made in order to reconstitute the structural model of the building since it is unavailable. Each structural element (beam, column) type is thus designed according to the valid construction norms (Eurocode 2). A nonlinear static analysis was performed on the structure by applying plastic hinges on the members for material nonlinearity properties. The target displacement using the pushover curve was plotted, the performance level of the structure presenting the different hinges at target displacement seen and force needed for collapse was presented. To compare our results with a more real situation (where foundation footings are not fixed), we considered the soil structure interaction (SSI) in which the foundation footings were modelled as a shell elements and the nature of the soil taken into consideration and modelled as spring elements both at the base and the sides of the footings. After this, we performed again the modal analysis and push over analysis, where we could observe a different behaviour of the structure under the action of given non-linear forces. The failure mechanism for the fixed footing was not the best as we could observe pillars going in to plasticity before the beams due to high values of axial forced induced by the fixed footing. Whereas in the case where we considered SSI, we observe the beams going in to collapse before the columns, thereby following the rule of performance-based design of buildings.

GENERAL CONCLUSION

In this work we have seen that reinforced concrete is one of the most used building construction material in the world, so its design should be well taken in to consideration. We saw that the reinforcement bars used in RC concrete buildings has ductile properties which characterize for the plastic behaviour of these types of building, so giving this buildings first, and elastic field, and the a plastic field before their collapse. So in this work, we considered a reinforced concrete building a six floors existing storey building in Yaounde-Cameroon and studied to get the different behaviours in the elastic and plastic fields. The seismology of Cameroon was presented in the literature review and showed that Cameroon is exposed to the occurrence of earthquake which was the main ground perturbation used in our analysis. The structure was first analysed in the elastic field on the basis of Eurocode 2 for the design the beams columns and footings. Then the complete structure being modelled on SAP 2000v.22 to carry out a modal analysis to get the periods of oscillation of the complete building under the influence of a dynamic load. These modal analysis gave us first a complete translation of the building in the x direction and then a rotational-translation in the y direction, followed by a complete rotation about the z axis (as gotten from the first three(3) modes of vibration. The second mode which showed a rotation was due to the fact that the ratio between the length and width of the building was not good (making our structure irregular). This necessitated a structural joint for the block in study. After the modal analysis was then performed a non-linear static analysis (pushover analysis) to get the plastic behaviour of our building. The results of these pushover analysis as seen at the end of chapter 3 in this work shows that the structure displaces about 35cm before collapse hinges occur in the x direction. The failure mechanism of the structure as seen in the results of the pushover analysis was not the best, since the columns went into collapse before the beams (seen by the formation of collapse hinges on the columns before beams). Then was later considered the soil structure interaction where the foundation footings were modelled as a shell elements and the nature of the soil taken into consideration and modelled as spring elements both at the base and the sides of the footings. From here the results of the modal analysis were the same in terms of vibration modes but different in terms of vibration periods. The pushover analysis was still carried out, but this time having results that gave the real behaviour of the building as we could observe storey displacements of about 75 cm before collapse hinges occurred. The failure mechanism here was better as the beams now gained plasticity before the columns due to the reduction in axial forces carried by the columns.

REFERENCES

- Abdelraheem, S. E., Ahmed, M. M., & Alazrak, T. M. (2014, November 29). Evaluation of soil–foundation–structure interaction effects on seismic response demands of multi-story MRF buildings on raft foundations. *International Journal of Advanced Structural Engineering*, 5, 1-18. doi:10.1007/s40091-014-0078-x
- Ahmed, A. (n.d.). *Evaluating the co-relationship between concrete flexural tensile strength and compressive strength Mohd . Ahmed *, Khalid Mohammad El Hadi , Mohammad Abul Hasan , Javed Mallick and. X*, 1–17.
- Allotey, N., & El Naggar, M. H. (2008). Generalized dynamic Winkler model for nonlinear soil-structure interaction analysis. *Canadian Geotechnics Journal*, 45(4), 560-573.
- Bagheri, M., Jamkhaneh, M. E., & Samali, B. (2018). Effect of Seismic Soil–Pile–Structure Interaction on Mid-and High-Rise Steel Buildings Resting on a Group of Pile Foundations. *International Journal of Geomechanics*. doi:10.1061/(ASCE)GM.1943-5622.0001222
- Carbonari, S., Dezi, F., & Leoni, G. (2011). Linear soil-structure interaction of coupled wall-frame structures on pile foundations. *Soil Dynamics and Earthquake Engineering*, 31, 1296-1309.
- Carbonari, S., Dezi, F., & Leoni, G. (2011). Linear soil-structure interaction of coupled wall-frame structures on pile foundations. *Soil Dynamics and Earthquake Engineering*, 31, 1296-1309.
- Chopra, A.K., and Goel, G.K. (2004). A Modal pushover analysis procedure to estimate to estimate seismic demands for unsymmetric-plan buildings, *Earthquake Engineering and Structural Dynamics*, Vol.33, pp.903-927
- Chu, D., & Truman, K. Z. (2004). Effects of pile foundation configurations in seismic soil-pile-structure interaction. *13th World Conference on Earthquake Engineering*. Vancouver, Canada: Canadian Association for Earthquake Engineering.
- CIM BÉTON " Les bétons: formulation, fabrication et mise en œuvre "
- Clough, R. W., & Penzien, J. (1993). *Dynamics of Structures*. New York: McGraw Hill.
- Djeukoua Nathou, G. L. (2019). *Compartive analysis of seismic protection system. (Master Thesis)*. National Adavanced School of Public Works.
- Dreux, G., & Festa, J. (1998). *New Guide of Concrete and Its Constituents*. Eyrolle Edition (8th edn), Paris, France p, 409.
- Durocrete (2013). *Mix design manual*.
- EN 1990: Eurocode: basis of structural design. Thomas Telford.
- EN 1992, (2004) ‘Design of concrete structures - Part 1-2: General rules - Structural fire design’,
- EN 1998-1 (2004) Eurocode 8: Design of structures for earthquake resistance.

- EN, B. (2000). 197-1, Cement-Part 1: Composition, specifications and conformity criteria for common cements. *British Standards Institution*.
- Forni, M. (sd). *Fondations spéciales et reprise en sous-oeuvre*. Eyrolles.
- Gonzalez Jamie 2018. Durability and concrete cover.
- Haseeb Jamal (January 02, 2018), Problems and Defects in Hardened Concrete.
- Hayashi, Y., & Takahashi, I. (2004). Soil-structure interaction effects on building response in recent earthquakes. *3rd UJNR Workshop on Soil-Structure Interaction*. Menlo Park, CA: USGS.
- Hokmabadi, A. S., & Fatahi, B. (2015). Influence of foundation type on seismic performance of buildings considering soil-structure interaction. *International Journal of Structural Stability and Dynamics*, 16, 29. doi: 10.1142/S0219455415500431
- Hokmabadi, A. S., Fatahi, B., & Samali, B. (2014). Assessment of soil pile-structure interaction influencing seismic response of mid-rise buildings sitting on floating pile foundations. *Compt Geotech*, 55(1), 172-186.
- Kosmatka, S. H., Kerkhoff, B., Panarese, W. C., MacLeod, N. F., & McGrath, R. J. (2003). Design and control of concrete mixtures, EB001. Portland cement Association, Skokie, Illinois, USA.
- Kramer, S. L. (1996). *Geotechnical Earthquake Engineering*. New Jersey, USA: Prentice Hall.
- Kutanis, M., & Elmas, M. (2001). Non-linear seismic soil-structure interaction analysis based on the substructure method in the time domain. *Turkish Journal of Engineering and Environmental Science*, 617-626.
- Liu, Y., Wang, X., & Zhang, M. (2015). Lateral vibration of pile groups partially embedded in layered saturated soils. *International Journal of Geomechanics*. doi:10.1061/(ASCE)GM.1943-5622.0000406
- Makhloufi Z, Bouziani T, Bédérina M and Hadjoudja M. (2014). Mix proportioning and performance of a crushed limestone sand-concrete. *Journal of building Materials and Structures*, 1(1), 10-22.
- Mbessa, M. (2000). Rôle des ultrafines dans les bétons industriels a hautes performances (Doctoral dissertation, Lyon, INSA)
- Mosley, W. H., Hulse, R., & Bungey, J. H. (2007). Reinforced Concrete Design to Eurocode 2 (EC2).
- Mouzzoun, M., Moustachi, O., Taleb, A., & Jala, S. (2013, Jan. - Feb.). Seismic performance assessment of reinforced concrete buildings using pushover analysis. *IOSR Journal of Mechanical and Civil Engineering (IOSR-JMCE)*, 5, 44-49.

Rafi, M. M., Lodi, S. H., & Nizam, A. (2013). Chemical and Mechanical Properties of Steel Rebars Manufactured in Pakistan and Their Design Implications. *Journal of Materials in Civil Engineering*, 26(2), 338-348.

Roesset, J. (1980). Stiffness and damping coefficients of foundations. *ASCE Geotechnical Engineering Division National Convention* (pp. 1-30). ASCE.

Shiming, W., & Gang, G. (1998). Dynamic soil-structure interaction for high rise buildings. *Dev. Geotech. Eng*, 203-2016.

Tabatabaiefar, S. H., Fatahi, B., & Samali, B. (2014). Numerical and Experimental Investigations on Seismic Response of Building Frames under Influence of Soil-Structure Interaction. *Advances in Structural Engineerig*, 17.

Tabatabaiefar, S., & Fatahi, B. (2014). Idealisation of soil-structure system to determine inelastic seismic response of mid-rise building frames. *Soil Dynamics and Earthquake Engineering*, 339-351.

Veletsos, A., & Meek, J. (1974). Dynamic behaviour of building-foundation systems. *Earthquake Engineering and Structural Dynamics*, 3, 121-138.

Wolf, J. P. (1985). *Dynamic Soil-Structure Interaction*. (U. S. River, Ed.) New Jersey: Prentice-Hall.

<https://civiltoday.com/civil-engineering-materials/concrete/225-pre-stressed-concrete>